pmod wrc

Annual Report
Jahresbericht 2017

Physikalisch-Meteorologisches Observatorium Davos und Weltstrahlungszentrum

Mission

Das PMOD/WRC

- dient als internationales Kalibrierzentrum für meteorologische Strahlungsmessinstrumente
- entwickelt Strahlungsmessinstrumente für den Einsatz am Boden und im Weltraum
- erforscht den Einfluss der Sonnenstrahlung auf das Erdklima.

Auftragerteilung

Das Physikalisch-Meteorologische Observatorium Davos (PMOD) beschäftigt sich seit seiner Gründung im Jahr 1907 mit Fragen des Einflusses der Sonnenstrahlung auf das Erdklima. Das Observatorium schloss sich 1926 dem Schweizerischen Forschungsinstitut für Hochgebirgsklima und Medizin Davos an und ist seither eine Abteilung dieser Stiftung. Auf Ersuchen der Weltmeteorologischen Organisation (WMO) beschloss der Bundesrat im Jahr 1970 die Finanzierung eines Kalibrierzentrums für Strahlungsmessung als Beitrag der Schweiz zum Weltwetterwacht-Programm der WMO. Nach diesem Beschluss wurde das PMOD beauftragt, das Weltstrahlungszentrum (World Radiation Center, WRC) zu errichten und zu betreiben.

Kerntätigkeiten

Das Weltstrahlungszentrum unterhält das Primärnormal für solare Bestrahlungsstärke bestehend aus einer Gruppe von hochpräzisen Absolut-Radiometern. Auf weitere Anfragen der WMO wurden 2004 das Kalibrierzentrum für Messinstrumente der atmosphärischen Langwellenstrahlung eingerichtet und 2008 das Kalibrierzentrum für spektrale Strahlungsmessungen zur Bestimmung der atmosphärischen Trübung. Seit 2013 wird auch das Europäische UV Kalibrierzentrum durch das Weltstrahlungszentrum betrieben. Das Weltstrahlungszentrum besteht heute aus vier Sektionen:

- Solare Radiometrie (WRC-SRS)
- Infrarot Radiometrie (WRC-IRS)
- Atmosphärische Trübungsmessungen (WRC-WORCC)
- UV Kalibrierzentrum (WRC-WCC-UV)

Die Kalibriertätigkeit ist in ein international anerkanntes Qualitätssystem eingebettet (ISO 17025) um eine zuverlässige und nachvollziehbare Einhaltung des Qualitätsstandards zu gewährleisten.

Das PMOD/WRC entwickelt und baut Radiometer, die zu den weltweit genauesten ihrer Art gehören und sowohl am Boden als auch im Weltraum eingesetzt werden. Diese Instrumente werden auch zum Kauf angeboten und kommen seit langem bei Meteorologischen Diensten weltweit zum Einsatz. Ein globales Netzwerk von Stationen zur Überwachung der atmosphärischen Trübung ist mit vom Institut entwickelten Präzisionsfilterradiometern ausgerüstet.

Im Weltraum und mittels Bodenmessungen gewonnene Daten werden in Forschungsprojekten zum Klimawandel und der Sonnenphysik analysiert. Diese Forschungstätigkeit ist in nationale, insbesondere mit der ETH Zürich, und internationale Zusammenarbeit eingebunden.

Das PMOD/WRC ist eine Abteilung der Stiftung
Schweizerisches Forschungsinstitut für
Hochgebirksklima und Medizin in Davos.

Physikalisch-Meteorologisches Observatorium Davos
und World Radiation Center (PMOD/WRC)
Dorfstrasse 33
7260 Davos Dorf
Schweiz

pmod wrc

Annual Report
Jahresbericht 2017

Table of Contents

Jahresbericht 2017

Werner Schmutz

Wissenschaft

Am 14. Juli 2017 morgens um 8 Uhr 36 konnten wir feiern: Nach einer 15-monatigen Warteperiode wurde der Satellit NorSat-1 in den Weltraum transportiert. Mit dabei war unser Compact Lightweight Absolute Radiometer (CLARA), ein Absolut-Radiometer der neusten Generation. Nach einer Ausgas-Periode von rund einem Monat wurde CLARA am 21. August 2017 erfolgreich in Betrieb genommen. Die wissenschaftliche Aufgabe für CLARA ist das Messen der Energie der Sonneneinstrahlung auf die Erde, die sogenannte Totaleinstrahlung, und die Überwachung deren Variationen in den kommenden Jahren. Da erwartet wird, dass die Sonnenaktivität in den nächsten 50 Jahren abnehmen wird, ist es spannend zu sehen, ob die Totalstrahlung ebenfalls abnehmen wird. Es ist allgemein akzeptiert, dass die Sonneneinstrahlung in Phasen mit der Sonnenaktivität variiert und daher wird eine Abnahme als solches keine Überraschung sein. Hingegen wird es bedeutsam sein, die Amplitude der Abschwächung zu messen, um beurteilen zu können, ob die solare Variation eine Auswirkung auf das Erdklima hat.

Die Inbetriebnahme von CLARA war eine passende Fortsetzung zum Abschluss des Multi-Institut-Projektes Future and Past Solar Influence on the Terrestrial Climate (FUPSOL). Ein letztes Treffen der teilnehmenden Wissenschaftler fand am 27./28. März 2017 in Davos statt. Eines der Hauptergebnisse des Projektes war die Voraussage, dass, falls die Sonne wiederum in eine grosse Inaktivitätsphase tritt, wie zum Beispiel während dem Maunder Minimum im 17. Jahrhundert, dann könnte die Totaleinstrahlung um bis zu 6 Wm^{-2} zurückgehen. Die Auswirkungen einer solchen Reduktion haben wir theoretisch mit Klimamodellen evaluiert und fanden, dass dies die anthropogene Erderwärmung in den nächsten 50 bis 100 Jahren um rund 0.5°C verringern könnte und somit die Geschwindigkeit der Zunahme etwas verlangsamen würde. Eine offensichtliche Schlussfolgerung ist, dass wir die Sonne im Auge behalten sollten.

Das abgeschlossene FUPSOL-Projekt war vom Schweizerischen Nationalfonds durch das Sinergia Programm finanziert, womit Forschungs-Kollaborationen mehrerer Institute gefördert werden. Das Drei-Jahres-Projekt war eine Fortsetzung einer Serie von Vorgängerprojekten, die alle dem Hauptforschungsthema des Instituts gewidmet sind: die Erforschung und Quantifizierung des Sonneneinflusses auf das Erdklima mit allen Aspekten, von der Rekonstruktion der historischen Sonneneinstrahlung bis zu vielfältigen Interaktionsprozessen mit der Erdatmosphäre. Nun, etwa achtzehn Jahre nach dem Start dieser Projekte, haben wir viele Fragen beantwortet und unser Verständnis der Sonne-Erde-Interaktion hat sich wesentlich verbessert. Unsere zahlreichen Publikationen zu diesem Thema werden von der internationalen Forschergemeinschaft zur Kenntnis genommen, wie man aus der Anzahl der Zitate schliessen kann, die diese erhalten. Der ganze Prozess wird aber bei Weitem noch nicht in seiner vollen Komplexität verstanden und wie es immer der Fall ist, hat unsere Forschung neue Fragen aufgeworfen, die sowohl international als auch von uns weiterverfolgt werden.

Entwicklung und Bau von Instrumenten

Die Instrumentenentwicklung im Institut wurde im letzten Jahr durch den Bau des Weltrauminstruments JTSIM-DARA dominiert, das als Nutzlast auf der chinesischen FY-3E Mission vorgesehen ist. Das PMOD/WRC trägt ein DARA-Typ Absolut-Radiometer zu einem chinesisch-schweizerischen Gemeinschaftsexperiment mit dem Namen Joint Total Solar Irradiance Monitor (JTSIM) bei, das zur präzisen Überwachung der Sonneneinstrahlung vorgesehen ist. Die Parallelentwicklung des bau-ähnlichen DARA Instruments für die europäische Technologie Mission PROBA-3 verlief im Vergleich zögerlich, da Randbedingungen der Schnittstellen zum Satelliten noch unklar waren. Anfang des Jahres 2017 haben wir die vom Institut gefertigten Teile von SPICE und EUI den Instituten ausgeliefert, die für die Experimente verantwortlich sind. Diese haben die fertig zusammengebauten Instrumente im August 2017 der Firma Astrium UK zur Integration in den Satelliten Solar Orbiter geliefert.

Dienstleistungsbetrieb Weltstrahlungszentrum

Die Infrastruktur und ein grosser Teil der indirekten Kosten sind durch den Dienstleistungsauftrag des Weltstrahlungszentrums finanziert. Der Status des Zentrums ist ausgezeichnet: Alle vier Sektionen sind gut organisiert und funktionieren reibungslos. Die Kalibriertätigkeiten, die beim Bureau International des Poids et Mesures als Kalibrier-Fähigkeiten des Weltstrahlungszentrums geführt werden, unterliegen einem Qualitätssystem, das international anerkannt werden muss. Eine im letzten Jahr von der Euramet Vereinigung durchgeführte Überprüfung bestätigte mit Komplimenten das gute Funktionieren unseres Qualitäts-Systems. Wir sind stolz darauf, dass am PMOD/WRC auch die Dienstleistungen in den entsprechenden Tätigkeitsfeldern auf Forschung an vorderster Front basiert. Das ist der beste Weg, einen Service anzubieten, denn eine Arbeit wird dann ausgezeichnet gemacht, wenn sie auf wahrem Interesse und Neugier basiert. Aktive Forschung ist für das Weltstrahlungszentrum Bedingung, damit wir auf dem Gebiet der Kalibrierung von Instrumenten zur Messung der Sonnenstrahlung führend bleiben.

Ein funktionierendes Weltstrahlungszentrum ist eine wünschenswerte Voraussetzung für den Start eines neuen Direktors des PMOD/WRC. Voraussichtlich wird die Übergabe an eine neue Leitung Ende dieses Jahres geschehen. Eine wichtige neue Ausgestaltung der Organisation des PMPOD/WRC-Betriebs ist eine Übereinkunft mit der ETH Zürich, dass der neue Leiter des PMOD/WRC auch zum affiliierten Professor im Departement Physik der ETH ernannt wird. Dies bringt einen besseren Bezug bei der Betreuung von Master- und Doktorandenarbeiten zur Hochschule. Dabei hofft man auch, dass weitere Zusammenarbeiten mit ETH-Instituten im Bau von Weltraum-Hardware zustande kommen, was die technische Abteilung des Observatoriums vergrössern und stärken würde.

Personelles

Dr. Thomas Carlund, der als Wissenschaftler in der WORCC Sektion arbeitete, hat das PMOD/WRC nach erfolgreichem Projektabschluss per Ende März 2017 verlassen und ist wieder in sein Heimatland Schweden zurückgekehrt. Herr Ioannis Panagiotis Raptis wurde als Gast im Rahmen einer H-2020-Kollaboration mit dem Observatorium Athen am Weltstrahlungszentrum von der WORCC Sektion betreut. Er ist im November 2017 wieder nach Griechenland zurückgekehrt, um seine Dissertation an der Universität Athen fertigzustellen. Dr. Hongrui Wang hat seinen Gastaufenthalt am Observatorium Ende 2017 beendet und kehrte nach China zurück. Weitere wissenschaftliche Gäste waren Franciele Carlesso, Doktorandin aus Brasilien, und Gian-Andrea Heinrich, Bachelor Student der ETH Zürich.

Matthias Gander als Entwicklungsingenieur und Mustapha Meftah als Struktur- und Thermik-Ingenieur verstärkten den Bereich Technik per 01. Februar 2017, damit die Anforderungen unserer Weltraumprojekte bewältigt werden konnten. Die Unterstützung durch Herrn Meftah war nur auf zwei Monate beschränkt, aber diese war trotz der knappen Zeit äussert wertvoll für den Fortschritt der Instrumentenentwicklung. Ende Juni 2017 kehrte Pierre-Luc Lévesque nach Kanada zurück, von wo er in Teilzeit-Auftragsarbeit bis Ende Jahr auch aus der Ferne seinen Beitrag für unsere Weltraumprojekte fertigstellen konnte. Fabrice Eichenberger startete im Januar 2017 als Zivildienstleistender und wurde danach ab Juli 2017 bis Februar 2018 als Ingenieur angestellt. Der Mechanik-Ingenieur Johnathan Kennedy ist per Ende Dezember 2017 ausgetreten.

Herzlich gratulieren können wir Frau Kathrin Anhorn und Alexandra Sretovic zur ausgezeichnet bestandenen Lehrabschlussprüfung zur Kauffrau. Frau Anhorn war nach dem Abschluss noch bis Ende Jahr als administrative Mitarbeiterin angestellt und so konnten wir noch ein paar Monate von ihrem Know-how profitieren. Frau Diana Dos Santos hat im August ihr erstes Lehrjahr begonnen. Ebenfalls gratulieren wir Jeanine Lehner zum erfolgreich abgeschlossenen kaufmännischen Jahrespraktikum. Ab August 2017 setzte sie an der Handelsschule in Chur ihre Ausbildung fort.

Ein willkommener Kontrast zu unserer normalen Tätigkeit war ein Konzert am 12. Juli 2017 auf dem Pausenplatz des Alten Schulhauses. Die Vorstellung fand im Rahmen des Davoser New Orleans Jazzfestivals statt und profitierte von ausgezeichneten Wetterbedingungen. Ein Teil unserer Belegschaft betreute mit Enthusiasmus den Anlass, umsorgte die Band und bot den Zuhörern Grilladen und Getränke an.

Dank

Das PMOD/WRC ist finanziell, personell und organisatorisch gut aufgestellt und ich bin dankbar, dass ich das Observatorium in gutem Zustand an eine neue Leitung werde übergeben können. Ich bin überzeugt, dass Forschung und Dienstleistung auch in Zukunft vorteilhaft voneinander profitieren können und dass das Institut eine strahlende Zukunft hat.

Ich danke dem Präsidenten der Stiftung, Dr. Walter Ammann, und dem Präsidenten der Aufsichtskommission, Prof. Dr. Bertrand Calpini, sowie den Mitgliedern der Aufsichtskommission und des Stiftungsratsausschusses für die wohlwollende Förderung des PMOD/WRC über all die Jahre. Ohne Betreuung auf strategischer Ebene wäre ein Institut wie das PMOD/WRC, weit weg von den Hochschulen, auf verlorenem Posten. Weitere Personen mit einflussreichem Wirken im Hintergrund sind der ständige Delegierte der Schweiz bei der Meteorologischen Weltorganisation, Peter Binder, sowie Lukas Schumacher, Leiter der Finanzen und Logistik an der MeteoSchweiz. Diesen Personen danke ich im Namen des Observatoriums ganz herzlich. Weiter danke ich den Partnern in der Finanzierung des Weltstrahlungszentrums, Bund, Kanton Graubünden und Gemeinde Davos, die mit der Grundfinanzierung die Existenz des Observatoriums ermöglichen.

Meine hohe Wertschätzung der Mitarbeitenden ist die letzte und wichtigste Aussage im Tätigkeitsbericht. Nur dank der ausgezeichneten Leistung der Mitarbeiterinnen und Mitarbeiter war der Erfolg des Observatoriums in den vergangenen Jahren möglich.

The launch of CLARA on a Soyuz rocket on 14th July 2017 was watched via a live-stream by PMOD/WRC staff.

The PMOD/WRC staff in May 2018 in front of the Observatory building.

Introduction

Werner Schmutz

On 14 July 2017, we celebrated the successful transfer of the NorSat-1 satellite to space after a waiting period of 15 months since the cancellation of its originally foreseen launch. Our new generation radiometer experiment, the Compact Lightweight Absolute Radiometer (CLARA), is onboard Norsat-1, which was successfully commissioned in the week of 21 August 2017 after an outgassing period of about one month. The science goal of CLARA is to measure the energy input from the Sun to the Earth, the so-called Total Solar Irradiance, and to follow solar irradiance variations in the coming years. As it is anticipated that the solar activity will decline in the next 50 years, it will be interesting to see whether the solar energy input to Earth will also decline. A variation in the solar irradiance in phase with its activity is commonly accepted by the solar community, however, more importantly, it will be interesting to observe the amplitude of such a variation in irradiance.

The CLARA 'first light' was a fitting continuation to the ending of the multi-institute project, Future and Past Solar Influence on the Terrestrial Climate. The final meeting was held in Davos on 27 — 28 March 2018. One of the main conclusions of the project was that if the Sun again enters a deep inactivity phase, a so-called Grand Minimum, such as for instance the Maunder Minimum in the 17th century, then we predict a reduction of the solar irradiance of up to 6 Wm^{-2}, or 0.5 % of its mean irradiance value. The impact of such a reduction has been evaluated theoretically with the use of climate models and it was found that a potential future decrease of the solar irradiance could contribute a slow-down of the global warming trend by up to 0.5°C in the next 50 to 100 years. An obvious conclusion is that we should keep an eye on the Sun to assess its impact on the Earth.

Last year's instrument development was dominated by the hardware development of JTSIM-DARA, which will be a payload on the Chinese FY-3E mission. PMOD/WRC is contributing a DARA-type radiometer to the Joint Total Solar Irradiance Monitor (JTSIM). Still also in its development phase is DARA for PROBA-3. However, because of lacking interface constraints the development could not advance as we would have liked. At the beginning of 2017, we delivered our hardware contributions to the Solar Orbiter instruments, SPICE and EUI. The integrated instruments were delivered in August 2017 by the PI institutes to Astrium UK for integration into the Solar Orbiter satellite.

The present status of the operational services of the World Radiation Center (WRC) is excellent. All four sections are set up well and are operating smoothly. Those calibration capabilities that are listed by the International Bureau of Weights and Measures are subject to an internationally approved quality management system. A recent external Euramet peer review of our system fully approved its effectiveness with acclamation.

The smoothly working operational status of the WRC is a good circumstance for the transition to a new head of the PMOD/WRC. It is intended that the hand-over takes place by the end of the current year. An important new arrangement is that the new director will also be nominated as an affiliated professor in the Department of Physics at the ETH Zurich. This will allow a better integration of Master and PhD students, who are working at PMOD/WRC, to the requirements of the university. There will also potentially be more collaborations in the field of hardware development with other ETH institutes, which could enlargen and strengthen the PMOD/WRC technical department. I am very glad to be in a position to report that the institute is in good shape and prepared for a future with a new vision, and am convinced of a bright future.

I acknowledge the continued and sympathetic full support of the Supervising Commission and the Board of Trustees, which is simply essential for the institute's existence. As a final note, I would like to express a deeply felt appreciation for my staff: It is primarily their dedication to our activities, which has made the institute's success possible.

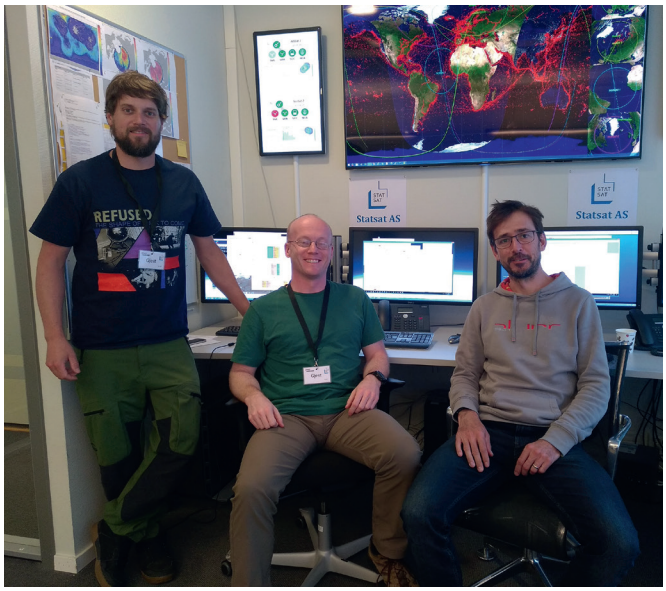

Commissioning team, left to right: Benjamin Walter (PMOD(WRC), Alex Beattie (UTIAS/SFL), Dany Pfiffner (PMOD/WRC) in the STATSAT NorSat-1 Mission Control Room (Oslo, Norway).

Operational Services

Quality Management System, Calibration Services, and Instrument Sales

Silvio Koller, Wolfgang Finsterle, Julian Gröbner, and Daniel Pfiffner

PMOD/WRC Quality Management System

The World Radiation Center has six different Calibration and Measurement Capabilities (CMCs) listed in the KCDB of BIPM. These include:

- Responsivity, solar irradiance pyranometer (1)
- Responsivity, solar irradiance pyrheliometer (1)
- Responsivity, solar irradiance broadband detector (4)

Depending on the instruments wavelength range, the CMCs belong to different WRC calibration sections. The four broadband detector CMCs are currently under review for modification with lower uncertainty values.

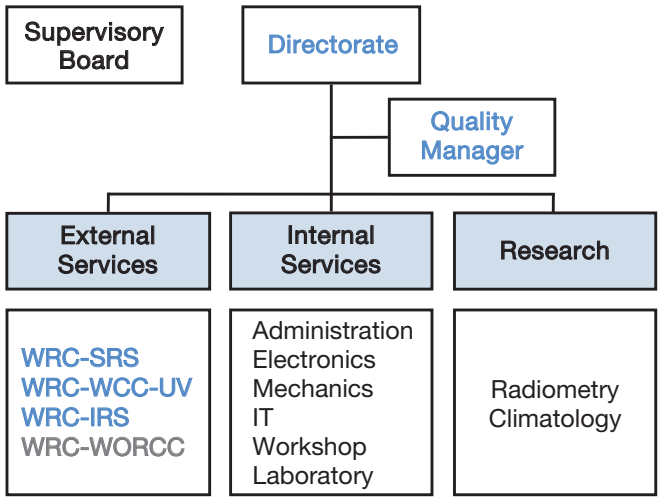

Figure 1. PMOD/WRC Quality Management System: Organisational chart. The WRC-SRS, WRC-WCC-UV and WRC-IRS sections (in blue) perform calibrations according to the EN ISO/IEC standard 17025.

The Quality Manager deputy function has been appointed to Ricco Soder. The WRC responsibility has been shared, and appointed to the lab. heads, Dr. Julian Gröbner and Dr. Wolfgang Finsterle.

Quality Management System Activities

Most of the QMS documentation was reorganised and partly rewritten or amended. The structure and numbering system is now uniform for all sections as well as the higher level, general documentation. Since the end of the year, the IRS calibration section is also fully covered by the PMOD/WRC QMS which follows the ISO/IEC 17025 standard.

In August, a peer review was held at PMOD/WRC by METAS and PTB auditors. Such audits are now foreseen more frequently within the D-A-CH NMI's in the frame of the EURAMET project 1083. The outcome was positive and confirmed the effectiveness of the PMOD/WRC QMS.

Calibration Services

The overall number of calibrations reached a new maximum. A total of 260 calibrations were conducted within the different WRC calibration sections, which is an increase compared to the long-term average shown in Figure 2.

Solar Radiometry Section (WRC-SRS)

In 2017, the WRC-SRS section calibrated 23 pyrheliometers and 92 pyranometers. All certificates were issued with the CIPM MRA logo for mutual recognition. The SRS section attended the National Pyrheliometer Campaign (NPC-2017) campaign in Boulder, USA (see Figure 3) and the WMO RPC RA-V.

Infrared Radiometry Section (WRC-IRS)

The WRC-IRS section performed 27 pyrgeometer calibrations in 2017. The IRS section attended inter-laboratory pyrgeometer comparisons at NREL, Southern Great Plains (SGP), Oklahoma, USA (see Figure 4).

Atmospheric Turbidity Section (WRC-WORCC)

The WRC-WORCC calibrated 22 Precision Filter Radiometers (PFR) against the WORCC Triad standard. In addition, two Precision Solar Spectroradiometers (PSR) were calibrated against a reference standard, traceable to the German National Metrology (PTB) Institute.

World Calibration Center for UV Section (WRC-WCC-UV)

The WCC-UV section calibrated 90 UVB broadband radiometers. Of this number, several certificates were issued for one instrument, but covered different units. In addition, two lamps/diodes were calibrated. These calibrations resulted in 252 certificates, 88 of them with a CIPM MRA logo.

The WCC-UV Section performed two quality assurance site audits of solar UV monitoring spectroradiometers at their respective field sites using the QASUME travelling reference spectroradiometer.

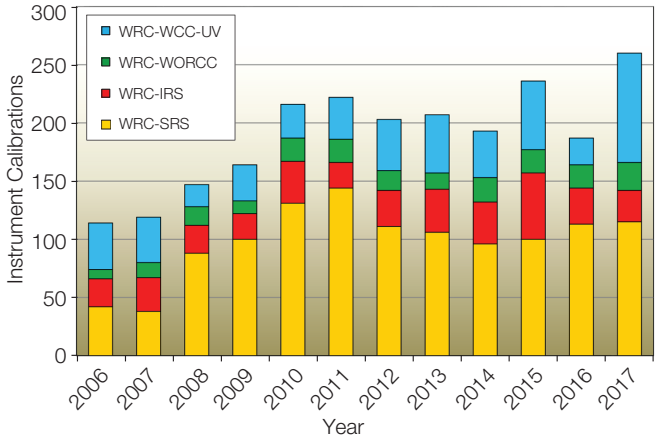

Figure 2. Statistics of instrument calibrations at PMOD/WRC for the 2006–2017 period. Note: One instrument can result in more than one calibration certificate.

Figure 3. Instruments from the SRS Section (far right) during the NPC-2017 campaign in Boulder (USA).

Figure 4. Radiometers to measure downwelling longwave radiation during the inter-laboratory comparisons at the SGP site in Oklahoma, USA.

Instrument Sales

In 2017, PMOD/WRC sold fewer instruments and accessories than in previous years. However, the number of PMO6-CC absolute radiometers purchased was similar to the long-term average.

The following instruments were sold:

- A PMO6-CC absolute radiometer to Chile.
- A PMO6-CC absolute radiometer to China.
- A PMO6-CC absolute radiometer to Shanghai/China.
- A PMO6-CC absolute radiometer to USA.
- Two VHS units to DWD, Germany.

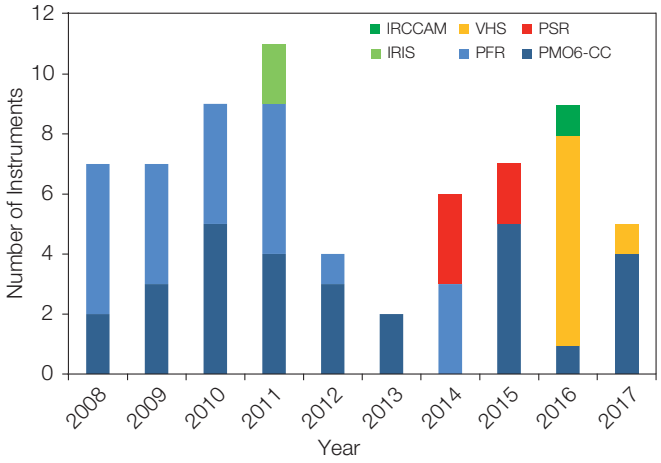

Figure 5. Number of PMOD/WRC instruments sold from 2008 up to and including 2017: i) IRCCAM = Infrared Cloud Camera, ii) VHS = Ventilated Heating Systems, iii) PSR = Precision Spectroradiometer, iv) IRIS = Infrared Integrating Sphere Radiometer, v) PFR = Precision Filter Radiometer, and vi) PMO6-CC = absolute cavity pyrheliometer.

Solar Radiometry Section (WRC-SRS)

Wolfgang Finsterle

The Solar Radiometry Section (SRS) of the WRC maintains and operates the World Standard Group (WSG) of Pyrheliometers which represents the World Radiometric Reference (WRR) for ground-based total solar irradiance measurements. The SRS operates a calibration laboratory according to the laboratory standard ISO/IEC 17025 for solar radiometers (pyrheliometers and pyranometers). During the 2017 calibration season, 115 calibration certificates were issued.

In 2017, the SRS/WRC calibrated 115 radiometers: these consisted of 92 pyranometers, 16 pyrheliometers with a thermopile sensor and seven absolute cavity radiometers. The WSG was operated on 84 days and the Cryogenic Solar Absolute Radiometer and Monitor for Integrated Transmittance (CSAR/MITRA) on 33 days (see article on page 12).

On 29 August, a peer-review audit of the SRS was conducted by experts from PTB (Germany) and METAS. The auditors concluded that the laboratory was generally in a good state and issued seven recommendations.

The SNF-sponsored project "Understanding and improving the cavity absorptance and instrumental degradation of TSI radiometers" aims to drastically reduce the largest uncertainty component in present TSI space radiometers. Alberto Remesal Oliva spent 5 weeks in Boulder, Colorado, USA, to work with NIST experts on the characterisation of black absorptive coatings, including sprayable as well as vertically aligned C-nanotubes and conventional black paints (see article by Alberto Remesal Oliva).

Between the end of April and July, an exchange student from Brazil (National Institute for Space Research, INPE) visited PMOD/WRC to work with SRS staff on the optical characterisation of black absorptive coatings. The results of this collaboration will be presented to the IAU General Assembly in Vienna in August 2018.

The SRS participated in the Regional Pyrheliometer Comparison (RPC) of WMO Regional Associations II and V (RPC RA-II&V), which was jointly organised by JMA (Japan) and the Bureau for Meteorology (Australia) on Mount Tsukuba, Japan, as well as in the National Pyrheliometer Comparison, NPC-2017, at NREL (USA). Two PMO6-cc and one AHF absolute cavity radiometer served as the SRS transfer standard in both comparisons. While weather conditions were good during RPC RA-II&V, the NPC was initially plagued by bad weather which prevented measurements during the first week of the event, after which the PMOD/WRC representative had to leave. Fortunately, a representative from Joint Research Centre (Italy) agreed to operate the SRS transfer standard during the second week, when a few sunny days occurred. The results of the NPC-2017 were published in the NREL technical report, NREL/TP-1900-70436, and confirm that the WSG has been stable since the last IPC (see Table 1). Results from the RPC RA-II&V are also shown in Table 1, the final report has been accepted and will soon be published by WMO.

Table 1. The WRR correction factors for the three transfer standard pyrheliometers determined in the RPC RAII&V and NPC-2017 agree extremely well with the results from IPC-XII in 2015. The US standard group maintained by NREL served as the independent reference during the NPC-2017. The observed relative changes are well below the significance threshold of the comparison and confirm the stability of the WSG. Because the SRS' transfer standard pyrheliometers were part of the reference group for the RPC RA-II&V, an independent assessment of their stability is not possible from that comparison.

	IPC-XII (2015)	RPC RA-II&V	NPC-2017
PMO6-CC 0401	1.020799	1.021102	1.02094
PMO6-CC 0803	1.000335	1.000021	1.00018
AHF 32455	1.001380	1.001296	1.00139

Regular confirmation of the stability of the WSG through participation in pyrheliometer comparisons is required by ISO 17025 to maintain the SRS' Calibration and Measurement Capabilities (CMCs). The SRS is leading the revision process for the ISO 9060 international standard (Solar energy – Specification and classification of instruments for measuring hemispherical and direct solar radiation). Two committee meetings and several telephone conferences were held in 2017 before a new Draft International Standard (DIS) was published. The DIS introduces a new classification scheme for pyranometers and pyrheliometers based on application specific requirements.

Figure 1. Panoramic view of the roof-top measurement site on Tsukubasan Keisei Hotel (Mt. Tsukuba, Japan) where the participants set up their equipment for the RPC RA-II&V.

Infrared Radiometry Section (WRC-IRS)

Julian Gröbner, Christian Thomann, and Stephan Nyeki

The Infrared Radiometry Section of the WRC maintains and operates the World Infrared Standard Group of pyrgeometers (WISG) which represents the world-wide reference for atmospheric long-wave irradiance measurements.

The WISG serves as the atmospheric long-wave irradiance reference for the calibration of pyrgeometers operated by institutes around the world. The WISG has been in continuous operation since 2004, and consists of four pyrgeometers which are installed on the PMOD/WRC roof platform.

The measurements of the individual WISG pyrgeometers with respect to their average are shown in Figure 1 for the period 2004 to the end of 2017. As can be seen, the internal consistency of the WISG is very satisfactory, with measurements from the four pyrgeometers agreeing to within ±1 Wm^{-2} over the whole time period. The WISG is currently seen as an interim transfer standard group with respect to its reference scale (WMO, 2006). The evidence for a revision of the reference scale comes from concurrent operation of the WISG alongside IRIS during night-time clear-sky conditions since 2008 as well as during several comparisons including the ACP (Reda et al., 2012), which yielded an underestimation of the WISG clear-sky longwave irradiance by 2–6 Wm^{-2}, depending on the amount of integrated water vapour (Gröbner et al., 2014).

An international intercomparison was organised at the Southern Great Plains test site (SGP) of the Atmospheric Radiation Measurement Program in Oklahoma, USA, from 16 Oct.–8 Dec. 2017 (Figure 2). During two periods (16–27 Oct., and 27 Nov.–8 Dec.), atmospheric longwave irradiance measurements were performed with several IRIS and ACP radiometers, as well as a number of pyrgeometers calibrated either with respect to the WISG or with calibrations obtained during the IPASRC-I campaign (Philipona et al., 2001). These measurements were complemented by additional information obtained by collocated instrumentation at SGP, such as a microwave radiometer, a thermal all-sky camera and the AERI spectrometer. A preliminary analysis of the data has confirmed previous comparisons as described in Gröbner et al. (2014). A more detailed investigation, including ancillary data from SGP, is currently being performed and first results are expected in the second quarter of 2018.

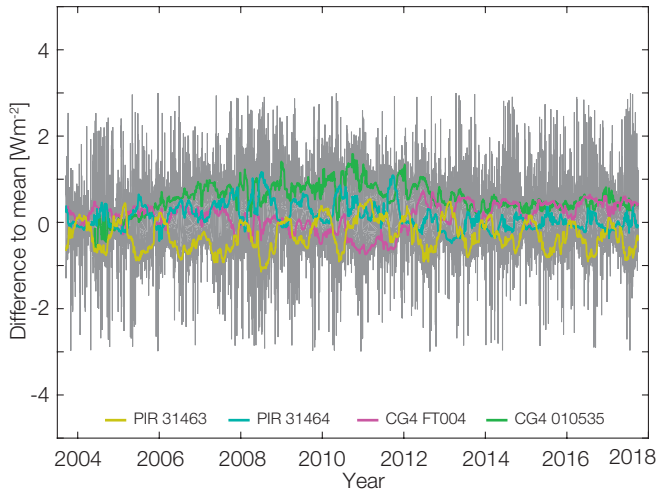

Figure 1. Night-time atmospheric long-wave measurements of the WISG pyrgeometers relative to their average. The coloured lines represent a 30-day running mean of each WISG pyrgeometer, while the grey shaded area represents the daily measurements.

Figure 2. View of the measurement platform at SGP (23 October 2017) showing the two ACP radiometers on the left, the four IRIS radiometers in the centre and the pyrgeometers on the right of the picture.

The results of the SGP campaign were also discussed during the first session of the WMO CIMO Task Team on Radiation References, which was held in the National Physical Laboratory (NPL) from 15–17 November, 2017 in Teddington, UK, and focussed on the traceability of terrestrial radiation measurements. During very constructive discussions among the participants, recommendations were formulated which will be submitted to the CIMO management group in spring 2018 and to the CIMO-17 session in October 2018 for endorsement.

References:

Gröbner J. et al.: 2014, J. Geophys. Res. Atmos., 119, doi: 10.1002/2014JD021630.

Philipona R. et al.: 2001, J. Geophys. Res., 106, 28129–28141.

Reda I. et al.: 2012, J. Atm. Sol.-Terr. Phys. 77, 132–143, doi: 10.1016/j.jastp.2011.12.011.

WMO: 2006, CIMO-XIV, Activity Report, WMO No. 1019 (Part II), 7–14 December 2006.

Atmospheric Turbidity Section (WRC-WORCC)

Stelios Kazadzis, Natalia Kouremeti, and Julian Gröbner

The Atmospheric Turbidity Section of WRC maintains a standard group of three Precision Filter Radiometers (PFR) that serve as a reference for Aerosol Optical Depth measurements within WMO. WORCC also operates the global GAW-PFR AOD network.

The WORCC standard group of three PFRs (referred to as the "PFR triad") was established in 2005 by WORCC in order to fulfil the WMO mandate regarding: "homogenisation of global AOD through provision of traceability to the World Standard Group (WSG) of spectral radiometers for contributing networks at co-located sites and/or periodic international filter radiometer comparisons, and further standardisation of evaluation algorithms." Since 2005, five different well-maintained instruments have been used as part of the PFR triad. Figure 1 shows the long-term (12 years) comparison of the PFR triad instruments. In the 12 years of 1-minute measurement data, >99% of retrieved AOD lies within the WMO U95 criterion, at all wavelengths. All differences of individual instruments with the triad are well within ±0.005 with only small shifts for different PFRs and particular wavelengths (Kazadzis et al., 2018).

Annual quality assured data from eight GAW-PFR stations were updated to 2017 and submitted to WDCA. In 2017, nine instruments of the extended GAW-PFR network and 13 additional customer instruments were calibrated against the reference Triad at Davos. All calibrations were documented according to the WRC quality management system.

The lunar PFR participated in a lunar AOD intercomparison held in Izaña, Tenerife, Spain during June 2017. In this campaign, two lunar irradiance models were used as well as three different photometer models (CIMEL CE318-T, the Lunar-PFR and a stellar photometer). The Lunar-PFR was also deployed at Ny Ålesund from Dec. 2016 to Feb. 2017 and Nov. 2017 to Feb. 2018 for AOD monitoring during the polar winter.

WORCC has started a close collaboration with AERONET Europe and SKYNET Europe/Asia. Two PFR instruments have been performing measurements in parallel with instruments from these networks at Valencia, Spain and Chiba, Japan for a year. A memorandum of understanding, including a four-year collaboration plan, was signed with CNR (Italy) which represents Skynet Europe for a close scientific collaboration on the traceability of SKYNET instruments linked with the PFR triad. Under this agreement, a reference POM-2 instrument was calibrated at Davos from Aug. to Sept. 2017. In addition, a PFR instrument is currently participating in the QUATRAM (QUAlity and TRaceabiliy of Atmospheric aerosol Meas.) campaign (www.euroskyrad.net/quatram.html). Similar agreements are planned with AERONET Europe.

Within the project "A travel standard for Aerosol Optical Depth in the UV", the UV version of the PFR (UV-PFR) has been tested as a reference instrument to calibrate Brewer spectrophotometers in order to determinate AOD. The UV-PFR was measuring during the whole of 2017 in Izaña, Spain. In a different campaign, a Precision Spectroradiometer (PSR) participated, under an ACTRIS transnational Access fund, in PRE-TECT (pre-tect.space.noa.gr) which was held in Crete, Greece, in April 2017.

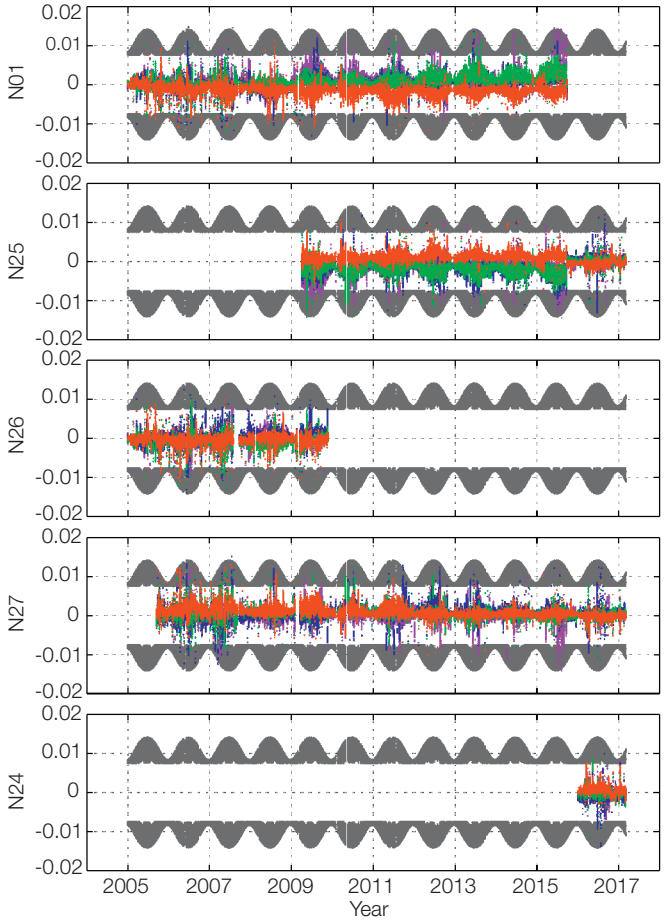

Figure 1. Daily difference of individual PFRs against the mean of the PFR triad at the four PFR wavelengths (coloured lines). Grey areas represent the WMO U95 limits.

Two years of PSR measurements at the Meteorological Observatorium Lindenberg, Germany, have been used in a study to investigate the ability of the PSR to determine columnar water vapour. Results from two retrieval methods were compared with various other methods (sun-photometer Cimel CE318, Global Positioning System, microwave radiometer profiler and radiosonde retrievals), and showed differences of up to 3.3% and 0.7% with coefficients of determination (R^2) in the ranges 0.87–0.95 and 0.96–0.98 for the two methods, respectively.

Three PSRs are being manufactured at PMOD/WRC and will all be operational during 2018. The instruments will be operated at Davos in parallel to the PFR triad to investigate their stability and accuracy. Moreover, the possibility of a future replacement of the WORCC standard by a "PSR-triad" and a move toward traceable spectral irradiance and AOD measurements will be investigated.

References: Kazadzis S., Kouremeti N., Nyeki S., Gröbner J., Wehrli C.: 2018, Geo. Instrum. Meth. Data Syst., 7, 39-53, doi.org/10.5194/gi-7-39-2018.

World Calibration Centre for UV (WRC-WCC-UV)

Julian Gröbner, Gregor Hülsen, and Luca Egli

The objective of the World Calibration Center for UV (WCC-UV) of WMO GAW is to assess the data quality of the Global GAW UV network and to harmonise the results from monitoring stations and programmes in order to ensure representative and consistent UV radiation data on a global scale.

The WCCUV-UV reference spectroradiometer, QASUME, was used during two quality assurance site visits. In June, we visited the headquarters of the Agencia Estatal de Meteorología (AEMET; see Figure 1). It was the 5th audit in Madrid (Spain) after 2009, 2011, 2013, and 2015. In September, we organised the 7th visit to the Agenzia Regionale per la Protezione dell Ambiente (ARPA) in the Valle d´Aosta, Italy. Reports describing the results of the campaign can be found on the WCC-UV website (see link further below).

The second main activity during 2017 was the participation in the 12th Regional Brewer Calibration Center-Europe (RBCC-E) campaign. Both global and direct irradiance measurements were conducted from May to June in El Arenosillo, Spain. The global UV irradiance spectra recorded by QASUME provided the reference data for the participating 21 Brewer spectrophotometers. Direct solar UV irradiance measurements were used to derive total column ozone which was compared to the reference data from the Regional Secondary Reference (Brewer 185) operated by the AEMET Izaña Observatory (Figure 2). The EMRP ENV59-ATMOZ project "Traceability for atmospheric total column ozone", coordinated by WCC-UV, was successfully finished in 2017 with a final workshop in El Arenosillo.

During Summer 2017 (May — October), we organised the International UV Filter Radiometer Comparison (UVC-II) at Davos. A total of 75 UV filter radiometers from 37 Countries participated in the campaign, of which 22 were from Europe (see Figure 3). The standard calibration methodology, using the instrument's spectral and angular response functions measured in the laboratory, exhibited remarkable agreement with the reference spectroradiometer, with expanded uncertainties ($k = 2$) of around 6% for most instruments.

Figure 1. View of the rooftop at AEMET, Madrid, Spain.

Figure 2. View of the measurement platform at the Istituto Nacional de Technica Aeroespacial (INTA). The input optic for direct irradiance measurement of QASUME can be seen at the front of the image.

Figure 3. Outdoor calibration during the 2nd International UV Filter Radiometer Comparison on the PMOD/WRC roof platform with a total of 75 UV radiometers.

Results of all QASUME site audits and campaign reports can be found on the WCC-UV website:

www.pmodwrc.ch/weltstrahlungszentrum/wcc-uv/
www.pmodwrc.ch/wcc_uv/wcc_uv.php?topic= qasume_audit

Instrument Development

The Cryogenic Solar Absolute Radiometer (CSAR) and the Monitor to Measure the Spectrally Integrated Transmittance of Windows (MITRA)

Benjamin Walter, Wolfgang Finsterle, and Nathan Mingard

The combined CSAR/MITRA instrument system is expected to replace the World Standard Group (WSG) in future to serve as a new World Radiometric Reference (WRR) for direct normal irradiance measurements. CSAR is a cryogenic radiometer operated under vacuum at -250°C allowing high measurement accuracies. Reflection and absorption losses at the CSAR entrance window are monitored with MITRA. The first seven irradiance measurements performed with CSAR/MITRA in 2017 support previous findings of a ~0.3% difference between the International System of Units (SI) radiometric scale represented by CSAR/MITRA and the currently used WRR scale. The following SI to WRR comparisons, however, revealed that the window cleanliness is still an unsolved issue. Modifications to CSAR and the new MITRA-III instrument were elaborated to finally resolve the window cleanliness problem.

CSAR/MITRA aims to reduce the uncertainty of direct normal incidence measurements from currently 0.3% (WSG) towards 0.01% on a worldwide basis, and to provide direct traceability of these measurements back to the SI scale. The effective spectrally integrated transmittance of the CSAR entrance window is permanently monitored for an identical window with MITRA to correct the power readings of CSAR for these losses. The basic assumption is that the transmittance of both windows is identical which strongly depends on their cleanliness.

Figure 1 illustrates a summary of the comparisons of the SI scale represented by CSAR/MITRA to the WRR performed in 2017, together with the respective MITRA transmittance measurements. The average of the first seven comparisons resulted in a difference of -0.26% ± 0.064% which agrees well with previous findings of a difference ~ -0.3%. The averages of the following four periods (indicated by the dashed red lines), where the windows were cleaned and changed between each period, shows significant differences although with reasonably good stability in-between periods.

This suggests that the CSAR/MITRA system is stable, but also that the CSAR and MITRA windows were not identical, most likely due to cleanliness issues as observed previously. Due to bad weather conditions and a busy schedule of the CLARA/NorSat-1 space radiometer, only few CSAR/MITRA measurements were performed in the second half of 2017.

To resolve the window cleanliness issue, a new MITRA-III instrument with four detectors is currently under construction which will also allow the transmittance of two windows to be compared. Furthermore, CSAR and MITRA-III will be modified so that the windows from each instrument can be exchanged amongst each other several times throughout a measurement day. Any difference in the spectrally integrated transmittance between both windows will thus be cancelled out when deriving a daily averaged SI to WRR comparison value. The next steps will include the installation of a vacuum valve behind the CSAR window which will allow the window to be removed without breaking the vacuum.

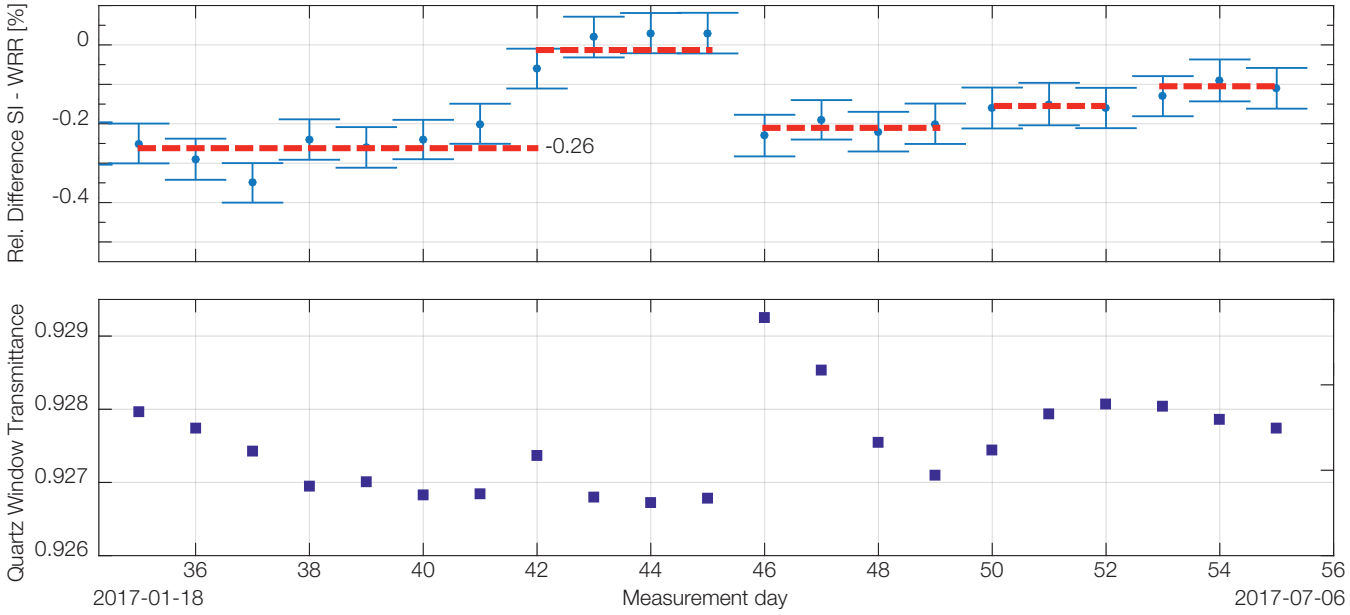

Figure 1. Top: Daily averages of 20 WRR to SI comparisons performed at PMOD/WRC with CSAR/MITRA in 2017. Altogether, 55 comparisons have been performed since June 2015. Bottom: corresponding daily averages of the spectrally integrated window transmittance as measured with MITRA.

Space Experiments

Manfred Gyo, Lloyd Beeler, Fabrice Eichenberger, Wolfgang Finsterle, Matthias Gander, Nuno Guerreiro, Patrik Langer, Pierre Luc Lévesque, Margit Haberreiter, Johnathan Kennedy, Silvio Koller, Philipp Kuhn, Nathan Mingard, Dany Pfiffner, Pascal Schlatter, Yanick Schoch, Marcel Spescha, Benjamin Walter, and Werner Schmutz

EUI

The Extreme UV Imager (EUI) experiment, a payload onboard the ESA/NASA Solar Orbiter Mission.

PMOD/WRC is responsible for the Optical Bench Structure (OBS) of the EUI instrument. At the beginning of 2017, all sub-parts were delivered to Centre Spatiale de Liège (CSL) . The sub-parts were integrated onto the OBS, and the optical parts of each channel were aligned. The channels were co-aligned to have the same field-of-view within the given uncertainties.

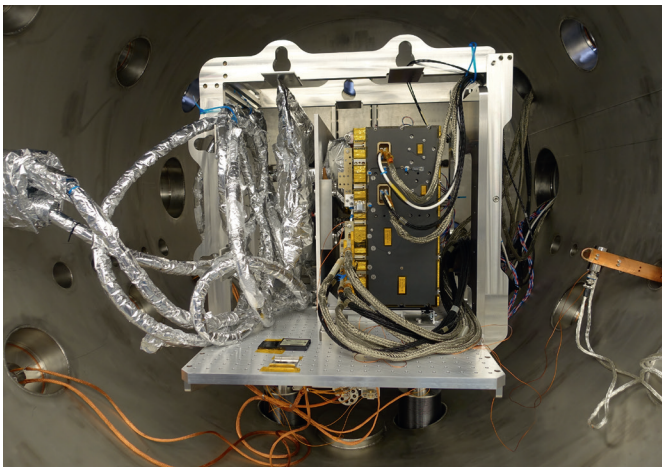

Figure 1. EUI Flight Model at PTB during end-to-end calibration with the Metrology Light Source (MLS).

After closing the instrument, the final acceptance test campaign was conducted on the Flight Model. All tests were successfully finished.

The last steps, performed under control of the consortium, were the end-to-end calibration campaign at the National Metrology Institute (PTB) in Berlin, Germany. The Metrology Light Source (MLS), a dedicated low-energy storage ring for metrology with synchrotron radiation, served as the stable source in the EUV wavelength range which was necessary for the end-to-end calibration.

After the successful calibration, the instrument was delivered to AIRBUS for integration and testing on the spacecraft. The integration is still on-going. Due to delays, the launch has been postponed to Spring 2020.

SPICE

The Spectral Imaging of the Coronal Environment (SPICE) experiment, a payload onboard the ESA/NASA Solar Orbiter Mission.

Low Voltage Power Supply (LVPS)

In 2017, a few capacitors in the electronics provided by PMOD/WRC had to be exchanged for ones with a higher stand-off to address the outcome of the solder verification. After the re-work, the test campaign at the Rutherford Appleton Laboratory (RAL) continued.

Slit Change Mechanism (SCM)

The pending qualification campaign was finished in the first quarter of 2017 with success. The slit change mechanism demonstrated that it will survive the required number of duty cycles in space. With the completion of the qualification task, the SCM industry contract with ALMATECH came to a finish.

SPICE Door Mechanism (SDM)

Parallel to the SCM activities, the qualification of the SDM was completed in the first few months of 2017. This industry contract with APCO Technologies was finished after the successfully completed qualification task.

SPICE Instrument

RAL Space finished the acceptance test campaign and the calibration of the SPICE Instrument, and delivered the instrument to AIRBUS for integration into the spacecraft. The integration is ongoing at AIRBUS.

In November, a Consortium Meeting at RAL took place to transfer the technical project lead from RAL to the operational project lead at IAS. A complete technical overview of the build-status was presented to the operational group.

Figure 2. Meeting of the SPICE Consortium in 2017.

CLARA

The Compact Lightweight Absolute Radiometer (CLARA), a payload onboard the Norwegian NorSat-1 micro-satellite.

As reported last year, the planned launch of NorSat-1 with CLARA (Figure 3) onboard did not occur in 2016. Fortunately, another launcher option was found and took place on 14 July 2017 on a Soyuz 2-1A at the Baikonur Cosmodrome, Kazakhstan (Figure 4).

A PMOD/WRC team was present at the Norwegian operations centre (STATSAT) in Oslo for the first switch-on of CLARA on the same day. An exciting moment was the verification of the first transmitted telemetry data. CLARA delivered nominal values for power consumption and temperatures. In the following days, instrument checks and status tests were conducted on NorSat-1 and CLARA. Before any irradiance measurements were conducted, an outgassing phase of about five weeks was scheduled.

CLARA 'first light' measurements were conducted on 21 – 24 August 2017. The first Total Solar Irradiance (TSI) measurements gave a mean value of 1361 $W m^{-2}$, which was very close to our expectations. The following weeks of commissioning showed larger pointing instability of the satellite than expected. Thus, several measurement sequences were introduced to verify CLARA's pointing sensitivity. Software routines were required to filter CLARA data in relation to information about the spacecraft's attitude. Although CLARA is still not in routine operation, it has already provided valuable scientific data.

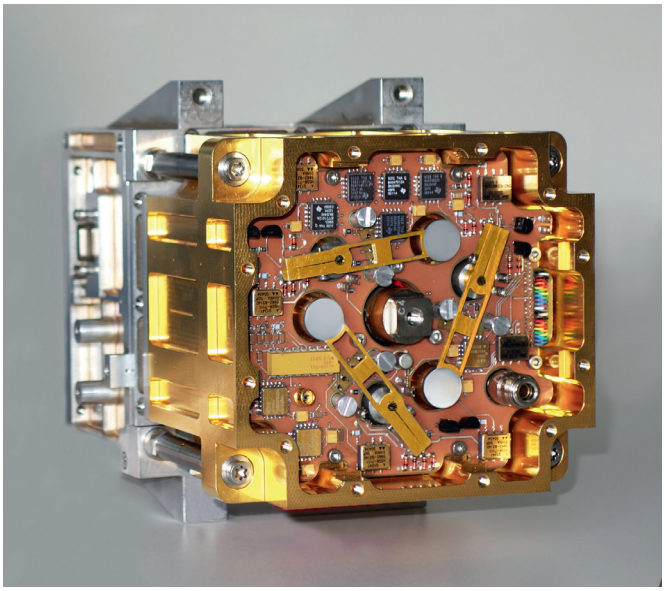

Figure 3. Close-up view of the CLARA radiometer with the front shield removed. CLARA's dimensions are 128 x 138 x 158 mm and weighs only 2.2 kg.

Figure 4. Soyuz 2-1A launch. Image credit: ROSKOSMOS, Russia.

The pointing stability of the satellite has been improved and further investigations are ongoing. Meanwhile, CLARA measurements provide information for the optimal cavity assignment and instrument parameter settings. Furthermore, an adapted backup regime for the detection of degradation has been determined.

PMOD/WRC thanks all involved parties, especially the Norwegian Space Centre for the opportunity to fly CLARA on the NorSat-1 micro-satellite.

The University of Toronto Institute for Aerospace Studies (UTIAS) provided the spacecraft platform and has always been a supporting and reliable partner. The Swiss Space Office funded the project in the framework of ESA's Science & Technology programme, PRODEX (PROgramme de Développement d'EXpériences scientifiques).

DARA

The Digital Absolute Radiometer (DARA), a payload onboard ESA's PROBA-3 formation flying mission.

Based on the outcome of the vibration test, which was conducted on the DARA engineering model, the structural design was improved. The focus was set on:

- Slipping and gapping prevention during the vibration test or later, at the spacecraft launch.
- Increasing the mechanical structure stiffness.
- Increasing the first eigen-mode frequencies.

All these points were addressed and the following structural analysis resulted in the expected behaviour. In parallel, a thermal analysis was conducted by our industry contractor, Almatech.

PMOD/WRC conducted a lifecycle test with the foreseen shutter mechanism for DARA. A setup of five stepper motors and shutter blades was installed in a vacuum chamber. The stepper motors performed 3.8 Mio. movements in about six weeks. In addition, the environmental temperature was cycled 11 times between -30°C and +70°C. Prior to the test, three of the motors underwent a vibration test to simulate real conditions. Such tests are required for design qualification reasons. The lifecycle test was successful and the shutter design can now be applied to both space experiments, DARA on the PROBA-3 satellite and JTSIM-DARA on the Chinese FY-3E mission.

Significant progress was made in 2017 on the development of the electronics. The Engineering Model (EM) electronics were fully tested and validated. Based on these results, the flight unit boards for DARA's sister experiment, JTSIM-DARA, were manufactured and tested. This instrument then allowed the calibration process of the entire electronic circuitry to be validated. The same process can now be applied to DARA.

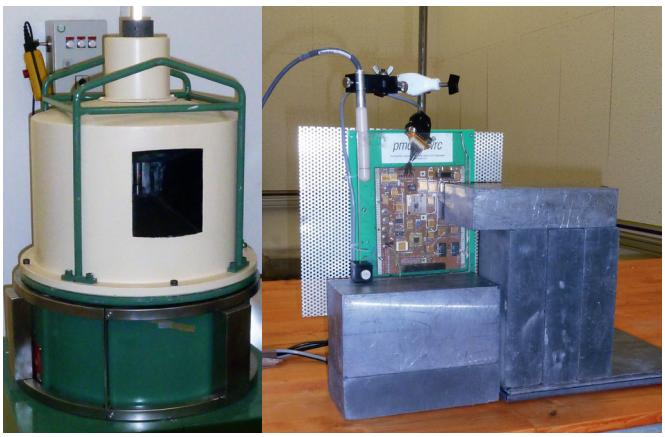

Figures 5 and 6. Radiation test source, and CPU test set-up.

In parallel, a dedicated controller (CPU) board (the radiation test sample) was built and assembled with qualified flight components. Some of these components are tolerant to ionising radiation up to a certain dose, others are unfortunately not available to the required standard. As the expected total dose on the PROBA-3 orbit is high, we conducted a radiation test on the test-board. The unshielded board functioned up to a total dose of 14.6 krad. The test is not fully representative since the ^{60}Co gamma-ray source does not simulate the real radiation environment. Nevertheless, the test indicated which components are most susceptible and consequently we will apply some spot-shielding on certain components. In addition, the aluminium housing of the instrument and the spacecraft itself will provide some shielding against harmful radiation.

Figure 5 shows the radiation source at the European Space Research and Technology Centre (ESTEC, Netherlands) test facility while Figure 6 shows the CUP during testing. Some parts of the circuit which are required to operate the test board are shielded with lead-alloy bricks in the figure.

Our industry contractor dlab GmbH, Winterthur reached an instrument development stage that allows us to fully run and control the instrument and to perform valid solar irradiation measurements with the DARA EM. At PMOD/WRC, we developed different data level transformation routines. To a first order approximation, the instrument measures tensions or currents, but these values need to be transformed and corrected for temperature variations and other adverse effects to achieve an accurate irradiance value at the end.

In the framework of the DARA project, PMOD/WRC hosted an ETHZ Bachelor thesis. Gian-Andrea Heinrich designed and implemented an optical test-setup to verify the pointing sensitivity of the DARA instrument. Any misalignments or deviations due to tolerances need to be corrected during the final mounting onto the spacecraft.

PROBA-3 is a highly demanding mission. The planned formation flight of two spacecraft is very complex and requires a lot of simulation work and resources. The foreseen launch date has therefore been moved to late 2020. This circumstance also slows down the development of DARA. However, PMOD/WRC is in an advantageous situation, in that the Chinese JTSIM-DARA project is very similar and both projects can therefore profit from each other. The DARA Critical Design Review (CDR) is planned for Spring 2018.

JTSIM-DARA

Joint Total Solar Irradiance Monitor-DARA (JTSIM-DARA), a payload onboard the Chinese FY-3E mission.

During 2017, the electronics of the JTSIM-DARA Proto Flight Model (PFM) were manufactured. The entire electronics team was extremely occupied with designing, ordering parts and equipping all the boards. At the end of the calendar year, the PFM electronics were fully functional and were able to be finalised. The test campaign on "board level" was successfully completed and the functional test on "instrument level" was also conducted. The electronics team was also able to calibrate parts of the electronics box while under a vacuum environment and over a wide temperature range.

A second meeting was held between PMOD/WRC and the Changchun Institute of Optics, Fine Mechanics and Physics Institute (CIOMP) in Changchun. Many technical details and interface aspects mainly related to communication were resolved during the meeting, and a much better understanding was reached by both sides.

Considering the numerous telephone conferences and email communications prior to this test campaign, and with the given cultural and linguistical differences between CIOMP and PMOD/WRC, a face-to-face workshop turned out to be the most effective approach to making significant progress. Nevertheless, due to an export restriction, the project schedule was further delayed. Under this restriction, no parts (e.g. simulator) could be exported, and the exchange of technical details was not possible. Further joint testing of JTSIM-DARA by CIOMP and PMOD/WRC had to be delayed until 2018.

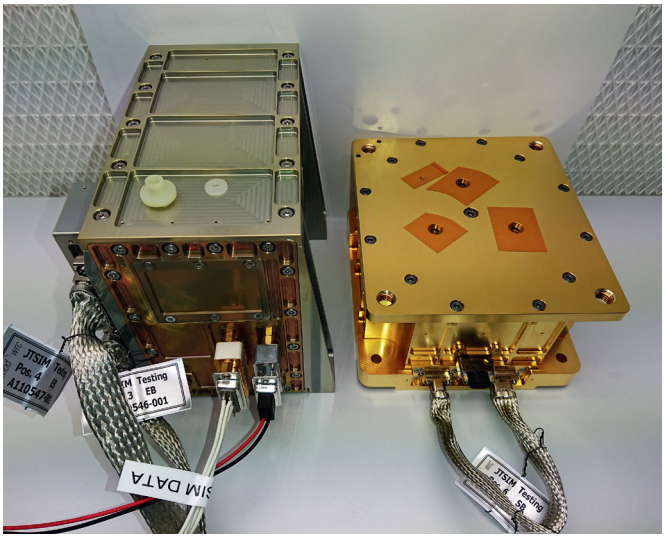

Figure 7. The JTSIM-DARA Flight Unit.

Figure 8. JTSIM-DARA being calibrated against the World Standard Group at PMOD/WRC.

In parallel, the mechanical side was worked on and good progress was made. After designing and simulating (mechanical and thermal model) the electronics and sensor boxes for JTSIM-DARA, the instrument had advanced enough to manufacture the mechanical parts. PMOD/WRC was able to manufacture the electronics box in-house (except surface treatment) whereas the whole sensor box and shutter mechanism were manufactured together with industrial partners.

The project will enter the final phase in 2018. The Flight Model will be calibrated at PMOD/WRC. The instrument will then be shipped to China to perform all environmental testing and finally a comprehensive test, calibration and qualification period is also planned in China, before the final instrument integration at the beginning of 2019.

Scientific Research Activities

Overview

Werner Schmutz

Projects at PMOD/WRC are related to solar radiation in which we address questions regarding the radiation energy budget in the terrestrial atmosphere, as well as problems in solar physics in order to understand the mechanisms concerning the variability of solar irradiance. Hardware projects at our institute are part of investigations into Sun-Earth interactions which involve measurements of solar irradiance.

The choice of projects to be conducted at the institute is governed by the synergy between the know-how obtained from the Operational Services of the World Radiation Center and other research activities. Basically, the same instruments are built for space-based experiments as are utilised for ground-based measurements. The research activities can be grouped into three themes:

- Climate modelling
- Terrestrial radiation balance
- Solar physics

Research activities are financed through third party funding. Last year, five projects were supported by the Swiss National Science Foundation and in addition, other funding sources were: i) a project through Swiss participation in the EU's COST actions, ii) two projects by MeteoSwiss in the framework of Swiss contributions to the Global Atmosphere Watch programme of the WMO, iii) a project through the Horizon 2020 programme of the European Commission, and iv) two projects through the European Metrology Research Programme. These funding sources have supported two PhD Theses and four post-doctoral positions.

Furthermore, two post-doctoral researchers, two PhD students, and one bachelor student have stayed at the observatory supported by external funding. Swiss participation in ESA's PRODEX (PROgramme de Développement d'Expériences scientifiques) programme funds the hardware development for space experiments. The institute's four PRODEX projects paid for the equivalent of five technical department positions. Another space-related contribution is the IDEAS+ project of the European Space Agency, which is using the institute's laboratory calibration equipment.

The project, *Future and Past Solar Influence on the Terrestrial Climate* (FUPSOL) ended in March 2017. It was funded through the so-called Sinergia programme of the Swiss National Science Foundation which supports multi-institute collaborative research. The past three-year project was the continuation of a previous three-year Sinergia project, and before, there were two so-called Poly-projects, with funding from the ETH Zürich, that has supported the main research theme of the observatory:

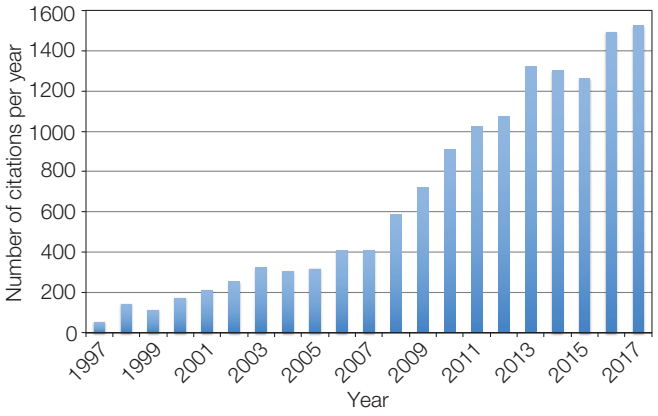

Figure 1. Number of annual citations to articles including an author with a PMOD/WRC affiliation. In April 2018, there were 14655 citations to 618 articles included in Thomson Reuter's Web of Science. The articles were selected using the search criteria address = (World Rad C*) OR (PMOD* NOT PMOD Technol* OR pmodak) OR (Phys* Met* Obs*).*

Quantifying the influence of the Sun on the terrestrial climate with all its aspects, starting with reconstruction of the historical variations of the solar irradiance to quantifying all possible interactions in the terrestrial atmosphere. About 18 years after the start of this project series, we have answered many questions and our understanding of the Sun-Earth connection has improved substantially.

Our results have been noted by the international community as can be concluded from the number of published papers and the citations they are receiving. However, the process is not yet understood in its full complexity and, as is always the case, our research has also created more new questions, which we are addressing in follow-up research projects, as outlined in the following pages of this annual report.

The institute's infrastructure and most of its overheads are paid for by the operational service of the World Radiation Center. We are especially proud of the fact that at the PMOD/WRC, the Center's services are based on research that is state-of-the-art in the respective fields. This is the best way to provide a service as it is common wisdom that tasks are only accomplished with excellence when based on genuine interest and curiosity.

The publications of the WRC sections are essential proof of this philosophy. Figure 1 statistically illustrates the good research reputation that PMOD/WRC staff have as well as the interest of the science community in results published by the institute. Nevertheless, it is fundamentally important that research connected to the calibration activities is conducted because only through active research can we strive to be a leading radiation calibration institute.

Solar Reference Spectrum

Margit Haberreiter and Werner Schmutz in collaboration with NPL (UK)

Currently, a number of Top-Of-the-Atmosphere (TOA) Solar Spectral Irradiance (SSI) datasets exist. To avoid systematic uncertainties in their applications, the Earth observing community has expressed the need for a recommended high-resolution solar reference spectrum.

We propose a new TOA SSI irradiance spectrum based on the following elements:

- The high-resolution component comes from synthetic spectra calculated with the radiative transfer code, NESSY, developed at PMOD/WRC (Haberreiter et al., 2008; Tagirov et al., 2017).
- The absolute scale is determined using the 2008 annual mean of the latest observational SSI composite (Haberreiter et al., 2017). This composite also takes into account the ATLAS3 observations by Thuillier et al. (2004). In addition, its integral is in agreement with the latest TSI value recommended by the IAU 2015 Resolution B3 (Prsa et al., 2016).

These elements guarantee that the correct absolute scale as well as the high-resolution information of the spectrum are within the uncertainty of the observations. The nominal solar luminosity and the nominal effective temperature are then further derived from the above-mentioned values. As such, the research activities at PMOD/WRC in solar physics and solar metrology have had a substantial impact on the IAU 2015 Resolution. IAU recommends using these values in all astronomical applications when stellar parameters are reported with respect to solar parameters as well as the corresponding SI units.

Figure 1 shows the un-scaled high-resolution spectrum calculated with the NESSY code in black and the 1-nm smoothed NESSY spectrum in red, both for the wavelength range from

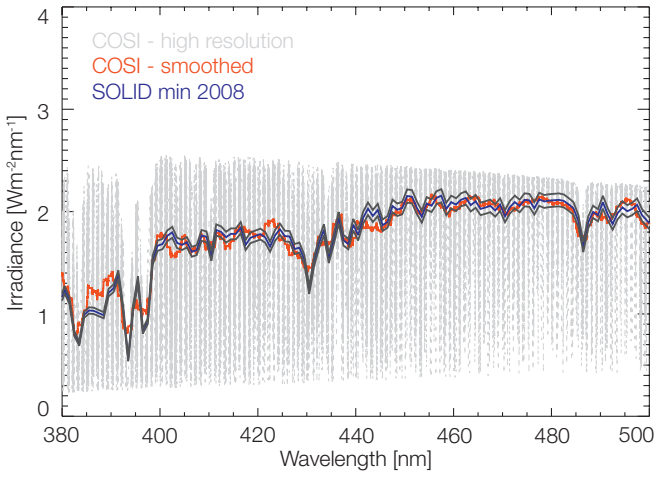

Figure 1. Calculated NESSY spectrum in high-resolution (black), the 1-nm smoothed NESSY spectrum (red) and the 2008 annual mean spectrum based on the SOLID observational SSI composite (blue).

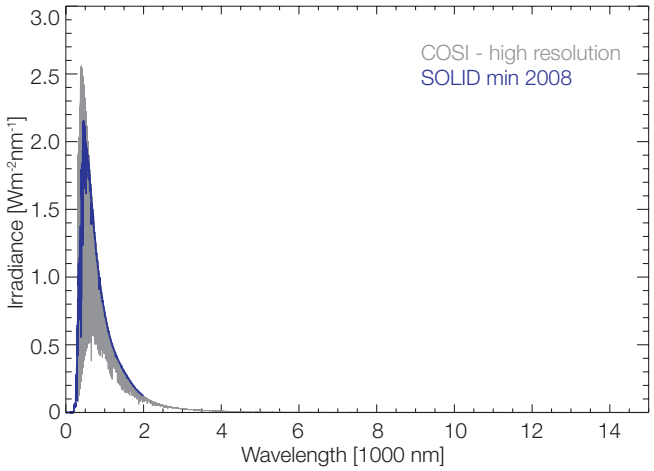

Figure 2. Same as Figure 1 except for the wavelength range from 380 nm to 15 µm.

380 nm to 500 nm. For comparison, the 2008 annual mean solar minimum spectrum that serves as the absolute scale for the high-resolution spectrum is shown in blue. Figure 2 then shows the complete set of the reference spectrum from 380 nm to 15 µm.

Details about the SOLID SSI composite can be found here (http://projects.pmodwrc.ch/solid/index.php/main-database). This reference spectrum is recommended by the CEOS Working Group on Calibration and Validation (CEOS WGCV), particularly the Infrared and Visible Optical Sensors Subgroup. Details can be found under the following links:

http://calvalportal.ceos.org/ceos-wgcv/ivos
http://ceos.org/ourwork/workinggroups/wgcv/subgroups/ivos

Currently, the detailed effect of the magnetic field on the solar spectrum is being investigated in collaboration with the ISSI International Team in a study called "Towards New Models of Solar Spectral Irradiance based on 3D MHD Simulations".

Acknowledgement: This work has been gratefully supported by D. Karbacher.

References:

Haberreiter M. et al.: 2008, Astron. Astrophys., 492, 833–840, doi: 10.1051/0004-6361:200809503.

Haberreiter M. et al.: 2017, J. Geophys. Res., 122, doi: 10.1002/2016JA023492.

Haberreiter M., Fox N., Schmutz W.: 2018, The CEOS solar reference spectrum, in preparation.

Prsa A. et al.: 2016, Astron. J. 152, id. 41, doi: 10.3847/0004-6256/152/2/41.

Tagirov R. et al.: 2017, Astron. Astrophys., 603, A27, doi: 10.1051//0004-6361/291628574.

Thuillier G. et al.: 2004, Adv. Space Res., 34, 256–261, doi:10.1016/j.asr.2002.12.004.

Contributions of Natural and Anthropogenic Forcing to the Early 20th Century Warming

Eugene Rozanov and Werner Schmutz in collaboration with IAC ETHZ (Switzerland)

In the framework of the FUPSOL project, we studied the influence of natural and anthropogenic factors on the ozone layer and climate evolution during the first half of the 20th century. We demonstrated that greenhouse gases are responsible for two thirds of the simulated 0.3 K global and annual mean surface warming, while one third is attributed to solar VIS and IR irradiance. The model underestimates the observed (0.4–0.5 K) terrestrial warming which hints at the possibility of a larger value than the applied solar forcing. The ozone response is driven by solar UV irradiance.

The observed early 20th century warming (1910–1940) is one of the most intriguing climate anomalies of the recent past. Several explanations of this warming, involving different combinations of natural and anthropogenic factors, have been suggested (e.g., Yamanouchi et al., 2011), but up to now the dominant process has not been established.

To investigate the contributions of natural and anthropogenic factors to the surface temperature increase, we performed a reference run and seven model experiments using the chemistry-climate model with an interactive ocean, SOCOL-MPIOM (Muthers et al., 2014). In the reference run, we applied all known climate drivers obtained from observations or reconstructed from proxies. For the experimental runs, we switched off one-by-one the following: the variability of energetic particle precipitation (PAR), solar UV irradiance (UV), solar visible and infrared irradiance (VIS), well-mixed greenhouse gases (GHG), tropospheric ozone precursors (OPR) and stratospheric aerosol (VOL).

The annual mean temperature trend (K/30 years) for the 1910–1940 period from the reference run with all considered forcing switched on is shown in Figure 1. The model simulates warming almost everywhere with maxima occurring over Central and Eastern Europe, Alaska, Australia, Northern Africa and Antarctica.

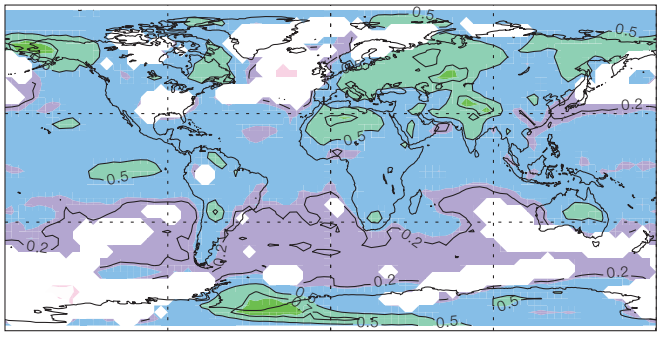

Figure 1. Annual mean temperature trend (K/30 years) for the 1910–1940 period from the reference run with all considered forcing switched on.

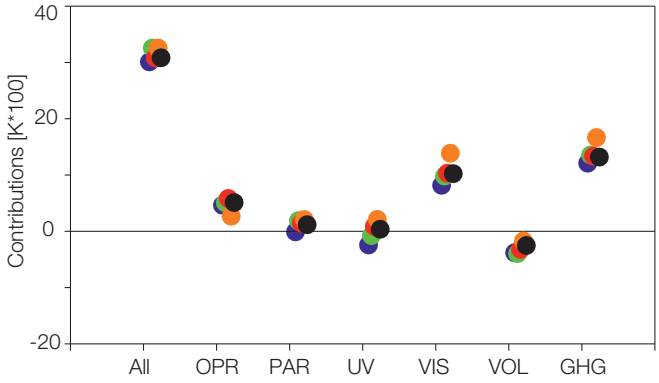

Figure 2. Global and seasonal mean temperature trend (K/30 years) for the period 1910–1940 from the reference run (All) and the contribution of different forcing. Black, blue, green, red and orange colours represent annual, boreal winter, spring, summer and autumn means.

The global mean, annual and seasonal mean values as well as the contribution from all considered forcings are shown in Figure 2. Model results suggest only 0.3 K warming on an annual mean global basis during the investigated period which is smaller than the observed trend by about 30%. Figure 2 shows that the main contributors are increases in well-mixed greenhouse gases (GHG, ~50%), deep penetrating solar irradiance (VIS, ~35%) and tropospheric ozone (OPR, ~15%). The other considered forcings (heavily absorbed UV, energetic particles and volcanic eruptions) do not significantly contribute to the annual and global mean warming.

On a regional scale, the warming in Europe in the first half of the 20th Century, is found to be driven by the increase in ozone precursor emissions. Because the GHG behaviour is well-constrained by observations and the solar forcing taken from Shapiro et al. (2011) has rather large uncertainties, better agreement with observations probably requires larger solar forcing or a search for as yet unknown additional climate drivers.

References:

Muthers S. et al.: 2014, The coupled atmosphere–chemistry–ocean model SOCOL-MPIOM, Geosci. Model Dev., 7, 2157–2179, doi:10.5194/gmd-7-2157-2014.

Shapiro A. I. et al.: 2011, A new approach to the long-term reconstruction of the solar irradiance leads to large historical solar forcing, Astron. Astrophys., 529, A67, doi: 10.1051/0004-6361/201016173.

Yamanouchi T.: 2011, Early 20th century warming in the Arctic: A review, Polar Sci., 5, 53–71, doi:10.1016/j.polar.2010.10.002.

Quantification of Solar Irradiance Forcing by Combining Climate and Phenological Models

Tatiana Egorova, Werner Schmutz, Timofei Sukhodolov, and Eugene Rozanov

The long-term time-series of the day of cherry blossoming in Kyoto, Japan, exhibits a substantial warming during the transition period from low solar activity to enhanced activity at the end of the Maunder Minimum. In an attempt to attribute this effect, we performed 100-year long runs of the MPI-Met Earth System Model (ESM) covering the period 1650–1750. The model is driven by the solar forcing reconstructed by Egorova et al. (2018). The simulations yield a substantial (around 0.5°C) surface warming in April during the first half of the 18th century which is comparable to the magnitude of the observed warming. However, the model failed to reproduce the warming in March.

One of the most promising proxies for a cold temperature anomaly in the late 17th and early 18th century, the so called Little Ice Age, is the date of cherry blossom in Japan which has an excellent historical coverage back to about 1500 and is closely related to climate, thus allowing local climate changes over the past 400 years to be assessed.

Figure 1 illustrates the close relationship between the derived surface temperature in Kyoto and Tokyo (e.g., Aono, 2015) and total solar irradiance reconstructed by Egorova et al. (2018). The average of the March temperatures of Kyoto and Edo matches the shape of the reconstructed solar irradiance very well between 1650 and 1850. The correlation between the two curves is strongly suggestive of a connection between the two time-series, implying that the relation is caused by the solar influence on the terrestrial climate.

In this project, we used the Earth System Model developed at the Max-Plank Institute for Meteorology in Hamburg, Germany (MPI-ESM). We performed 100-year long simulations (1650–1750) driven by evolving solar irradiance (Egorova et al., 2018) and analysed spring temperatures over Kyoto.

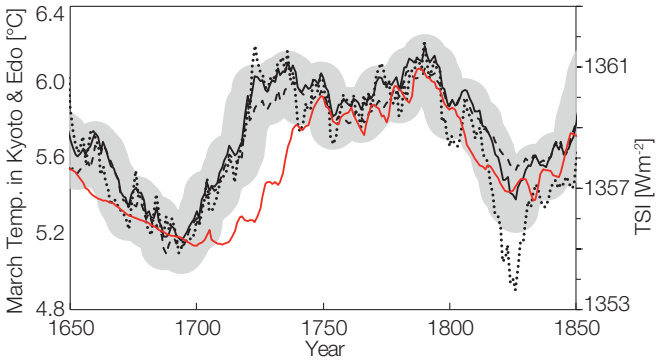

Figure 1. Mean March temperatures at Kyoto and Edo (Tokyo), Japan (black line and grey shaded area), derived from the date of cherry blossoming by Aono and Kazui (2008, dotted line) and Aono (2015, dashed line) compared to TSI reconstructed by Egorova et al. (2018) (red line).

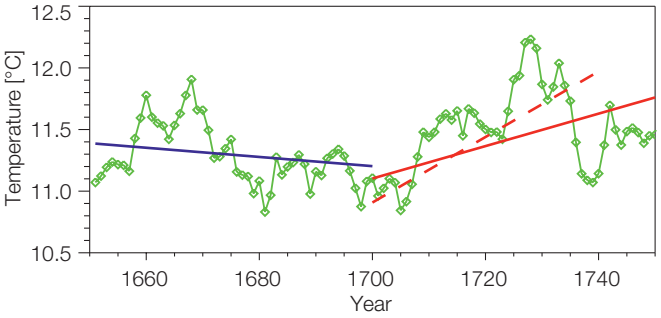

Figure 2. Surface temperature (°C) over Kyoto in April (green) simulated with MPI-ESM and smoothed with an 11-year window. Linear fits are plotted in blue for 1650–1700 and in red for 1700–1750 (solid line) and 1700–1740 (dashed line).

Figure 2 illustrates the evolution of the April mean surface temperature during the simulation period in Kyoto, and linear fits for three different periods. During the last half of the 17th century, there is a cooling tendency related to the decline of solar activity (see Figure 1). After 1700, the temperature tends to increase in agreement with the TSI enhancement. The March temperature does not reveal any significant trends. The magnitude of the April warming during the recovery from the period of extremely low solar activity is about 0.5–0.7°C, depending on the chosen period. This difference is explained by the appearance of local extremes caused by the ENSO-like ocean variability and can be avoided if a larger number of runs for the ensemble simulation is used. Another problem is the absence of interactive chemistry in the version of the used model which could lead to problems with March temperatures.

Therefore, further progress requires the use of ensemble model runs and coupling to interactive chemistry, to activate the top-down mechanism of the influence of solar irradiance on climate. It will allow the magnitude of the warming to be established, and prepare the model for the coupling with a phenology model to describe the chain of processes from solar variability to the day of cherry blossoming.

References:

Aono Y., Kazui K.: 2008, Phenological data series of cherry tree flowering in Kyoto, Japan, and its application to reconstruction of springtime temperatures since the 9th century, Int. J. Climatol. 28, 905, doi: 10.1002/joc.1594, 2008.

Aono Y.: 2015, Cherry blossom phenological data since the seventeenth century for Edo (Tokyo), Japan, and their application to estimation of March temperatures, Int. J. Biometeorol. 59, 427, doi: 10.1007/s00484-014-0854-0.

Egorova et al.: 2018, Revised historical solar forcing using updated model and proxy data, Astron. Astrophys., in press, doi.org/10.1051/0004-6361/201731199.

Prediction of Sudden Stratospheric Warming Events with the Chemistry-Climate Model, SOCOL

Eugene Rozanov in collaboration with the Central Aerological Observatory (Russia)

In the framework of our collaboration with the Central Aerological Observatory (CAO; Russia) we evaluated the possibility of predicting Sudden Stratospheric Warming events (SSW) using the Chemistry-Climate Model (CCM), SOCOL, in the specified dynamics mode, assimilating observed meteorological data.

The purpose of this experiment with CCM SOCOLv3 (Stenke et al., 2013) was to assess the feasibility of using this model for short-term forecasts of the thermodynamic parameters and chemical composition of the middle atmosphere. Accurate reproduction of the short-term atmosphere variability by models is impossible without the assimilation of meteorological observations. In our experiments, CCM SOCOL assimilates three thermodynamic parameters: the atmospheric temperature, divergence and vorticity of the wind field according to 6-hourly Japanese Meteorological Agency (JMA) reanalysis data, available at 60 hybrid model levels from the surface to 60 km in altitude with a high spatial resolution (approximately 0.56°x0.56°).

In order to evaluate the predictive capabilities of the model, it is necessary to find out the time period when the calculated values of the parameters will begin to deviate significantly from the observational data, after the model is switched to free running mode without nudging. As a test experiment, we chose sudden stratospheric warming (SSW) events, which cannot normally be reproduced with a free running model. The classic features of a major SSW are: (i) a strong and sudden (several tens of degrees over several days) temperature increase in the stratosphere of the polar and subpolar zones, and (ii) a change in the direction of the 10 hPa zonal wind from westerly to easterly at 60ºN (circulation reversal). In total, eight such events were simulated from 2000 to 2010.

Each experiment consisted of three runs of the model switching off the data assimilation process at 4, 8, and 12 days before the event to evaluate the predictive capabilities of the model and one run with continuous nudging to assess the effectiveness of the nudging procedure itself. The simulated temperature and wind were compared with the ERA-Interim reanalysis data set.

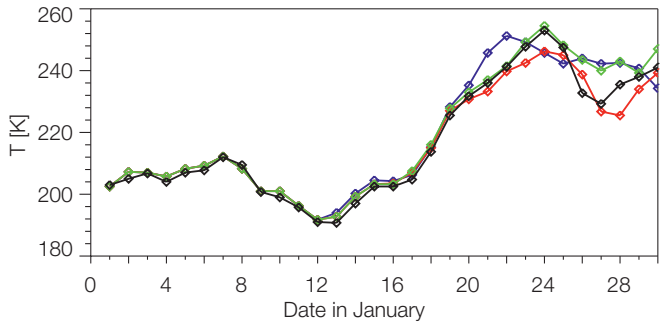

Figure 1. Temperature at 10 hPa over the Plesetsk site during the stratospheric warming event. The simulated data are shown by the red, blue and green lines which represent the cases when nudging was stopped 12 (blue), 8 (red) and 4 (green) days, respectively, before the event on 24 January. The reanalysis data are shown by the black line.

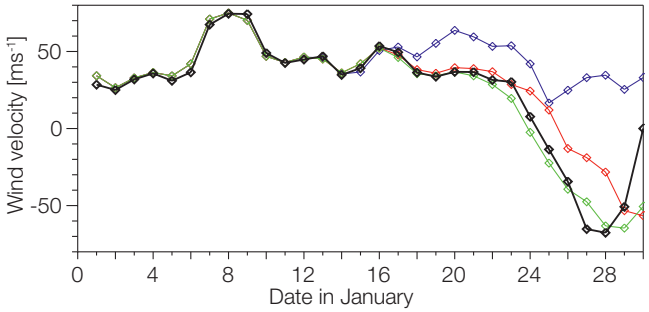

Figure 2. Zonal wind velocities, otherwise same as Figure 1.

Figures 1 and 2 illustrate the results of one particular SSW simulation in January 2009 over the Plesetsk rocket launch site. The results of model experiments showed that the temperature behaviour is adequately predicted by the model for at least a week in advance for all the events studied. Wind velocities can be robustly predicted four days in advance. In some cases it can be predicted for a longer period, but no more than a week ahead. One of the reasons for the instability of wind predictability is the accumulation of the interpolation errors in the applied nudging process. In the reanalysis database which is used for the data assimilation procedure, the values of the horizontal wind components are given. For the model calculations, they must be converted to the divergence and vorticity of the wind field. After performing the calculations, the divergence and vorticity of the wind components are reversed.

Repeated use of this sequence can lead to degradation of the quality of the prediction through accumulation of numerical noise. One way to avoid this is to use divergence and vorticity directly from the meteorological reanalysis. Successful prediction of the circulation and temperature allows the assumption that the chemical fields such as total column ozone can also be accurately predicted up to one week in advance. The study of this possibility is ongoing.

References: Stenke A., Schraner M., Rozanov E., Egorova T., Luo B., Peter T.: 2013, The SOCOL version 3.0 chemistry-climate model: description, evaluation, and implications from an advanced transport algorithm, Geosci. Model Dev., 6, 1407–1427, doi:10.5194/gmd-6-1407-2013.

Atmospheric Impacts of the Strongest Known Solar Particle Storm of 775 AD

Timofei Sukhodolov, Eugene Rozanov, Werner Schmutz, and William Ball in collaboration with IAC ETHZ (Switzerland) and University of Oulu (Finland)

Sporadic Solar Energetic Particle (SEP) events affect the Earth's atmosphere and environment through depletion of the ozone layer. The greatest SEP storm known for the last 11 millennia occurred in 774–775 AD, serving as a likely worst-case scenario. In this study, we present a systematic analysis of the impact such an extreme event can have on the Earth's atmosphere using our chemistry climate model, SOCOLv3, driven by ionisation rates calculated with the cosmic ray cascade model, CRAC:CRII.

Typically, HO_x and NO_x production during SEP events leads to additional ozone depletion followed by a decrease in temperature. This temperature anomaly then modulates the Polar-Night Jet Oscillation (PJO) and creates a positive and, later, a negative wind anomaly both propagating down. The overall impact is stronger in the winter hemisphere because of air isolation by the polar vortex and the fact that coupling between the polar stratosphere and troposphere is the strongest during winter.

Figure 1a-d illustrates all these effects for the event in 775 AD as a difference in northern polar NO_x, ozone, temperature and zonal wind between the modelling runs with and without the event in ionisation rates. Further propagation of the anomaly down to the troposphere is described by the so-called "top-down mechanism", which results in the modulation of the tropospheric circulation with local weather consequences. In accordance with this, the model suggests that monthly mean near-ground land temperatures differ by up to 4 K (Figure 1e-f) between the ensemble runs with and without the event. For December 774 AD, the model yields an acceleration of the tropospheric mean flow in the northern hemisphere and thus a more pronounced meridional circulation causing warming over Siberia. Conversely for January 774 AD, the model predicts more significant (orange contour) cooling in Siberia, Europe and Canada caused by the negative stratospheric zonal mean wind anomaly.

Thus, we showed that such a severe event can perturb the polar stratosphere for at least one year, leading to regional changes in the surface temperature during northern hemisphere winters. More details can be found in a recently published paper by Sukhodolov et al. (2017).

References: Sukhodolov T. et al.: 2017, Atmospheric impacts of the strongest known solar particle storm of 775 AD, Nature Scientific Reports, 7, 45257-45257, doi: 10.1038/srep45257.

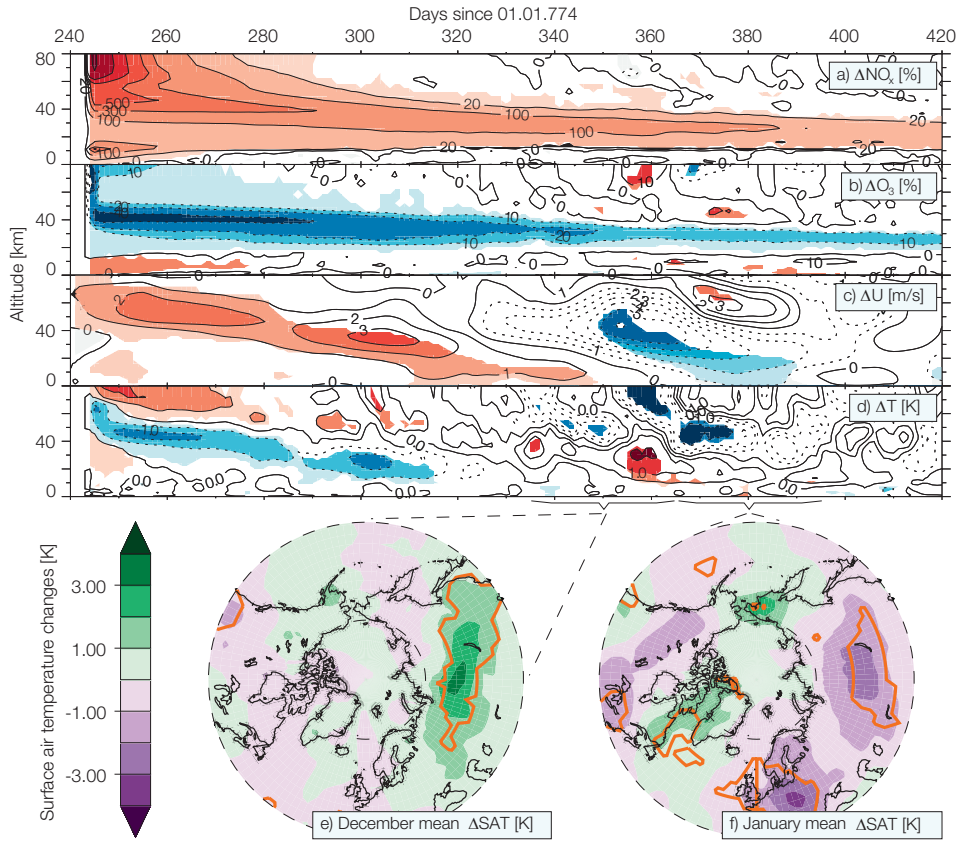

Figure 1. Atmospheric effects due to the SEP event on 1 Sept. 774 (day 244). Panels a) to d): NO_x, O_3, zonal wind (U) and temperature (T) anomalies, respectively, averaged over the northern polar region (70–90°N for NO_x, O_3 and T and 50°–70°N for U) and averaged over all 30 ensemble members. Zonal wind changes are shown as 20-day running means. Coloured areas are significant at a 95% confidence level. Panels e) and f): Monthly mean surface air temperature (SAT) changes (K) in December 774 AD and January 775 AD due to the event. The orange contours indicate significance at the 95% confidence level. Dashed lines mark the 40°N and 70°N latitudes. Figure credit: Nature Scientific Reports.

Further Improvement of the Coupled Aerosol-Chemistry-Climate Model, SOCOL-AER

Timofei Sukhodolov and Eugene Rozanov in collaboration with IAC ETHZ (Switzerland)

In the framework of the project VEC we have continued work on our main modelling tool, the aerosol-chemistry-climate model (ACCM) SOCOL-AER. We have improved the treatment of water uptake by sulphate aerosol particles, aerosol mass conservation, and wet and dry deposition schemes, as well as revised the sulphur emissions. Overall, this led to a better representation of tropospheric sulphate, while maintaining a good agreement with recently revised stratospheric observations.

The performance of SOCOL-AER was documented for background (Sheng et al., 2015) and high aerosol loading conditions (Sukhodolov et al., 2018). The model showed very good performance in reproducing the stratospheric aerosol evolution. Detailed information about processes contributing to the background aerosol layer, presented in Sheng et al. (2015), has been used as a reference by many observational and modelling groups in the international aerosol community for several years. Good representation of the stratospheric volcanic cloud was also confirmed by a recent model intercomparison study by Marshall et al. (2018). However, that study also revealed clear problems in how SOCOL-AER treats tropospheric removal of the sulphate aerosols. In addition, recently revised stratospheric observations provided new stratospheric aerosol burden dataset. All this motivated us to look for further upgrades of our model.

Compared to the version used in all recent publications, we have now improved the treatment of water uptake by sulphate aerosol particles, corrected the aerosol mass conservation, revised the sulphur natural and anthropogenic emissions, and significantly improved dry and wet deposition schemes. To illustrate the model improvements, we compare 2000–2002 mean sulphur wet deposition from two versions of the model with observations compiled by Vet et al. (2014).

Figure 1 shows that the previous model version, which used a constant wet deposition lifetime, overestimates sulphur wet deposition in dry regions (e.g. southwestern USA) and underestimates the deposition in wetter regions. The updated model version, with an interactive wet deposition scheme based on Henry's law equilibrium constants for wet scavenging of gases and radius-dependent calculation of nucleation and impaction scavenging for wet removal of aerosols, falls closer to the observations, and reveals a higher R2 value than the older model version. Publication discussing this and other recent improvements in detail is now in preparation.

References: Marshall L. et al.: 2018, Atmos. Chem. Phys., 18, 2307–2328, doi: 10.5194/acp-18-2307-2018.

Sheng J.-X. et al.: 2015, J. Geophys. Res. Atmos., 30 120, 2014JD021 985, doi: 10.1002/2014JD021985.

Sukhodolov T. et al.: 2018, Geosci. Model Dev. Discuss., doi: 10.5194/gmd-2017-326.

Vet R. et al.: 2014, Atmos. Environ., 93, 3–100.

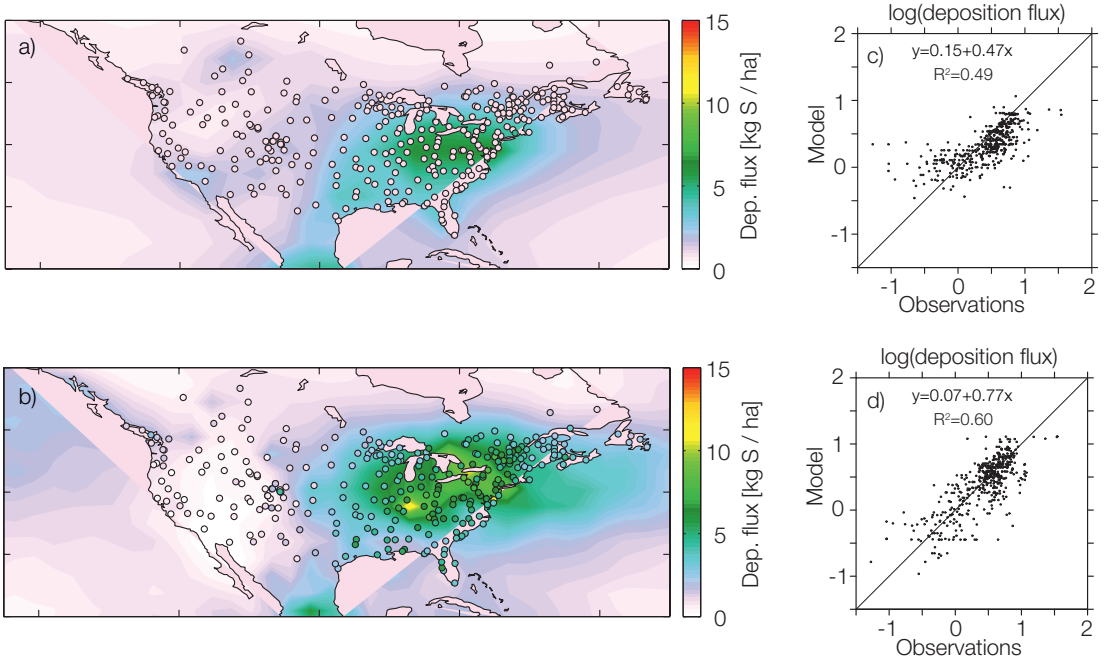

Figure 1. Mean sulphur wet deposition for the 2000–2002 period from the model calculations and from the station observations compiled by Vet et al. (2014). Panels a) and b) compare SOCOL-AER (background contours) with North American station observations (filled circles) for the Sheng et al. (2015) and updated model versions, respectively. Panels c) and d) show log-log scatterplots of the modelled and observed sulphur wet deposition at all stations in the Vet al. (2014) assessment.

Comparison of the Observed and Simulated Influence of the Solar Irradiance Variability on the Atmosphere

Eugene Rozanov in collaboration with Prague Univ. (Poland), IAC ETHZ (Switzerland), SOLARIS-HEPPA WG3 members and PIs of all participating in IGAC/SPARC CCMI models

In the framework of Working Group 3 of the SPARC core project SOLARIS-HEPPA, we compared the observed solar signal resulting from solar irradiance forcing against the results of specified dynamics experiments performed as part of the IGAC/SPARC CCMI activity.

Past studies have identified disagreement between chemistry-climate models (CCM) and satellite data in the characterisation of the atmospheric response to solar irradiance variability. One possible cause could be related to CCM biases in the simulation of atmospheric circulation and temperature. The IGAC/SPARC CCMI-1 activity provides a novel resource to investigate this problem using simulations with meteorology nudged towards reanalysis fields. Within this framework, we compared the simulated atmospheric response to spectral solar irradiance with the reanalysis products used for the model nudging and satellite measurements.

Figure 1 illustrates the tropical mean temperature response to solar irradiance decadal scale variability obtained using multivariate linear regression analysis (e.g., Kuchar et al., 2017) of the REF-C1SD results and ERA-Interim reanalysis. All models simulate a double peak structure of the temperature response with two warming spots in the lower and upper stratosphere. The lower stratosphere warming is not of solar origin (Kuchar et al., 2017) while the solar influence in the upper stratosphere has been robustly attributed to the heating by enhanced solar irradiance. Even though all considered models assimilated ERA-Interim

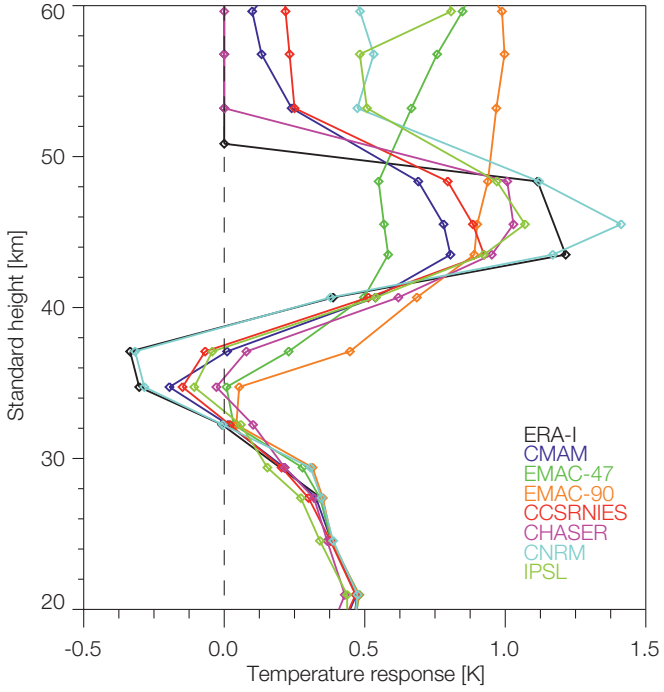

Figure 1. The tropical mean temperature responses to solar cycle extracted from the results of REF-C1SD runs with models nudged to ERA-I meteorology.

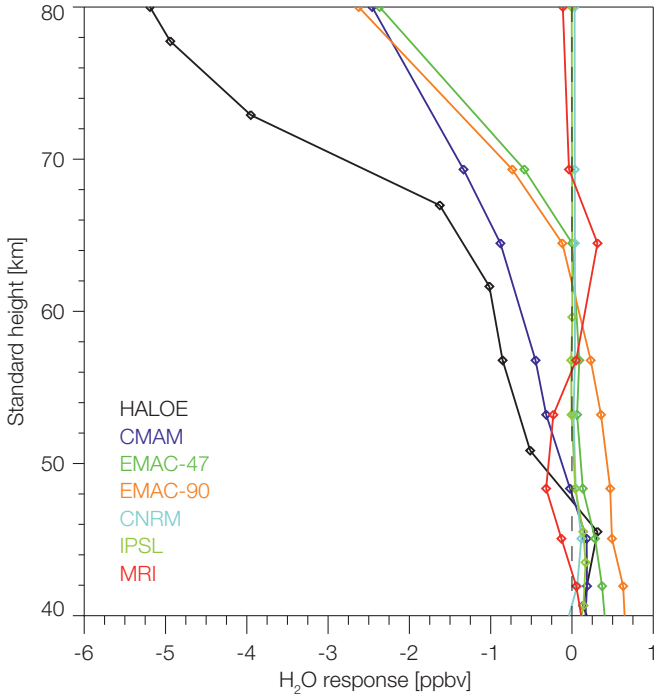

Figure 2. The tropical mean water vapour responses to the solar cycle extracted from the results of REF-C1SD runs.

temperature, the solar response is not the same for all models above 30 km. Most models except EMAC reproduce sharp warming around 50 km, but the magnitude of the warming varies from 0.7 K (CMAM model) to 1.4 K (CNRM model). The disagreement between models increases in the mesosphere where the temperature response varies from 0.2 to 1 K. This problem can be related to the absence of any assimilation above 60 km as well as to the different response of O_3 and H_2O in this layer.

Figure 2 illustrates the tropical H_2O simulated and observed response to solar irradiance variability. A pronounced negative response extracted from HALOE data is partially reproduced only by three models above 70 km and only CMAM from 50 to 65 km. This problem has potential implications for the ozone and temperature response in the mesosphere and is most probably related to the treatment of H_2O photolysis by solar irradiance in the Lyman-alpha and Schumann-Runge band (e.g., Sukhodolov et al., 2016).

The analysis of zonal wind, ozone and some other species are on-going. All participating models are described in Morgenstern et al. (2017).

References: Kuchar A. et al.: 2017, 122, 9076–9093, doi:10.1002/2017JD026948.

Morgenstern, O. et al.: 2017, Geosci. Model Dev., 10, 639-671, doi: 10.5194/gmd-10-639-2017.

Sukhodolov T. et al.: 2016, J. Geophys. Res. Atmos., 121, doi:10.1002/ 2015JD024277.

Study to Determine Spectral Solar Irradiance and its Impact on the Middle Atmosphere (SIMA)

William Ball, Eugene Rozanov, and Werner Schmutz in collaboration with multiple international partners

The SIMA project aims to use stratospheric ozone and temperature observations as a detector, and our integrated physical knowledge encapsulated within chemistry climate models to estimate top-of-atmosphere irradiance changes required to force the variability observed in the atmosphere.

The project requires accurate estimates of the solar cycle changes in the upper stratosphere from ozone observations. However, when solar cycle ozone changes are estimated from the multiple available ozone composites spanning several decades, different magnitudes are found which leads to high uncertainty in the incoming solar irradiance.

In order to make progress, we set about resolving the differences between the composites, developing new techniques and algorithms (Ball et al., 2017a) to achieve this. This has now led to a suite of new ozone composites that account for jumps, drifts and sampling issues in the data. These composites are known as the BAyeSian Integrated and Consolidated (BASIC) ozone composites.

As a consequence of this work, we are confidently able to show that there is a recovery underway in the upper stratosphere (Figure 1) as a result of the Montreal Protocol, and that there is no post-1998 hemispheric asymmetry in hemispheric ozone trend profiles which was a question raised in the most recent WMO 2014 ozone assessment report. The results and composite will be included in the forthcoming SPARC LOTUS (Stratosphere-Troposphere Processes and Their Role in Climate) report on uncertainties in long-term ozone trends.

A second major outcome has been the detection of a decline in the lower stratosphere that is offsetting the recovery in the upper stratosphere. The implication is that, between 60°N and 60°S, the ozone layer may not be recovering as anticipated from chemistry climate model projections (Figure 2).

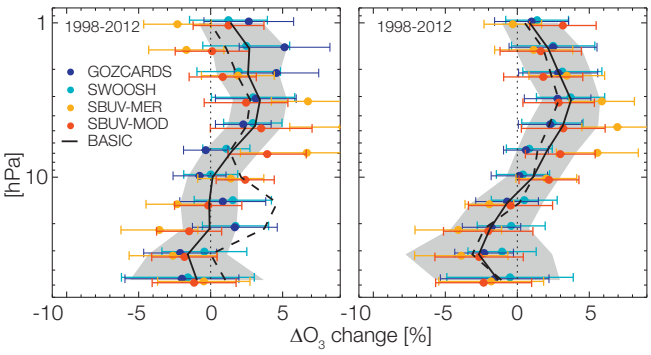

Figure 1. The 1998–2012 changes in ozone in the Northern (left) and Southern (right) hemispheres. The BASIC result, using dynamical linear modelling to estimate changes, is the solid black line with grey shading representing uncertainties. Figure from Ball et al. (2017), copyright EGU.

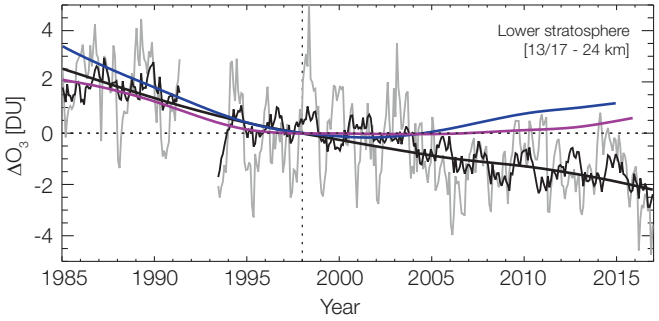

Figure 2. Integrated lower stratospheric ozone changes (1998–2016). Observed (black/grey), SOCOL-model (purple), WACCM-model (blue). Figure from Ball et al. (2018a), copyright EGU.

Currently, the cause is not understood and it is now a major question for the scientific community to address. The press release in February 2018 of the publication by Ball et al. (2018a) received world-wide press attention. The effort to correct the ozone data was essential for the SIMA project, but has also led to major insights into the ozone layer, and is spurring new research into lower stratospheric variability.

We have accounted for artefacts in the ozone data and now have arguably the most advanced and accurate ozone composite currently available. Our initial results show a high agreement in solar cycle ozone changes in the upper stratosphere with respect to models in specified dynamics mode (Ball et al., 2018b). We are therefore now in a position to estimate the Spectral Solar Irradiance (SSI) from changes in ozone and temperature.

References:

Ball W. T., Alsing J., Mortlock D. J., Rozanov E. V., Tummon F. Haigh J. D.: 2017, Reconciling differences in stratospheric ozone composites, Atmos. Chem. Phys., 17, 12269–12302.

Ball W. T. et al.: 2018a, Evidence for a continuous decline in lower stratospheric ozone offsetting ozone layer recovery, Atmos. Chem. Phys., 18, 1379–1394.

Ball W. T. et al.: 2018b, in prep., Estimate of ultraviolet solar cycle changes from stratospheric ozone and temperature observations.

Study of the Interplanetary Magnetic Field Variability Influence on Surface Pressure over High Latitudes

Eugene Rozanov in collaboration with SpbSU (Russia)

In the framework of the European COST CA-15211 Action, "Atmospheric Electricity Network: coupling with the Earth System, climate and biological systems", we studied possible connection between the B_y component of interplanetary magnetic field (IMF), clouds and surface pressure over the high latitude zone. We demonstrated that the observed influence of the IMF variability can be partially reproduced by the chemistry-climate model if a dependence of the cold droplets growth efficiency on the IMF is introduced.

The Earth system is sensitive to different external forcings such as solar irradiance, solar wind, galactic cosmic rays, supernova explosions, passage through interstellar dust or galactic shoulders, etc. Traditionally, only solar irradiance variability has been included in pure climate models. Energetic particles have recently attracted some attention, but they are not yet recognised as a major climate driver by the science community. The role played by interplanetary magnetic field (IMF) disturbances is even less understood. It was pointed out in several recent papers (e.g., Lam and Tinsley, 2016) that IMF variability can directly influence polar ionospheric potential, resulting in changes of the surface pressure, tropospheric geopotential height and temperature. The physical mechanism behind this relationship has not yet been established.

One hypothesis is related to the influence of electrical charge on cloud microphysics. Harrison et al. (2015) have demonstrated that the probability of the confluence of cloud droplets is higher in electrified clouds, leading to faster formation of rain droplets. In climate models, this process is parameterised and its efficiency depends on the autoconversion rate (A_c). In this work, we attempt to introduce the dependence of A_c on IMF variability in the chemistry-climate model (CCM), SOCOL. First of all, we compared model results for the standard and decreased (75%) value of A_c in order to check the model sensitivity to this process. The model shows an expected and substantial increase in cloud amount caused by slower formation of raindrops. The difference reaches 50% in the tropical area, but it is also observable over the Antarctic, reaching 50% in some locations.

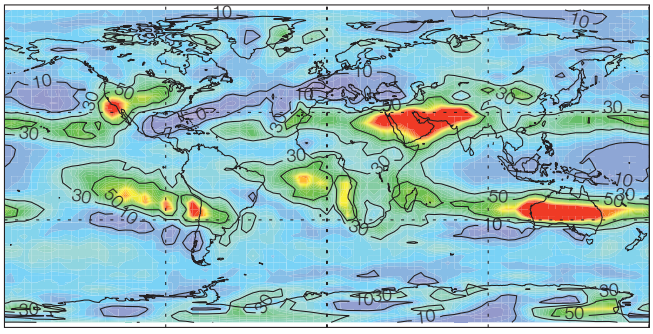

Figure 1. The increase in cloud amount (%) caused by a 75% decrease in the cloud autoconversion rates.

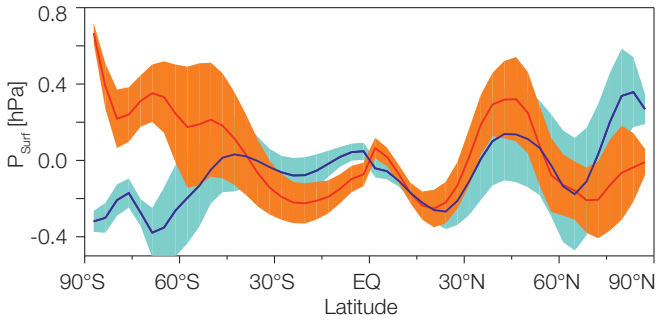

Figure 2. Surface pressure anomalies for days when the interplanetary magnetic field B_y component exceeds 3 nT (blue line) and when B_y is less than -3 nT (red line). The shading marks variability among ensemble members.

After this, we introduced a dependence on A_c from the observed variability of the IMF B_y component. Then we performed two 2-year long ensemble runs using a standard model configuration (reference run) and with switching on the dependence of A_c on B_y.

The resulting anomalies of surface pressure are shown in Figure 2 for different latitudes. The introduced mechanism significantly affects the surface pressure only over the polar regions where the troposphere is sensitive to cloud properties. These results agree with an analysis of observational data described by Lam et al. (2013), however the magnitude of the pressure anomalies is about 60% lower over the Southern hemisphere. Over the Northern hemisphere, both simulated and observed surface pressure anomalies are less pronounced. It should also be noted that the signs of the pressure anomalies differ from the observations. This can be related to the arbitrary choice of the influence of B_y on A_c. We assumed that positive B_y means that A_c increases, however, in reality the dependence can have the opposite sign. The analysis of other atmospheric parameters such as cloud cover, temperature and circulation response to B_y variability is ongoing.

References:

Harrison R. G., Nicoll K. A., Ambaum M. H. P.: 2015, On the microphysical effects of observed cloud edge charging, Q. J. R. Meteorol. Soc., doi:10.1002/qj.2554.

Lam M., Chisham G., Freeman M. P.: 2013, The interplanetary magnetic field influences mid-latitude surface atmospheric pressure, Environ. Res. Lett., 8, 045001, doi:10.1088/1748-9326/8/4/045001.

Lam M., Tinsley B.: 2015, Solar wind-atmospheric electricity-cloud microphysics connections to weather and climate, J. Atmos. Solar-Terr. Phys., 149, 277–290, doi: 10.1016/j.jastp.2015.10.019.

Evaluation of the Arosa Total Ozone Representativeness for the Analysis of the Global Ozone Field

Eugene Rozanov, Luca Egli, and Julian Gröbner in collaboration with MeteoSwiss (Switzerland)

In the framework of the supported project INFO3RS, we evaluated the connection of the total column ozone (TOC) time-series simulated over Arosa and all other locations in the world. We have shown that annual mean Arosa TOC correlates well with other locations over the northern and southern middle latitudes. For the tropical area and high latitudes, the correlation is generally small. This opens the possibility of applying the conclusions based on TOC observations over Arosa to a much wider area.

The observations of TOC are required to trace expected future ozone recovery as well as to understand the ozone behaviour in the past. The INFO3RS project aims to develop a homogeneous TOC time-series for Arosa spanning the period from 1926 into the future. The availability of such long time-series for one place requires the representativeness of the Arosa TOC measurements to be evaluated with respect to global ozone. These tasks will be fulfilled using a simulation of the TOC evolution with a state-of-the-art chemistry climate model for various scenarios. Therefore, the time when the ozone recovery can be expected will be obtained by combining the data-set analysis, the corresponding observational uncertainties and calculations from models.

To quantify the representativeness of the Arosa measurements with respect to an evaluation of the global trend, we used the results from our chemistry-climate model (CCM), SOCOLv3, (Stenke et al., 2013) with runs performed in the framework of the IGAC/SPARC CCMI project. In the framework of this activity, we simulated the ozone layer and climate evolution during the 1960–2100 period using observed boundary conditions until 2009 and one subset of the recommended scenarios for the future (Morgenstern et al., 2017).

Using monthly mean model output, we calculated correlation coefficients between simulated monthly mean total ozone time-series (1960–2009) over Arosa and all other locations. The correlation maps for the annual and February mean values are shown in Figures 1 and 2, respectively. Annual mean TOC over

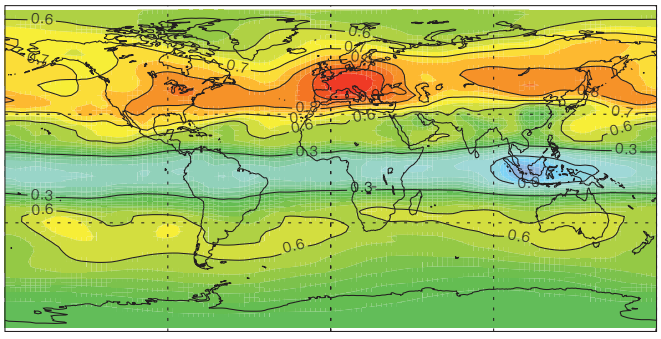

Figure 1. The correlation coefficient between the simulated annual mean total ozone time-series (1960–2009) over Arosa, using CCM SOCOLv3, and all other locations.

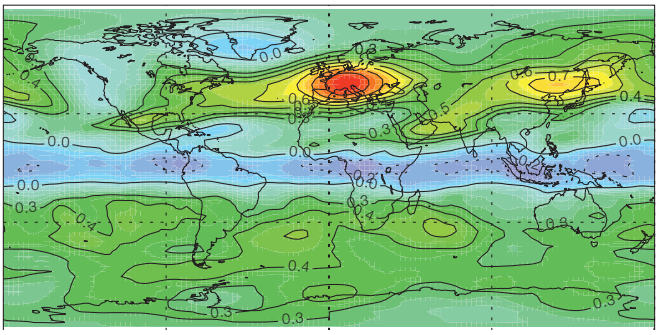

Figure 2. February mean values, otherwise same as in Figure 1.

Arosa correlates well (correlation coefficient $R>0.7$) with other locations over the Northern middle latitudes. The highest correlation ($R>0.8$) is observed over Europe, Eastern US and Eastern Russia. Weaker values ($R>0.6$) are found over the southern middle latitudes. The correlation with TOC over high and low latitudes is generally small, except for the maritime continent, where $R>0.6$. These results are related to the similarity of the ozone forming processes over middle latitudes, where the structure of atmospheric dynamics plays a dominate role. For the high latitudes, the chemistry contribution become more important and the differences in the environmental properties such as lower temperature as well as different gas and aerosol composition lead to different ozone behaviour.

The difference between middle and high latitudes is even more pronounced for February mean values. In this case, the correlation of the TOC field with Arosa remains high over Europe and East of Russia, while the correlation with the TOC inside the polar vortex disappears completely. This emphasises the difference between the processes defining ozone over the middle latitudes and inside the polar vortex. The correlation with the tropics and Southern hemisphere also decreases due to the seasonal dependence of transport and chemical processes in the case of an absence of the polar vortex and supressed meridional transport.

From this preliminary study, we can conclude that annual mean Arosa TOC values are only highly representative of the northern middle latitudes. On a monthly scale, regions with a high correlation are limited to Europe, US and part of Russia. A similar analysis using observations and models for other months is ongoing. The project INFO3RS is partially financed by a grant from the MeteoSwiss GAW-CH programme.

References: Morgenstern O. et al.: 2017, Review of the global models used within the Chemistry-Climate Model Initiative (CCMI), Geosci. Model Dev., 10, 639-671, doi: 10.5194/gmd-10-639-2017.

Stenke A. et al.: 2013, The SOCOL version 3.0 chemistry-climate model: description, evaluation, and implications from an advanced transport algorithm, Geosci. Model Dev., 6, 1407–1427, doi:10.5194/gmd-6-1407-2013.

Multi-Model Comparison of the Volcanic Sulphate Deposition After the 1815 Eruption of Mt. Tambora

Timofei Sukhodolov, Eugene Rozanov, and William Ball in collaboration with Univ. Leeds (UK) and VolMIP participants

As a part of the Model Intercomparison Project on the climatic response to Volcanic forcing (VolMIP), four state-of-the-art global aerosol models, including our model, SOCOL-AER, simulated the Mt. Tambora eruption in 1815 and compared the resulting sulphur deposition with ice core data. Overall, this study showed very high inter-model differences, which initiated further model inter-comparison activities in this direction. SOCOL-AER showed clear problems in simulating absolute values of the sulphate aerosol deposition, but also revealed the best agreement of the evolution of aerosol deposition with observations among participating models.

The eruption of Mt. Tambora in 1815 was the largest volcanic eruption of the past 500 years. The eruption had significant climatic impacts, leading to the "year without a summer" in 1816. The eruption also resulted in one of the strongest and most easily identifiable volcanic sulphate signals in polar ice cores, which are widely used to reconstruct the timing and atmospheric sulphate loading of past eruptions. We analysed the volcanic sulphate deposition in model simulations of this eruption using four state-of-the-art global aerosol models (CESM1(WACCM), MAECHAM5-HAM, SOCOL-AER and UM-UKCA) and compared the simulated deposited sulphate to a comprehensive array of ice core records.

Figure 1 shows the simulated area-mean volcanic sulphate deposition to the Antarctic and Greenland ice sheets over time, compared to the D4 and DIV2010 observational data sets with the highest temporal resolution and most precise dating. We find that deposition in both ice sheets peaks first in MAECHAM5-HAM, followed by SOCOL-AER, then UM-UKCA and CESM1(WACCM). The main phase of deposition recorded in both ice cores falls in time between that simulated by MAECHAM5-HAM and the other models. Compared to DIV2010 and D4, the deposition in MAECHAM5-HAM is too quick, but too slow in CESM1(WACCM) and UM-UKCA, although the main features are still relatively well-captured by all models. The onset and duration of deposition to the ice sheets simulated by SOCOL-AER is the closest to the data from both ice cores, suggesting a good representation of the stratospheric aerosol evolution, while the simulated deposition magnitude is too large due to a simplified deposition scheme.

Thus, the models differ substantially in their simulation of the Mt. Tambora volcanic sulphate deposition, with differences in the timing, spatial pattern and magnitude. Deposition is a result of the whole chain of the aerosol life cycle – formation, stratospheric transport, and the stratosphere-troposphere exchange with further quick removal. Therefore, differences in model resolution, modelled stratospheric winds, treatment of aerosol microphysics, sedimentation, and deposition schemes have all contributed to the range in model-simulated volcanic sulphate deposition.

A detailed analysis of the differences in sulphur chemistry and the aerosol formation and transport in each model will further help to interprete these results. Dedicated multi-model comparison projects with process-oriented comparisons, such as the Interactive Stratospheric Aerosol Modelling Intercomparison Project (ISA-MIP) (Timmreck et al., 2018), will be imperative to disentangle the reasons for model differences. Simulations of the next large-magnitude volcanic eruption in the frame of the Science Response Plan for the Next Volcanic Eruption with Major Impact on Climate (VolRES) will also enable additional model intercomparisons, the characterisation of important processes and further improvement of the models. The results of this study are presented and discussed in greater detail in a recent publication by Marshall et al. (2018).

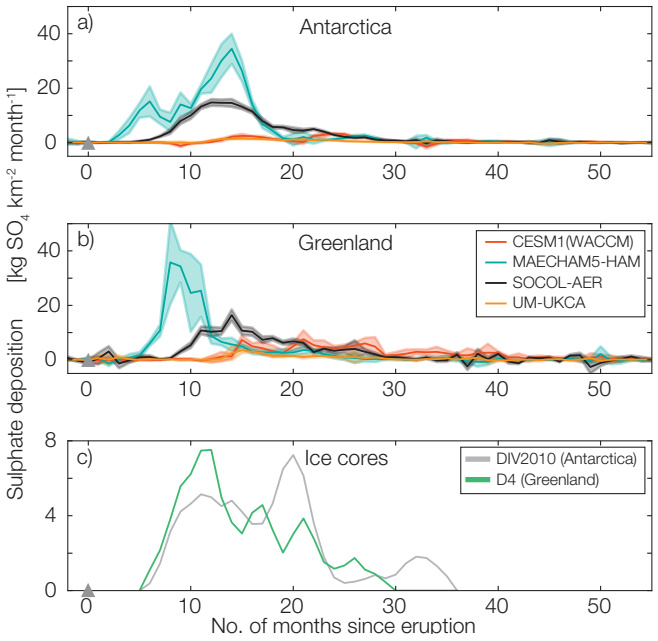

Figure 1. Simulated area-mean volcanic sulphate deposition ($kgSO_4$ km^{-2} $month^{-1}$) to: Panel a) the Antarctic ice sheet, and panel b) the Greenland ice sheet for each model (colours). Each ice sheet mean is defined by taking an area-weighted mean of the grid boxes in the appropriate regions once a land-sea mask has been applied. Solid lines mark the ensemble mean and shading is 1σ. Panel c): Deposition fluxes from two monthly-resolved ice cores (DIV2010 from Antarctica and D4 from Greenland). The scale is reduced in (c). The grey triangles mark the start of the eruption (1 April 1815). Figure credit: Atmos. Chem. Phys.

References:

Marshall L. et al.: 2018, Multi-model comparison of the volcanic sulfate deposition from the 1815 eruption of Mt. Tambora, Atmos. Chem. Phys., 18, 2307-2328, doi: 10.5194/acp-18-2307-2018.

Timmreck C. et al: The Interactive Stratospheric Aerosol Model Intercomparison Project (ISA-MIP): in review, 2018, Motivation and experimental design, Geosci. Model Dev. Discuss., doi: 10.5194/gmd-2017-308.

First Tests of a New Atmosphere-Ocean-Aerosol-Chemistry-Climate Earth System Model, SOCOLv4.0

Timofei Sukhodolov, Eugene Rozanov, and Tatiana Egorova in collaboration with IAC ETHZ (Switzerland)

Our group studies climate and ozone layer changes caused by different natural and anthropogenic forcing agents using numerical models. Since 2001, we have been working on the development and application of the chemistry-climate model, SOCOL (SOlar-Climate-Ozone Links). We completed our third version of the model in 2013. Since then, the model has undergone many further improvements branching into several specialised versions. In the framework of the VEC project, we combine multiple versions into one complete up-to-date Earth System Model (ESM). Here, we present the first description of a new Atmosphere-Ocean-Aerosol-Chemistry-Climate (AOACCM) Earth System Model (ESM), SOCOLv4.0.

Since the publication of SOCOLv3 by Stenke et al. (2013), the SOCOL model has undergone further improvements, such as the addition of VOC chemistry and an interactive lightning parameterisation, upgraded heating rate parameterisation, the photolysis rate parameterisation, and the parameterisations of energetic particle effects. In close collaboration with other Swiss institutes, we have added the ocean/sea-ice dynamics model. The performance of the Atmosphere-Ocean-Chemistry-Climate Model (AOCCM) SOCOL-MPIOM in simulating past climate has been evaluated and documented in the framework of the SNF Sinergia project, FUPSOL. In the framework of the SNF project IASSA, we have extended the model by adding the sulphur group to gas phase chemistry and aerosol microphysics. The performance of the new Aerosol-Chemistry-Climate Model (ACCM) SOCOL-AER was documented for background and high aerosol loading conditions, after which it has been further improved, among other things, by adding new dry and wet deposition schemes.

For the next step, it was necessary to combine multiple model versions and add the possibility of considering multiple feedbacks in the Earth system. To do this, we have developed the fourth version of the model in the framework of the SNF VEC project. It is based on the combination of the MPIMet (Hamburg, Germany) Earth System model (Giorgetta et al., 2013) consisting of ECHAM6 for the atmosphere and MPIOM for the ocean as well as JSBACH for terrestrial biosphere and HAMOCC for the ocean´s biogeochemistry, with the latest versions of chemical (MEZON) and microphysical (AER) modules used in SOCOLv3 and SOCOL-AER.

We have now just completed operational testing on the next generation of SOCOLv4.0. Figure 1 illustrates the components and information flow in AOACCM ESM SOCOL v4.0. The model treats the majority of processes responsible for the Earth system behaviour from the ground up to the mesopause. In addition to the interactive gas-phase/heterogeneous chemistry and bin-resolved stratospheric sulphate aerosol, the model can simulate the dynamical vegetation, carbon cycle, emission of sulphur containing species from the ocean and other necessary quantities to simulate direct forcing and feedbacks responsible for the ozone and aerosol layer evolution. Figure 2 shows altitude-latitude ozone and sulphate aerosol distributions calculated with SOCOLv4.0. The model already produces realistic ozone and aerosol layers and is now undergoing a process of tuning and verification in the framework of the ongoing SNF VEC project.

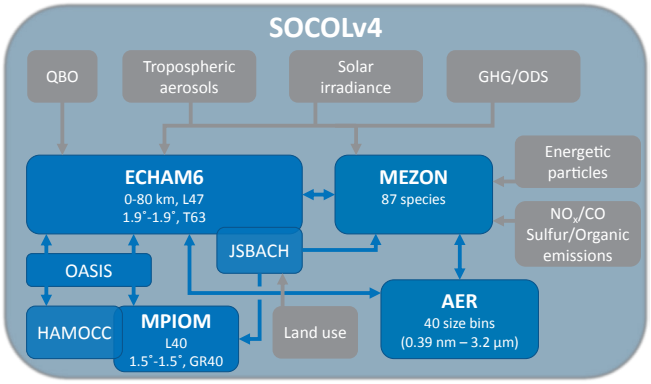

Figure 1. Components and information flow in the Atmosphere-Ocean-Aerosol-Chemistry-Climate Earth System Model, SOCOL v4.0.

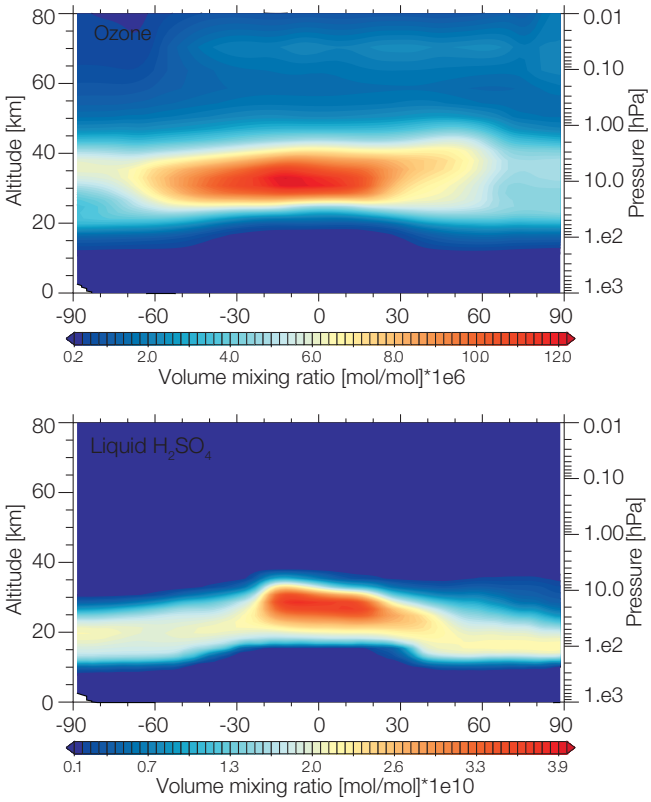

Figure 2. Zonal mean ozone (upper panel) and liquid H_2SO_4 (lower panel) mixing ratios for Jan. 2000 calculated with AOACCM ESM SOCOLv4.0.

References: Giorgetta M. et al.: 2013, JAMES, 5(3), 572–597, doi: 10.1002/jame.20038.

Stenke A. et al.: 2013, Geosci. Model Dev., 6, 1407–1427, doi: 10.5194/gmd- 6-1407-2013.

First Results of the Entire Atmosphere Global Model (EAGLE)

Timofei Sukhodolov and Eugene Rozanov in collaboration with IZMIRAN (Kaliningrad, Russia) and MPIMet (Hamburg, Germany)

Historically, numerical models of the upper (>80 km) and lower atmosphere layers (<80 km) have developed almost independently by just prescribing the lower/upper boundary conditions, which is usually a very rough approximation of the physics happening below/above. With increasing knowledge about atmospheric sciences related to progress, both in measurements and models, it has become clear that the interrelation between atmospheric layers is important and needs to be addressed explicitly. Here, we present a step in this direction with a focus on the ionosphere by showing first results of the Entire Atmosphere Global Model (EAGLE) that combines models of the upper and lower atmospheres.

The Earth's ionosphere is a complex system of coupled dynamical, radiative and chemical processes. Ionospheric variability is mostly defined by the solar radiation flux and geomagnetic activity, but still a significant part of it (~20%) is associated with the forcing coming from the lower and middle atmosphere. The main mechanisms responsible for this connection are planetary waves, atmospheric tides, and gravity waves. A proper representation of all these processes is crucial for understanding the ionosphere itself and its connection to the lower layers.

To calculate the state and variability of the lower and middle atmosphere, we use HAMMONIA (Hamburg Model of the Neutral and Ionized Atmosphere). This model is mostly based on the fifth version of the general circulation model of the atmosphere ECHAM5, but also contains several important additions, such as the extension of the top boundary up to 250 km, inclusion of the chemical module MOZART3 and others (Schmidt et al., 2006), which allow a good representation of the lower thermosphere. HAMMONIA is applied here with a horizontal resolution of ~2×2° and 119 vertical layers from the ground up to ~200–250 km. The state and variability of the upper atmosphere are calculated by the Global Self-consistent Model of the Thermosphere, the Ionosphere and the Protonosphere (GSM TIP, Namgaladze et al., 1988). This model is based on the system of quasi-hydrodynamic equations of continuity, motion and heat balance for neutral and charged particles of the cold near-earth plasma in conjunction with the equation for the electric potential in the altitude range from 80 km to a geocentric distance of ~15 Earth radii and with a horizontal resolution of 5×5°.

In order to couple both models, we programmed a coupler interface that prepares fields of both models to be transited to each other in the overlap region (~80–200 km) and allows HAMMONIA and non-parallel (GSM TIP) codes to simultaneously run in parallel. In future, it is also planned to transfer nitrogen oxide production and Joule heating from GSM TIP to HAMMONIA, but here, as a first step, we discuss only the one-way coupling through specification of the GSM TIP temperature and neutral wind fields. Neutral density is specified only at 80 km as a lower boundary condition.

Figure 1 shows the vertical structure of the zonal mean temperature in January 2009. One of the characteristic features of this region is the existence of the cold summer mesopause, which is mostly a result of momentum deposition from gravity waves. HAMMONIA (Figure 1b) perfectly reproduces this region compared to the MIPAS observations (Figure 1a), since the model dynamics is continuous from the surface. The decoupled GSM TIP model (Figure 1c) cannot reproduce this region and shows a clear lack of cooling at the polar summer mesopause, which also leads to a cold shift of the above temperatures. This is due to missing wave-forcing information that is necessary to generate a vortex at about 90–100 km. Therefore, we have chosen to couple HAMMONIA and GSM TIP in the 80–120 km region (Figure 1d), which allows both models to transfer forcings to each other while allowing a realistic mesopause region to be maintained. This illustrates the importance of the coupling processes and necessity of a combined model, which we are continuing to work on.

Acknowledgements: This investigation was performed with the financial support of the Russian Science Foundation grant No. 17-17-01060.

References: Namgaladze A. A. et al.: 1988, Pure Appl. Geophys., 127(2/3), 219–254.

Schmidt H. et al.: 2006, J. Climate, 19, 3903–3931.

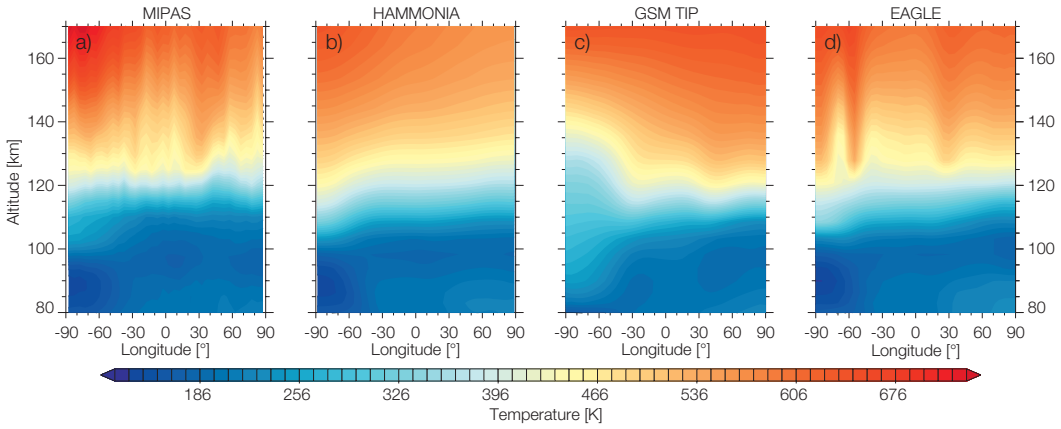

Figure 1. The January 2009 monthly zonal mean temperature from 80 to 175 km ie upper mesosphere/lower thermosphere region. Panel a): MIPAS observations, b) HAMMONIA, c) GSM TIP, d) EAGLE.

ATMOZ – Traceability for Atmospheric Total Column Ozone

Luca Egli, Julian Gröbner, and Natalia Kouremeti in collaboration with partners from the EMRP-ENV59 ATMOZ project

The European joint research EMRP project, ATMOZ "Traceability for Atmospheric Total Column Ozone", has significantly enhanced the reliability of total column ozone data measured at the Earth's surface with Dobson, Brewer and array spectroradiometers. New methods of observation (techniques, instruments and software) have been developed to provide traceable total ozone column measurements with an uncertainty of less than 1%.

Since the 1980's, it is known that human-produced chlorofluorocarbons (CFCs) have led to recurring massive losses of total ozone in the Antarctic (ozone hole) and at mid-latitudes in Europe (Molina and Rowland, 1974). The Montreal protocol and its amendments have been successful in reducing the emission of ozone-depleting substances. However, monitoring of the recovery of the ozone layer requires accurate long-term observations with reliable and well understood instruments and the development of future instrumentations for the continuation of the long-term time-series. Without solving this problem, the recovery of the ozone layer cannot be shown and the worldwide efforts of reducing ozone concentrations cannot be demonstrated.

The project, coordinated by the World Calibration Center for UV radiation (WCC-UV) has addressed the problems by:

- Characterising the most important reference ozone network instruments, such as Dobsons and Brewers.
- Developing new devices for field characterisation of worldwide network instruments.
- Developing a potential new generation of ozone monitoring instruments.
- Generation of new reference data sets such as new ozone absorption cross-sections and a new extraterrestrial reference solar spectrum.
- Establishing an overall uncertainty budget of ozone measurements to be used by the end-user ozone community.

Figure 1. The members of the EMRP consortium at the field campaign at Izaña, Tenerife, Spain. The consortium consists of partners from national metrology institutes, industry and universities.

The project results represent important improvements towards more reliable measurements of total column ozone and the harmonisation of global ozone monitoring networks:

- The importance and impact of well characterized Dobson and Brewer instruments has been demonstrated to the TOC (Total Ozone Column) monitoring community in two field campaigns, two stakeholder workshops and training seminars. In addition to the laboratory-based methods for the characterisation and calibration of the network instruments, the project can now also provide methods and devices for in-field characterisations and calibrations to the end-user.
- The new extra-terrestrial spectrum displays a traceable benchmark dataset for traceable spectral solar irradiance, with low and known uncertainty.
- The overall uncertainties of ground-based ozone monitoring are now well quantified. A software tool is available to assess the overall uncertainty of ozone measurements by different network instruments.
- The scientific ozone community now has a tool to homogenise the different ground-based ozone networks with well-quantified uncertainties.
- The technical advances made during the project have prepared the development of a potential new generation of cost effective, robust and reliable instruments for monitoring ozone with the requested uncertainty for the next decades.

The project has made significant improvements in explaining substantial differences and in quantifying the corresponding uncertainties of worldwide monitoring TOC from the Earth's surface with different instrument types, and has therefore led to a homogenisation of ozone monitoring data products.

Furthermore, the project provides the technical and research foundation to replace ageing instruments with more cost effective, robust and accurate instruments of the latest generation to detect the recovery of the global ozone layer during the next decades.

Acknowledgment: The EMRP is jointly funded by the EMRP participating countries within EURAMET and the European Union

References: Molina M. J. and Rowland F. S.: 1974, Stratospheric sink for chlorofluoromethanes-chlorine atom catalyzed destruction of ozone, Nature, 249, 810–812.

Spectral Snow Albedo Measurements at Weissfluhjoch, Davos, Switzerland

Luca Egli and Julian Gröbner in collaboration with Medical Univ. Innsbruck (Austria) Gigahertz-Optik GmbH (Germany) and WSL Institute for Snow and Avalanche Research SLF (Switzerland)

Measurement of spectral snow albedo is essential for global climatology models and different snow cover properties. PMOD/WRC and partners have quantified the uncertainty of snow albedo measurements with state-of-the-art array spectroradiometer and calibration laboratory facilities. The expanded uncertainty of spectral snow albedo is around 2%.

The quantification of the albedo of snow is important for global energy budgets in the cryosphere, such as melt energy in snow hydrology or the evolution of snow cover properties, such as weak layer formation in avalanche forecasting (Zatko and Warren, 2015). Furthermore, snow albedo is essential for modelling of solar irradiance at the Earth's surface (Mayer and Kylling, 2005).

In winter 2016/2017, the WSL Institute for Snow and Avalanche Research (SLF) began a comprehensive measurement campaign at the Alpine experimental site at Weissfluchjoch 2450 m a.s.l in Davos, Switzerland. The campaign aimed to measure turbulent and latent heat fluxes, snow transport, stable water isotopes exchange, density, snow density and snow impurities using microcomputer tomography. In conjunction with this measurement campaign, the Medical University of Innsbruck and the PMOD/WRC provided daily spectral snow albedo measurements. The instrumentation used for the entire campaign (USB4000 CCD array spectrometer from Ocean Optics) was developed and thoroughly characterised, calibrated, optimised and tested during the EMRP project ENV03, taking advantage of the characterisation and calibration expertise of the PMOD/WRC and the corresponding laboratory facilities.

On specific days, a commercially available weatherproofed new generation of array spectroradiometer instrument (BTS2048-VL-TEC-WP from Gigahertz Optik GmbH), as calibrated and

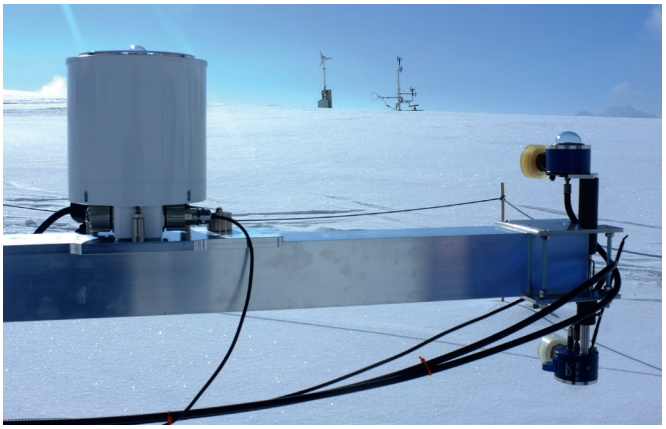

Figure 1. On the left: Standalone waterproofed and temperature stabilised BTS2048-VL-TEC-WP instrument from Gigahertz Optik GmbH. On the right: Two global entrance optics connected with a fibre to the temperature stabilised Ocean Optics array spectroradiometer from the Medical University Innsbruck towards the bottom.

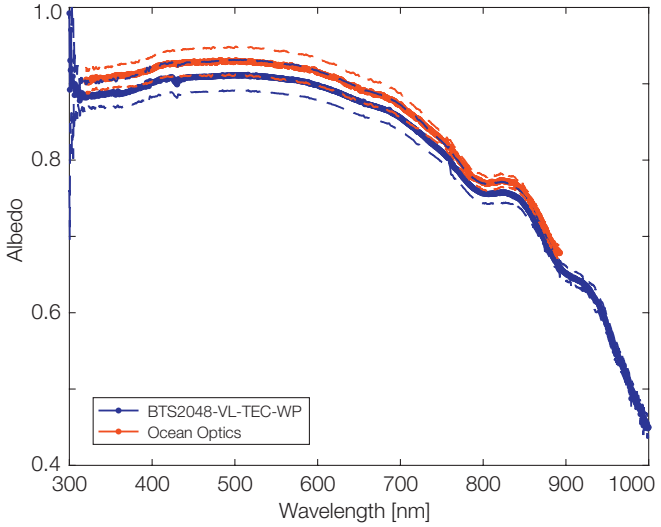

Figure 2. Spectral snow albedo measured on 29 March 2017 with two different instruments. The instruments agree within the expanded measurement uncertainty of 2% (dashed lines).

characterised by the manufacturer, was tested and compared with the main instrument. The comparison revealed an agreement between both instruments of 2% which is within the measurement uncertainty of 2% (Figure1). During the campaign, snow albedo spectral data in the 320–870 nm wavelength range for the Ocean Optics instrument and 300–1000 nm for the BTS were measured, accounting for effects observed in the laboratory such as cosine error and azimuth biases. On-site effects such as the different height of the entrance optics above snow cover and orientation of the optics were measured to evaluate an overall uncertainty of snow albedo measurements in the field.

The uncertainty estimate showed that absolute snow albedo can be measured with an expanded ($\sigma = 2$) absolute uncertainty of 2%. The spectral measurements agree with snow albedo measurements from UVA broadband radiometers operated at the experimental site by PMOD/WRC during the entire season. Accounting for the effect of changing distance from the snow surface to the entrance optics, the deviation (1 σ) can be quantified at about 2% per meter height difference. This effect has to be considered if the albedo sensor is mounted at a fixed height and when the snow cover is increasing and decreasing during the season, resulting in a changing distance. The high-quality snow albedo data was compared with impurities and specific surface area of the snow cover. First results show that spectral snow albedo information may be used to retrieve these two snow cover properties by accurate radiation observations.

References: Zatko M. C., Warren S. G.: 2015, Annals of Glaciology 56, doi: 10.3189/2015AoG69A574.

Mayer B., Kylling A.: 2005, Atmos. Chem. Phys., 5, 1855-1877.

Trends in Surface Radiation and Cloud Radiative Effect at Four Swiss Sites for 1996–2015

Stephan Nyeki, Christine Aebi, and Julian Gröbner in collaboration with DWD (Lindenberg, Germany) and MCH (Payerne, Switzerland)

The trends of surface downward shortwave and longwave radiation (DSR, DLR) were analysed at four stations (between 370 and 3580 m asl) in Switzerland for the 1996–2015 period. The calculated Cloud Radiative Effect (CRE) was found to decrease by 2.3–3.1 Wm^{-2} /decade, implying a reduction in cloud cover and/or a shift towards a different cloud type.

The trends of surface radiation for the 1996–2015 period at four Swiss SaCRAM stations were investigated in this work which is an update of previous studies (Philipona et al., 2004; Wacker et al., 2011). Our objectives are: i) to assess whether trends in all-sky and cloud-free surface radiation (ie downward shortwave radiation, DSR; downward longwave radiation, DLR) can be determined and explained with any greater certainty, and ii) to assess the trends in the cloud radiative effect (CRE).

Surface radiation and meteorological data were obtained for the four MeteoSwiss SaCRAM stations: Davos (DAV, 46.814°N, 9.846°E, 1594 m asl), Jungfraujoch (JFJ, 46.549°N, 7.986°E, 3580 m), Locarno (LOC, 46.180°N, 8.783°E, 367 m) and Payerne, (PAY, 46.815°N, 6.944°E, 491 m). Trend analysis was conducted with a linear least square method. All-sky DSR trends at all four stations are mainly positive, but few are significant at the 95% confidence level. In contrast, all-sky DLR trends are positive (0.6–4.8 Wm^{-2}/decade) and significant (except for PAY). Larger DLR trends are found for cloud-free conditions (2.7–5.4 Wm^{-2}/decade), while all trends are significant at the 95% confidence level. These DLR results were partly observed in previous studies (e.g. Wacker et al., 2011) but not to the convincing and widespread extent as observed in this study.

The effect of clouds on the surface radiation budget can be expressed by the CRE which is the difference between observed radiation fluxes at the ground and modelled fluxes in the absence of clouds. CRE is determined by summing the shortwave and longwave cloud effects (SCE and LCE, respectively). Trend analysis of the SCE time-series gave positive trends (0.1–3.6 Wm^{-2}/decade) at all stations (see Table 1). As the SCE annual average at all stations is negative (-48 to -72 Wm^{-2}), the increasing trend represents a decrease in the magnitude of the SCE. In contrast, the LCE trends are negative (-0.2 to -1.2 Wm^{-2}/decade) at three stations which is consistent with the SCE trends. As a result of these SCE and LCE trends, CRE trends are all positive but not significant. Our study suggests that the net radiative cooling due to clouds, the CRE, has decreased by 2.3–3.1 Wm^{-2}/decade over the 1996–2015 period which implies a decrease in cloud cover or a shift towards a different cloud type. However, it is not possible to quantify and verify these cloud changes in detail as cloud cameras, ceilometers, lidar, etc have only been installed to varying degrees at the four SACRaM stations in recent years.

Although accurate DSR and DLR time-series have been available for more than 20 years in Switzerland, the detection of trends with high confidence remains difficult due to the relatively small changes in surface radiation and cloud properties which are close to the measurement uncertainty. Therefore, it is important to continue providing facilities to maintain such radiation and ancillary atmospheric observations of the highest possible accuracy during day and night-time conditions. In particular, the continuous observations of clouds are essential for climate monitoring. The development of cloud and infrared cameras to monitor and characterise clouds (Aebi et al., 2017; and references therein) will therefore be an important step towards this goal.

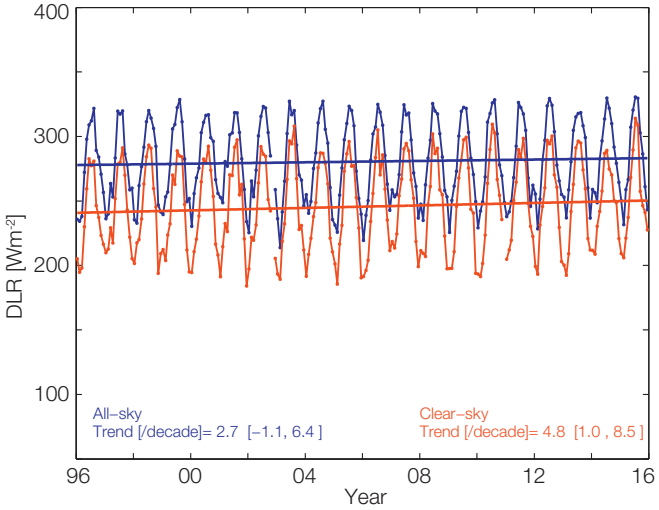

Figure 1. Monthly average DLR values during all-sky (blue) and cloud-free (red) conditions at Davos from 1996–2015. The trend analyses for the all-sky and cloud-free time-series are represented by the lines.

Table 1. Trend analysis of the shortwave and longwave cloud effects (SCE and LCE), and cloud radiative effect (CRE) for the 1996–2015 period at all four stations. Trend values are in Wm^{-2}/decade. JFJ results not shown as time-series of integrated water vapour are possibly erroneous.

Station	SCE	LCE	CRE
DAV	3.1	-0.2	3.1
JFJ	0.1	-	-
LOC	3.4	-0.7	2.7
PAY	3.6	-1.2	2.3

References: Aebi C., Gröbner J., Kämpfer N., Vuilleumier L.: 2017, Atmos. Meas. Tech., 10, 4587–4600, doi.org/10.5194/amt-10-4587-2017.

Philipona R. et al.: 2004, Geophys. Res. Lett., 31, L03202, doi:10.1029/ 2003GL018765.

Wacker S. et al.: 2011, J. Geophys. Res., 116, D10104, doi:10.1029/2010JD015343.

ATLAS – A Pulsed Tunable Laser System for the Characterisation of Spectrometers

Natalia Kouremeti, Julian Gröbner, Stelios Kazadzis, and Gregor Hülsen

A pulsed Tunable LAser system for the characterisation of Spectrometers (ATLAS) is an ESA-funded project which started in March 2015. ATLAS's main aim is the improved characterisation of array spectroradiometer systems that are widely used for satellite validation of various atmospheric products.

The ATLAS project aims to improve the accuracy of array spectroradiometers used for satellite validation of various atmospheric products. The objectives of the second phase of the project (July 2016–Dec 2017) were the characterisation of a Pandora (LuftBlick GmbH) instrument operated at Davos. Aspects investigated were: the wavelength scale, stray light and non-linearity, and the absolute irradiance calibration. In addition, a comparison of the aerosol optical depth (AOD) against the reference PFR-Triad and a comparison of total column ozone against the collocated Brewer #163 spectrophotometer were conducted. Pandora instruments as part of the Pandonia network are key instruments for ground-based trace gas retrievals and satellite validation.

Pandora has two operational spectrometers covering the spectral ranges 273–540 nm (UV) and 387–940 nm (Vis). The dispersion functions for Pandora 120 have been determined with an uncertainty of about 10 pm. The full-width -at-half-maximum (FWHM) of the spectrometers is quite constant over the detector's wavelength range and is on average 0.43 nm ± 0.02 nm and 0.92 nm ± 0.14 nm for the UV and Vis spectrometers, respectively.

The line spread functions (LSF) were determined for the two spectrometers by applying a new method of combining a highly overexposed laser measurement with the rest of the non-saturated and saturated measurements. This methodology led to a reduction in the noise and the expanded uncertainty of the straylight correction matrix, especially in the background regions of about 4–14% depending on the features of the LSF (Figure1). The LSF of the UV (Figure 2) and Vis spectrometer, covering six orders of magnitude,

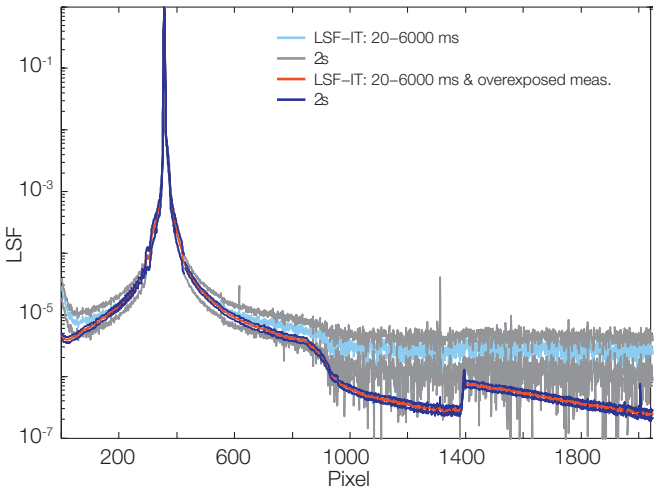

Figure 1. Example of a combined line-spread function along with the uncertainty estimate based on the old and new method.

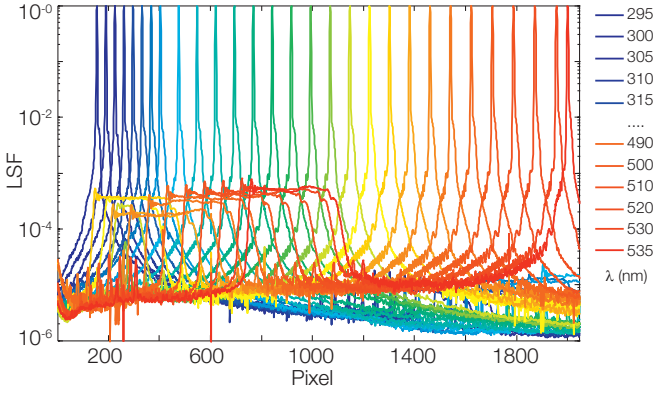

Figure 2. Line-spread functions of the Pandora-120 spectrometer.

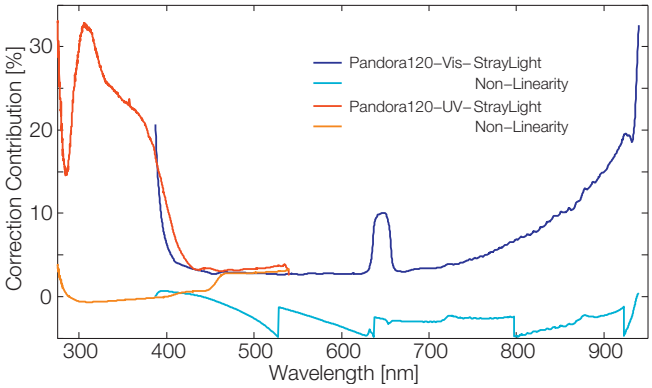

Figure 3. Stray-light and non-linearity contribution to the direct irradiance response function of the Pandora-120 spectrometer.

were converted to a stray-light matrix by finding the in-band region, based on an agreement of better than 20% between the measured slit function and a 2nd order Gaussian fit.

The absolute irradiance calibration and non-linearity correction were determined in the PMOD/WRC direct irradiance calibration setup, including a 3 m long motorised linear stage and a secondary irradiance reference (lamp type FEL, QASUME spectral irradiance reference). The effect of the stray-light and non-linearity contributions on the response functions of the two Pandora-120s is shown in Figure 3. Especially for the UV spectrometer, the stray- light contribution to the FEL spectrum is about 30% up to 400 nm while for the Vis spectrometer it is substantially lower at ~10%. The stray-light correction has already been incorporated by LuftBlick GmbH in their algorithms for ozone and AOD retrievals (testing phase).

The comparison with the collocated Brewer#163, calibrated yearly against the reference Brewers of the RBCC-E Triad, showed an agreement >20 DU for one year of synchronous operation. The comparison revealed a dependency on the stratospheric temperature of about 1 DU/K. A comparison with the PFR-Triad revealed the potential of Pandora to provide AOD information in addition to trace gases once the fibre stability has been improved. The comparison and improvement of algorithms as well as operational procedures is continuing during the third phase of ATLAS (2018–2019).

Aerosol Optical Depth Traceability: WORCC Activities and Collaborations

Stelios Kazadzis, Natalia Kouremeti, and Julian Gröbner in collaboration with CNR (Italy), AEMET (Spain), Univ. Valencia (Spain)

PMOD/WORCC maintains a standard group of three Precision Filter Radiometers that serve as a reference for Aerosol Optical Depth measurements within WMO. During 2017, a series of scientific activities and collaborations towards AOD traceability with various networks/instruments were undertaken.

PMOD/WORCC has signed a four-year memorandum of understanding with the SKYNET network of sun-photometers in order to form a framework for organising joint WORCC and SKYNET/Europe activities on: i) aerosol optical depth (AOD) traceability, ii) measurement quality improvement, iii) intercomparison studies in different environments, and iv) validation and interpretation of the results. Measurement traceability and data quality are essential requirements by the WMO for monitoring atmospheric aerosol optical properties by international radiometer networks. The SKYNET network has recently been included as a WMO-GAW contributing network. Hence, a programme of traceability to CIMO defined standard instruments and methods, together with intercomparisons and calibration of ESR/SKYNET master instruments through PMOD/WRC is necessary. Based on this collaboration activity, two long-term campaigns at Valencia (Spain) and Chiba (Japan) have been organised with the participation of WORCC/PFR instruments and reference instruments from SKYNET Europe and Asia. In addition, during August–September 2017, a reference SKYNET instrument visited WORCC and performed parallel measurements alongside the WORCC triad. The transfer of the triad scale was based on a signal and not an AOD comparison.

Following this calibration activity, a long-term campaign started in October 2017 in Rome. A major objective of the QUAlity and TRaceabiliy of Atmospheric aerosol Measurements (QUATRAM) campaign is an assessment of the calibration activity previously held in Davos using parallel measurements of a PFR and 11 additional AOD measuring instruments. The campaign will last until July 2018 and the long-term comparison results will be assessed (http://www.euroskyrad.net/quatram.html). PMOD/WORCC has started a collaboration with the AEMET Izaña Atmos. Res. Center (IARC) which hosts the WMO Regional Brewer Calibration Centre (RBCC) for Europe and Africa. IARC is an absolute calibration site for AERONET, AERONET-Europe, PHOTONS (PHOtométrie pour le Traitement Opérationnel de Normalisation Satellitaire, France) and RIMA (Red Ibérica de Medida Fotométrica de Aerosoles, Iberia) photometer networks, and is an absolute calibration site for PMOD/WRC instruments. A total of twelve years of AOD measurements from three PFRs and 15 CIMEL instruments operated at IARC have been analysed and compared. The dataset included up to 67,000 synchronous AOD measurements and results showed an agreement between 91.7% and 97.4% at four different wavelengths (380, 440, 500, 865 nm), where the percentage values describe the number of measurements within the WMO limits for AOD intercomparisons (0.005+0.01/*m*, where *m* is the air mass).

Figure 1. View of the instruments participating in QUATRAM.

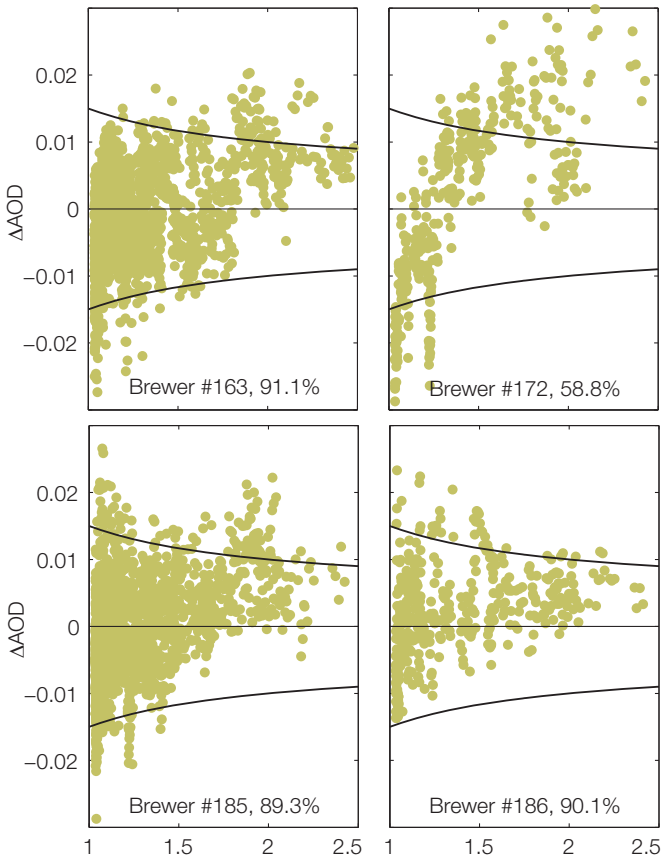

Figure 2. Selected results from the Brewer/UV-PFR intercomparison.

The results of an intercomparison campaign between Brewer spectroradiometers and the WORCC UV-PFR reference instrument (Carlund et al., 2017) have been analysed and are presented in Solano et al. (2018). The results show a precision better than 0.01 and an uncertainty of less than 0.05 for well-maintained instruments comparing AODs in the UV wavelengths (Figure 2).

References: Carlund T., Kouremeti N., Kazadzis S., Gröbner J.: 2017, Atmos. Meas. Tech., 10, 905-923, doi:10.5194/amt-10-905-2017.

López-Solano A. et al.: 2018, Atmos. Chem. Phys., 18, 3885-3902, https://doi.org/10.5194/acp-18-3885-2018.

The 2nd International UV Filter Radiometer Comparison UVC-II

Gregor Hülsen and Julian Gröbner

A UV filter radiometer comparison was organised by PMOD/WRC in Summer 2017. A total of 75 broadband radiometers from 37 institutions participated in the campaign. The relative differences between the solar measurements derived from the user calibration and those derived from the calibration performed at PMOD/WRC varied from 0.04% to larger than 50% for specific instruments.

The 2nd international UV Filter Radiometer Comparison (UVC-II) was held at the WCCUV of PMOD/WRC from 25 May to 5 October 2017. This campaign followed three similar campaigns held in 1995 in Helsinki (Finland), 1999 in Thessaloniki (Greece), and 2006 in Davos (Switzerland). A total of 75 broadband radiometers from 37 institutions participated in the most recent campaign. The radiometers were for the most part reference instruments from their respective regional or national networks. Nine different radiometer types participated and included the following: i) Kipp & Zonen / Sintec (28 in total), ii) Yankee UVB 1 (11), iii) analogue and digital Solar Light V. 501 (19/9), iv) Delta Ohm LP UVI 02 (2), v) EKO MS 212W (2), vi) Sensor 1E.1-081 (1), vii) Genicom GUVB (1), viii) Eppley TUVR (1), and ix) Middleton Solar UVR1-B2 (1). The filter weighting functions mostly approximated the erythemal action spectrum, while some approximated the UVB, UVA and UV spectra.

The two reference spectroradiometers, QASUME and QASUMEII (Hülsen and Gröbner, 2007) belonging to the WCCUV, agreed to within ±2% throughout the campaign. The atmospheric conditions during the campaign varied from fully overcast to clear skies, and allowed a reliable calibration of all instruments. The standard calibration methodology (Hülsen et al., 2016) using the instrumental spectral and angular response functions measured in the laboratory and an absolute outdoor calibration relative to the QASUME-II spectroradiometer, provided traceable measurements to SI with expanded uncertainties ($k=2$) of about 6% for most instruments.

Figure 1. Outdoor calibration during the 2nd International UV Filter Radiometer Comparison (UVC-II) on the PMOD/WRC roof platform with a total of 75 UV radiometers.

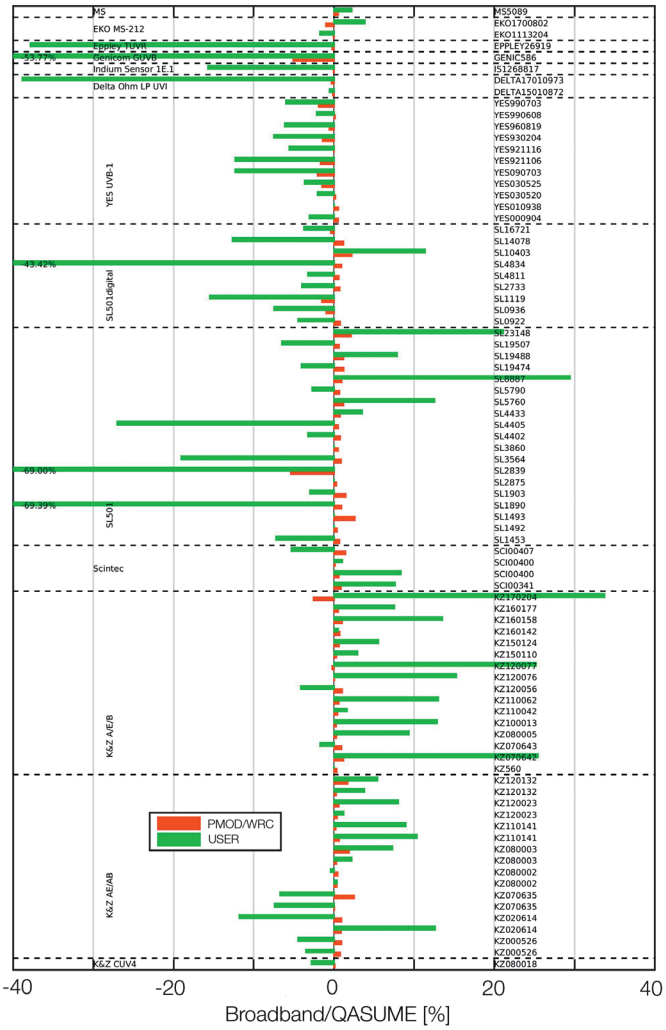

Figure 2. Comparison of the original (USER, green) and the new (PMOD/WRC, red) calibration.

Broadband radiometer measurements were analysed both with the PMOD/WRC calibration as well as the calibration used by the home institutes. The average date of the user calibration was five years prior to this campaign (e.g. 2012) and 40 out of the 75 instruments used a single calibration factor, instead of the suggested calibration matrix. The relative differences between the measurements using the user calibration and those from PMOD/WRC varied from 0.04% to larger than 50% for specific instruments.

References: Hülsen G., Gröbner J.: 2007, Characterisation and calibration of ultraviolet broadband radiometers measuring erythemally weighted irradiance, Appl. Opt. 46, 5877–5886.

Hülsen G., Gröbner J., Nevas S., Sperfeld P., Egli L., Porrovecchio G., Smid M.: 2016, Traceability of solar UV measurements using the QASUME reference spectroradiometer, Appl. Opt. 55, 7265–7275.

Cloud Fraction Analysis by Thermal Infrared and Visible All-Sky Cameras

Christine Aebi and Julian Gröbner in collaboration with Univ. Bern (Switzerland)

In the framework of the project, A Comprehensive Radiation Flux Assessment (CRUX), a new instrument has been developed: the thermal Infrared Cloud Camera (IRCCAM). The cloud fraction determined from IRCCAM is analysed and compared with the cloud fraction retrieved from two visible all-sky cameras and from the Automated Partial Cloud Amount Detection Algorithm (APCADA) using pyrgeometer data.

The thermal infrared cloud camera (IRCCAM) consists of a commercial microbolometer camera (Gobi-640-GigE) looking downward on a gold-plated spherical mirror in order to image the whole upper hemisphere. The IRCCAM is sensitive in the 8–14 µm wavelength range and has been measuring continuously during day and night-time in Davos since September 2015. An algorithm allows the cloud fraction from the IRCCAM images to be determined (Aebi et al., 2018). For a two-year period, these data have been compared with cloud fraction data retrieved from two visible all-sky cameras (Mobotix Q24M and Schreder VIS-J1006) as well as cloud fraction data calculated with APCADA.

Figure 1 shows, as an example, the cloud fraction detected by the cameras on 4 April 2016. The IRCCAM detected a cloud fraction >0.98 at the beginning of the day. A large fraction of the clouds had disappeared by about 6 UTC when the visible cameras started to measure. At this time the cloud fraction was around 0.1 and cumulus clouds were present. The larger difference between the instruments can be explained by the fact that the clouds are located in the vicinity of the horizon and thus in a region that not all algorithms are able to analyse. The best agreement between the different cameras and algorithms was at about 10 UTC (Figure 2). The cloud types present during the afternoon were cumulus and cirrostratus. Thin and high-level cirrostratus are difficult to detect with the IRCCAM and visible all-sky camera algorithms (Aebi et al., 2017). The visible all-sky cameras agree in more than 94% of cases to within ±2 oktas (cloud fraction = 0.25) and in 77–94% of cases to within ±1 okta (0.125). Thus, these cameras are taken as a reference to validate the cloud fraction retrieved from the newly developed IRCCAM.

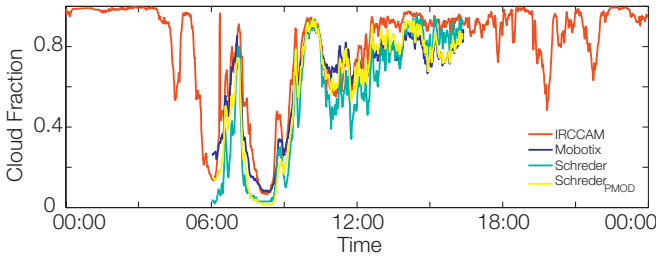

Figure 1. Fractional cloud coverage determined by the cameras and algorithms (red: IRCCAM; blue: Mobotix; cyan: Schreder; yellow: Schreder$_{PMOD}$) on 4 April 2016.

The median difference in the cloud fraction between the IRCCAM and Mobotix is 0.01 with 5th and 95th percentile values of -0.26 and 0.18, respectively. In this data set, 90% of the IRCCAM data agree to within ±2 oktas in comparison to the cloud fraction determined by the visible all-sky Mobotix camera. The median difference in cloud fraction between the IRCCAM and Schreder camera is 0.07 and thus slightly higher than the median difference in cloud fraction between the IRCCAM and Mobotix camera. However, 90% of data in this data set also agree to within ±2 oktas.

The differences in the detection of the cloud fraction between the IRCCAM and other instruments have also been analysed separately for various cloud types, times of the day and different seasons. The differences between seasons and between day and night-time data are not significant. Low-level clouds are best detected with median values of ~0.0, followed by mid-level and high-level clouds. Thus, the performance of IRCCAM in detecting the cloud fraction is comparable to state-of-the-art cloud detection instruments (Boers et al., 2010). All the results presented here are further discussed in Aebi et al. (2018).

References: Aebi C., Gröbner J., Kämpfer N., Vuilleumier L.: 2017, Atmos. Meas. Technol. 10, 4587–4600, doi: 10.5194/amt-10-4587-2017.

Aebi C., Gröbner J., Kämpfer N.: 2018, Atmos. Meas. Technol. Disc., 2018, 1–32, doi: 10.5194/amt-2018-68.

Boers R. et al.: 2010, J. Geophys. Res., 115, doi: 10.1029/2010JD014661.

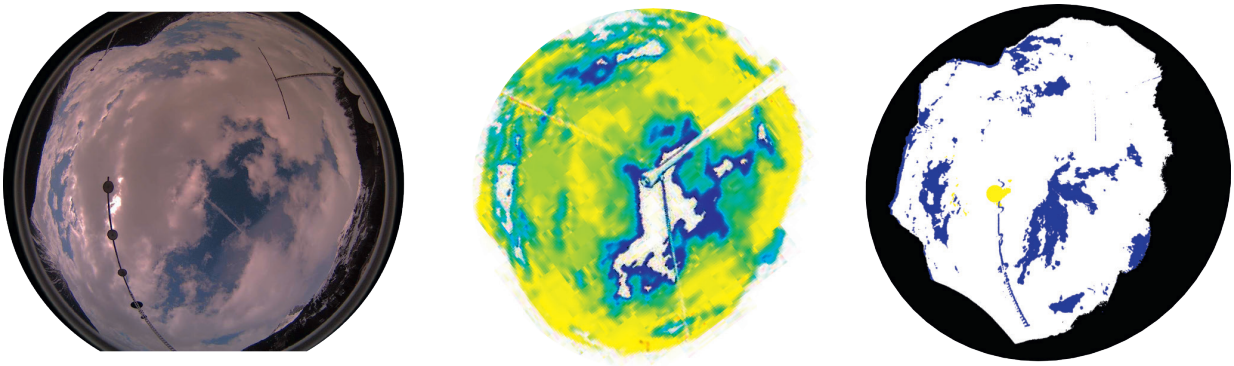

Figure 2. Cloud situation at 10 UTC, 4 April 2016. Left panel: image from Mobotix. Centre and right panels: cloud fraction determined from IRCCAM and Mobotix, respectively.

GEO-CRADLE Project: The Solar Energy Nowcasting System (SENSE)

Stelios Kazadzis in collaboration with the National Observatory of Athens (Greece)

GEO-CRADLE (http://geocradle.eu/en/) has received funding from the EU Horizon 2020 Research and Innovation Programme (February 2016–November 2018) with the aim of promoting the uptake and exploitation of Earth Observation (EO) activities in North Africa, Middle East and the Balkans. To this end, the project has brought together 25 partners from three continents to work in a highly-complementary team that combines a strong background in EO coordination activities with proven scientific excellence in four key thematic areas: i) Adaptation to climate change, ii) improved food security & water extremes management, iii) access to raw materials, and iv) access to energy.

GEO-CRADLE includes four pilot areas that have been chosen in order to build the scientific basis that will lead to a specific application for the Eastern Mediterranean, the Middle East and North African area under study. PMOD/WRC leads the Solar Energy Nowcasting SystEm (SENSE) pilot area. The aim of the pilot is to coordinate, improve and support the regional EO infrastructures and capabilities related to solar radiation and solar energy related applications. The aim for this pilot is an operational, real-time system for solar energy, solar irradiance and related now-casting applications.

SENSE is based on the synergy of radiative transfer model simulations, speed-up technologies (neural networks and multi-regression function techniques), and real-time atmospheric parameter inputs from the Meteosat Second Generation and the Copernicus Atmosphere Monitoring Service (Kosmopoulos et al., 2018).

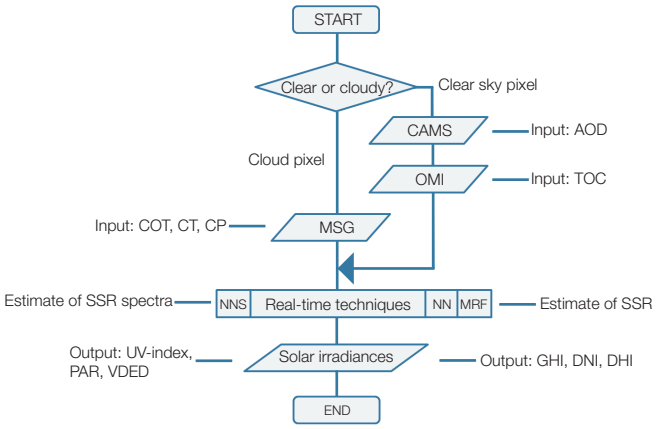

Figure 1. Flowchart illustration of SENSE. The initial pixel classification followed by the clear or cloudy sky inputs to SENSE resulting in the spectral and integrated SSR-related products and services.

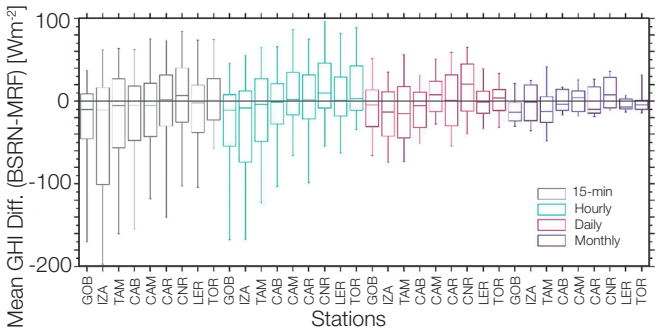

Figure 2. Shown is the difference in Global Horizontal Irradiance (GHI) for validation of SENSE against BSRN ground-based measurements under various climatological conditions (from southern Africa to northern Europe) and time horizons (from 15-min to monthly averages).

It can be integrated in any already existing information system (Figure 1), providing high resolution data (spectral: 1 nm, spatial: 5 km, temporal: 15 min.) to support solar energy planning, and transmission/distribution operators, and is capable of producing more than 1 million outputs in less than 1 minute.

By using the networking platform of GEO-CRADLE, the SENSE pilot has succeeded in stimulating the interest of relevant energy stakeholders and end-users, and has provided targeted solar energy applications, products and services (http://solea.gr/), aiming to be a starting point for energy related investments and activities towards and beyond GEO, GEOSS and Copernicus.

Such end-users were the Ministry of Electricity and Renewable Energy of Egypt, the Independent Power Transmission Operator of Greece, the shipping companies Superfast and Blue Star Ferries, Magdi Yacoub Heart Foundation Aswan Heart Centre and research groups from various Universities and research institutes.

References:

Kosmopoulos P. G., Kazadzis S., Taylor M., Raptis P. I., Keramitsoglou I., Kiranoudis C., Bais A. F.: 2018, Assessment of the surface solar irradiance derived from real-time modelling techniques and verification with ground-based measurements, Atmos. Meas. Tech., 11, 907–924.

Kosmopoulos P. G., Kazadzis S., Taylor M., Athanasopoulou E., Speyer O., Rapris P. I., Marinou E., Proestakis E., Solomos S., Gerasopoulos E., Amiridis V., Bais, A. F.: 2017, Dust impact on surface solar irradiance assessed with model simulations, satellite observations and ground-based measurements, Atmos. Meas. Tech., 10, 2435–2453.

NLTE Calculations of the Solar Spectrum Using Cross-Influence of Solar Atmosphere Structures

Nuno Guerreiro and Werner Schmutz in collaboration with MPS (Göttingen, Germany)

The computational resources to simulate 3-D magneto-hydrodynamic (MHD) models of the solar atmosphere and include a complete treatment of radiative transfer are prohibitive. In order to overcome this problem and calculate the solar spectrum in non-local thermodynamic equilibrium (NLTE), we develop a method working in 1D and cross-influencing different atmospheric structures at each depth point. This is expected to represent the effects of spatial and temporal variations in a simplified manner.

The constraints imposed by computational resources to calculate the solar spectrum have been tackled using 1-D models such as COSI and NESSY (Shapiro et al., 2010; Haberreiter et al., 2008; Tagirov et al., 2017). These widely-used models yield relatively good results. However, they depict an average composition and structure of the atmosphere that cannot fully reproduce the solar spectrum.

We have developed a method with 1-D models that can include several atmospheric structures and allows them to cross-influence each other. The cross-influence of the structures at each depth point in our method is governed by the following equation:

$$J_k^j new \approx J_k^j \Lambda^* + (1 - \Lambda^*) \sum_i \alpha_i J_k^j$$

where $J_k^j new$ represents the cross-influenced intensity of structure k at depth point j. The term J_k^j represents the intensity of structure k being cross-influenced by all other structures at point j, where Λ^* is the diagonal component of the Λ-acceleration. The term α_i represents the fractional contribution from the structure i.

The implications of the cross-influence for the solar spectrum can be seen in Figure 1. The top panel shows the radiative flux from two models used by Fontela et al. (1999). The black solid line represents the faint supergranular cell interior (FAL99_A), while the dotted blue line represents the average supergranule cell interior (FAL99_C) in the visible region of the spectrum. The dashed dotted red line shows the influence on FALL99_C from cross-influencing with FALL99_A. The green dashed line shows the influence of cross-influencing FALL99_A with FAL99_C. We used a 50% weight for each structure. The bottom panel displays the relative flux of cross-influenced structures to the same structures without cross-influencing.

The red line represents the cross-influenced FAL99_C divided by the flux of the same structure without cross-influence. The blue line represents the cross-influenced FALL99_A flux divided by the flux of the same structure without cross-influence. Both in the visible region of the spectrum. Essentially, the bottom panel illustrates the scale of the variation in the spectrum that occurs when we include the cross-influence effect.

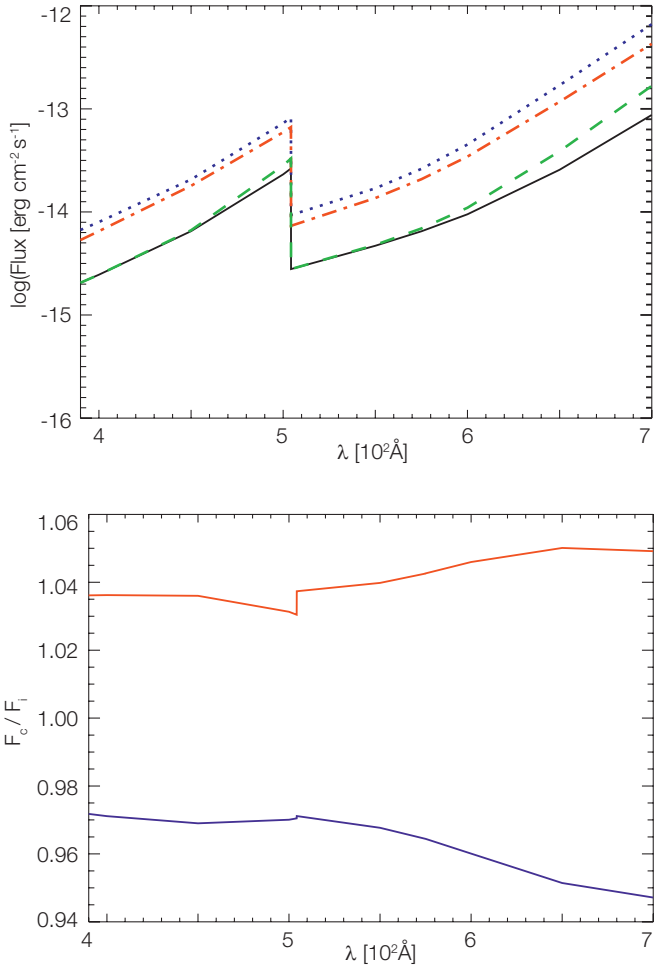

Figure 1. Top panel: Flux of the FALL99_A (black solid line), FALL99_C (dashed blue line) models and the flux resulting from the cross-influence of FALL99_A with FALL99_C (green dashed line), and FALL99_C with FAL99_A (dotted dashed red line).

Bottom panel: The ratios between the flux resulting from cross-influencing the two structures and the fluxes for each structure without cross-influence. The blue line stands for the cross-influenced FALL99_C model divided by the flux of the same model without cross-influence and the red line represents the cross-influenced FALL99_A flux divided by the flux of the same structure without cross-influence.

References:

Haberreiter M. et al.: 2008, Solving the discrepancy between the seismic and photospheric solar radius, Astron. Astrophys. 492, 833.

Fontela J. et al.: 1999, Calculation of solar irradiances. I. Synthesis of the solar spectrum, Astrophys. J., 518, 480.

Shapiro A. et al.: 2010, NLTE solar irradiance modeling with the COSI code, Astron. Astrophys., 517, A48.

Tagirov R. et al.: 2017, NESSY: NLTE spectral synthesis code for solar and stellar atmospheres, Astron. Astrophys., 603, 27.

Characterisation of a New Carbon Nanotube Detector Coating for TSI radiometers

Alberto Remesal Oliva, Wolfgang Finsterle, and Benjamin Walter

Three cavity detectors coated with spray-on carbon nanotubes from Surrey NanoSystems (www.surreynanosystems.com) were characterised. The cavity detectors are to be used in the Digital Absolute Radiometer (DARA), developed and built for the PROBA-3 satellite, as described by Sutter (2015) and Walter et al. (2017).

Three cavity detectors coated with spray-on carbon nanotubes were evaluated in two different experiments. The first cavity was exposed to a high-power UV laser to study the accelerated ageing of the carbon nanotubes under optical conditions similar to one year of Total Solar Irradiance (TSI) space measurements. The second cavity was tested in a thermal cycling test chamber simulating thermal variations onboard a satellite. The third cavity served as a reference and was therefore not subjected to any tests. We studied the reflectance of the detectors and evaluated the coating qualitatively by Scanning Electron Microscopy (SEM) before and after the tests to evaluate the performance of the coating, and to identify differences in the absorptance and in the structure of the carbon nanotubes.

Thermal cycling: Our radiometer (Cavity 3) was subjected to thermal cycling for 21 cycles over six days. Each cycle lasted 6.5 hours, with a maximum temperature of 80°C and a minimum of -20°C. The temperature cycle was thermally controlled every minute by a thermistor inside the chamber in order to check the stability of the test.

UV Ageing: Cavity 1 was subjected to a high-power UV laser (λ = 248 nm). Our goal was to simulate the equivalent UV dose for one year of full time solar exposure. The sample was installed inside a vacuum chamber maintained below a pressure of 6 x 10^{-4} mbar and the cavity was thermally controlled by a thermistor with a maximum temperature of 85°C. The cavity radiometer was exposed during 5 hours to 3.6 million pulses of approximately 20 mJ/pulse with a frequency of 200 pulses/s, with an average irradiance of 2 Wcm^{-2}.

Measurements of Cavity 3 before and after thermal cycling show no significant differences, and indicate that the thermal cycling had not affected the carbon nanotubes within the uncertainties shown for Cavity 2. This is shown in Figure 1. Although there is no significant difference in the SEM images (see Figure 2) after accelerated UV laser ageing, Cavity 1 suffered a significant increase in the coating reflectance, as observed in Figure 3.

The temperature reached in the carbon nanotubes is most likely higher than that measured in the cavity, and might be above the temperature limit of the hydrophobic film. This overheating of the coating might induce breaks in the protection film and damage of the carbon nanotubes.

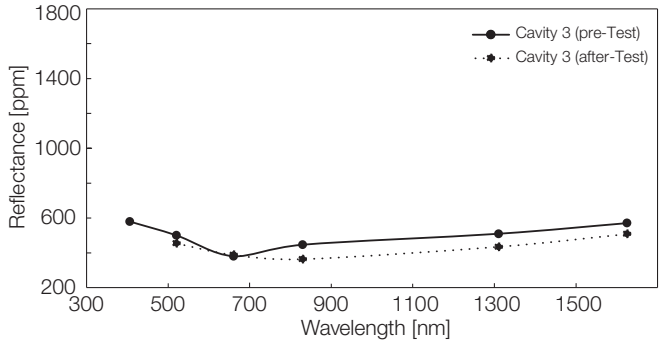

Figure 1. Comparison of Cavity 3, before and after treatment.

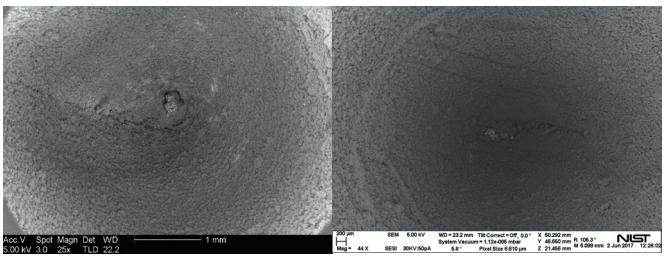

Figure 2. SEM pictures of Cavity 1. Left and right panels: Pre and post-treatment with UV light, respectively. No significant visual differences can be detected.

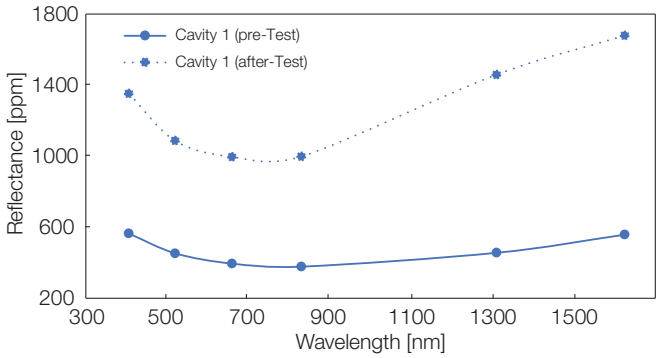

Figure 3. Comparison of Cavity 1, before and after treatment.

Acknowledgement: This work is supported by SNF grant 200021 162926.

References:

Suter M., 2015, Advances in Solar Radiometry, PhD Thesis Univ. Zürich, Zürich, Switzerland.

Walter B. et al.: 2017, The CLARA/NORSAT-1 solar absolute radiometer: instrument design, characterization and calibration, Metrologia, 54, 674-682, doi: 10.1088/1681-7575/aa7a63.

Publications and Media

Refereed Publications

Aebi C., Gröbner J., Kämpfer N., Vuilleumier L.: 2017, Cloud radiative effect, cloud fraction and cloud type at two stations in Switzerland using hemispherical sky cameras, Atmos. Meas. Tech., 10, 4587–4600, doi.org/10.5194/ amt-10-4587-2017.

Anderson D., Nicely J., Wolfe G., Hanisco T., Salawitch R., Canty P., Baidar S., Bannan T., Blake N., Chen D., Dix B., Fernandez R., Hall S., Hornbrook R., Huey L., Josse B., Jöckel P., Kinnison D., Koenig T., Le Breton M., Marécal V., Morgenstern O., Oman L., Pan L., Percival C., Plummer D., Revell L., Rozanov E., Saiz-Lopez A., Stenke A., Sudo K., Tilmes S., Ullmann K., Volkamer R., Weinheimer A., Zeng G.: 2017, Formaldehyde in the tropical western Pacific: Chemical sources and sinks, convective transport, and representation in CAM-Chem and the CCMI models, J. Geophys. Res. Atmos., 122, 11201–11226, doi:10.1002/2016JD026121.

Ball W., Alsing J., Mortlock D., Rozanov E., Tummon F., Haigh J.: 2017, Reconciling differences in stratospheric ozone composites, Atmos. Chem. Phys., 17, 12269–12302, doi: 10.5194/ acp-17-12269-2017.

Brönnimann S., Jacques-Coper M., Rozanov E., Fischer A., Morgenstern O., Zeng G., Akiyoshi H., Yamashita Y.: 2017, Tropical circulation and precipitation response to ozone depletion and recovery, Environ. Res. Letts., 12, 064011, doi: 10.1088/1748-9326/aa7416.

Carlund T., Kouremeti N., Kazadzis S., Gröbner J.: 2017, Aerosol optical depth determination in the UV using a four-channel precision filter radiometer, Atmos. Meas. Tech., 10, 905–923, doi:10.5194/amt-10-905-2017.

Drosoglou T. et al.: 2017; Comparisons of ground-based tropospheric NO2 MAX-DOAS measurements to satellite observations with the aid of an air quality model over the Thessaloniki area, Greece, Atmos. Chem. Phys., 17, 5829–5849, doi:10.5194/acp-17-5829-2017

Funke B., Ball W., Bender S., Gardini A., Harvey V., Lambert A., López-Puertas M., Marsh D., Meraner K., Nieder H., Päivärinta S.-M., Pérot K., Randall C., Reddmann T., Rozanov E., Schmidt H., Seppälä A., Sinnhuber M., Sukhodolov T., Stiller G., Tsvetkova N., Verronen P., Versick S., von Clarmann T., Walker K., Yushkov V.: 2017, HEPPA-II model-measurement inter-comparison project: EPP indirect effects during the dynamically perturbed NH winter 2008–2009, Atmos. Chem. Phys., 17, 3573–3604, doi:10.5194/acp-17-3573-2017.

Gröbner J., Kröger I., Egli L., Hülsen G., Riechelmann S., Sperfeld, P.: 2017, The high-resolution extraterrestrial solar spectrum (QASUMEFTS) determined from ground-based solar irradiance measurements, Atmos. Meas. Tech., 10, 3375–3383, doi.org/10.5194/amt-10-3375-2017.

Guerreiro N., Haberreiter M., Hansteen V., Schmutz W.: 2017, Small-scale heating events in the solar atmosphere. II. Lifetime, total energy, and magnetic properties, Astron. Astrophys., 603, A103 (11 pp), doi: 10.1051/0004-6361/201629795.

Haberreiter M., Schöll M., Dudok de Wit T., Kretzschmar M., Misios S., Tourpali K., Schmutz W.: 2017, A new observational solar irradiance composite, J. Geophys. Res.-Space Phys., 122, 5910–5930, doi: 10.1002/2016ja023492.

Jungclaus J., Bard E., Baroni M., Braconnot P., Cao J., Chini L., Egorova T., Evans M., González-Rouco J., Goosse H., Hurtt G., Joos F., Kaplan J., Khodri M., Goldewijk K., Krivova N., LeGrande A., Lorenz S., Luterbacher J., Man W., Maycock A., Meinshausen M., Moberg A., Muscheler R., Nehrbass-Ahles C., Otto-Bliesner B., Phipps S., Pongratz J., Rozanov E., Schmidt G., Schmidt H., Schmutz W., Schurer A., Shapiro A., Sigl M., Smerdon J., Solanki S., Timmreck C., Toohey M., Usoskin I., Wagner S., Wu C.-J., Yeo K.-L., Zanchettin D., Zhang Q., Zorita E.: 2017, The PMIP4 contribution to CMIP6 – Part 3: The last millennium, scientific objective, and experimental design for the PMIP4 past1000 simulations, Geosci. Model Dev., 10, 4005–4033, doi: 10.5194/gmd-10-4005-2017.

Koenigsberger G., Schmutz W., Skinner S.L.: 2017, Does the Wolf-Rayet binary CQ Cephei undergo sporadic mass transfer events?, Astron. Astrophys., 601, A121 (9 pp), doi: 10.1051/0004-6361/201630360.

Kosmopoulos P.G., Kazadzis S., Taylor M., Athanasopoulou E., Speyer O., Raptis P. I., Marinou E., Proestakis E., Solomos S., Gerasopoulos E., Amiridis V., Bais A., Kontoes C.: 2017, Dust impact on surface solar irradiance assessed with model simulations, satellite observations and ground-based measurements, Atmos. Meas. Tech., 10, 2435-2453, doi:10.5194/ amt-10-2435-2017.

Kuchar A., Ball W., Rozanov E., Stenke A., Revell L., Miksovsky J., Pisoft P., and Peter T.: 2017, On the aliasing of the solar cycle in the lower stratospheric tropical temperature, J. Geophys. Res. Atmos., 122, 9076–9093, doi:10.1002/ 2017JD026948.

Lamberts A., Millour F., Liermann A., Dessart L., Driebe T., Duvert G., Finsterle W., Girault V., Massi F., Petrov R. G., Schmutz W., Weigelt G., Chesneau O.: 2017, Numerical simulations and

infrared spectro-interferometry reveal the wind collision region in γ^2 Velorum, Mon. Not. R. Astron. Soc., 468, 2655–2671, doi: 10.1093/mnras/stx588.

Liang Q., Chipperfield M., Fleming E., Abraham N., Braesicke P., Burkholder J., Daniel J., Dhomse S., Fraser P., Hardiman S., Jackman Ch., Kinnison D., Krummel P., Montzka S., Morgenstern O., McCulloch A., Mühle J., Newman P., Orkin V., Pitari G., Prinn R., Rigby M., Rozanov E., Stenke A., Tummon F., Velders G., Visioni D., Weiss R.: 2017, Deriving global OH abundance and atmospheric lifetimes for long-lived gases: A search for CH_3CCl_3 alternatives, J. Geophys. Res. Atmos., 122, 11914–11933, doi:10.1002/2017JD026926.

Malik A., Brönnimann S., Stickler A., Raible C., Muthers S., Anet J., Rozanov E., Schmutz W.: 2017, Decadal to multi-decadal scale variability of Indian summer monsoon rainfall in the coupled ocean-atmosphere-chemistry climate model SOCOL-MPIOM, Climate Dynamics, 49, 3551-3572, doi: 10.1007/s00382-017-3529-9.

Matthes K. et al.: 2017, Solar forcing for CMIP6 (v3.2), Geosci. Model Dev., 10, 2247–2302, doi:10.5194/gmd-10-2247-2017.

Morgenstern O., Hegglin M., Rozanov E., O'Connor F., Abraham N., Akiyoshi H., Archibald A., Bekki S., Butchart N., Chipperfield M., Deushi M., Dhomse S., Garcia R., Hardiman S., Horowitz L., Jöckel P., Josse B., Kinnison D., Lin M., Mancini E., Manyin M., Marchand M., Marécal V., Michou M., Oman L., Pitari G., Plummer D., Revell L., Saint-Martin D., Schofield R., Stenke A., Stone K., Sudo K., Tanaka T., Tilmes S., Yamashita Y., Yoshida K., and Zeng G.: 2017, Review of the global models used within the Chemistry-Climate Model Initiative (CCMI), Geosci. Model Dev., 10, 639–671, doi: 10.5194/gmd-10-639-2017.

Nyeki S., Wacker S., Gröbner J., Finsterle W., Wild M.: 2017, Revising shortwave and longwave radiation archives in view of possible revisions of the WSG and WISG reference scales: methods and implications, Atmos. Meas. Tech., 10, 3057-3071, doi.org/10.5194/amt-10-3057-2017.

Raptis P. I., Kazadzis S., Psiloglou B., Kouremeti N., Kosmopoulos P., Kazantzidis A.: 2017, Measurements and model simulations of solar radiation at tilted planes, towards the maximization of energy capture, Energy, 130, 570-580, doi:10.1016/j.energy.2017.04.122.

Revell L., Stenke A., Luo B., Kremser S., Rozanov E., Sukhodolov T., Peter T.: 2017, Impacts of Mt Pinatubo volcanic aerosol on the tropical stratosphere in chemistry–climate model simulations using CCMI and CMIP6 stratospheric aerosol data, Atmos. Chem. Phys., 17, 13139–13150, doi: 10.5194/acp-17-13139-2017.

Schmalwieser A. W., Gröbner J., Blumthaler M. et al.: 2017, UV Index monitoring in Europe, Photochem. Photobiol. Sci., 16, 1349–1370, doi: 10.1039/C7PP00178A.

Shapiro A. I., Solanki S. K., Krivova N. A., Cameron R. H., Yeo K. L., Schmutz W. K.: 2017, The nature of solar brightness variations, Nature Astronomy, 1, 612–616, doi: 10.1038/s41550-017-0217-y.

Stübi R., Schill H., Klausen J., Vuilleumier L., Gröbner J., Egli L., Ruffieux D.: 2017, On the compatibility of Brewer total column ozone measurements in two adjacent valleys (Arosa and Davos) in the Swiss Alps, Atmos. Meas. Tech., 10, 4479–4490, doi.org/10.5194/amt-10-4479-2017.

Sukhodolov T., Usoskin I., Rozanov E., Asvestari E., Ball W.T., Curran M.A.J., Fischer H., Kovaltsov G., Miyake F., Peter T., Plummer C., Schmutz W., Severi M., Traversi R.: 2017, Atmospheric impacts of the strongest known solar particle storm of 775 AD, Scientific Reports, 7, 45257, doi: 10.1038/srep45257.

Sukhodolov T., Rozanov E., Ball W.T., Peter T., Schmutz W.: 2017, Modeling of the middle atmosphere response to 27-day solar irradiance variability, J. Atmos. Sol.-Ter. Phys., 152, 50–61, doi: 10.1016/j.jastp.2016.12.004.

Sukhodolov T., Usoskin I., Rozanov E., Asvestari E., Ball W., Curran M., Fischer H., Kovaltsov G., Miyake F., Peter T., Plummer C., Schmutz W., Severi M., Traversi, R.: 2017, Atmospheric impacts of the strongest known solar particle storm of 775 AD, Nature Scientific Reports, 7, 45257–45257, doi: 10.1038/srep45257.

Tagirov R., Shapiro A.I., Schmutz W.: 2017, NESSY: NLTE spectral synthesis code for solar and stellar atmospheres, Astron. Astrophys., 603, A27 (15 pp), doi: 10.1051/0004-6361/201628574.

Thuillier G., Zhu P., Shapiro A.I., Sofia S., Tagirov R., van Ruymbeke M., Perrin J.-M., Sukhodolov T., Schmutz W.: 2017, Solar disc radius determined from observations made during eclipses with bolometric and photometric instruments on board the PICARD satellite, Astron. Astrophys. 603, A28 (12 pp), doi: 10.1051/0004-6361/201629386.

Tsekeri A., Lopatin A., Amiridis V., Marinou E., Igloffstein J., Siomos N., Solomos S., Kokkalis P., Engelmann R., Baars H., Gratsea M., Raptis P. I., Binietoglou I., Mihalopoulos N., Kalivitis N., Kouvarakis G., Bartsotas N., Kallos G., Basart S., Schuettemeyer D., Wandinger U., Ansmann A., Chaikovsky A.P., Dubovik O.: 2017, GARRLiC and LIRIC: Strengths and limitations for the characterization of dust and marine particles along with their mixtures, Atmos. Meas. Tech., 10, 4995-5016, doi:10.5194/amt-10-4995-2017.

Walter B., Voegeli C., Horender S.: 2017, Estimating sediment mass fluxes on surfaces sheltered by live vegetation , Boundary Layer Met., 163, 273–286, doi:10.1007/s10546-016-0224-z.

Walter B., Levesque P.-L., Kopp G., Andersen B., Beck I., Finsterle W., Gyo M., Heuerman K., Koller S., Mingard N., Remesal Oliva A., Pfiffner D., Soder R., Spescha M., Suter M., Schmutz W.: 2017, The CLARA/NORSAT-1 solar absolute radiometer: instrument design, characterization and calibration, Metrologia, 54, 674–682, doi: 10.1088/1681-7575/aa7a63.

Wang H.R., Qi J., Li H.D., Fang W.: 2017, Initial in-flight results: The Total Solar Irradiance Monitor on the FY-3C satellite, an instrument with a pointing system, Sol. Phys., 292, 9, doi: 10.1007/s11207-016-1027-6.

Wang H.R., Wang Y.P., Ye X., Yang D.J., Wang K., Li H.D., Fang W.: 2017, Instrument Description: The Total Solar Irradiance Monitor on the FY-3C satellite, an instrument with a pointing system, Sol. Phys., 292, 8, doi: 10.1007/s11207-016-1026-7.

de Wit T. D., Kopp G., Frohlich C., Scholl M.: 2017, Methodology to create a new total solar irradiance record: Making a composite out of multiple data records, Geophys. Res. Lett., 44, 1196–1203, doi:10.1002/2016GL071866.

Zerefos C. S., Eleftheratos K., Kapsomenakis J., Solomos S., Inness A., Balis D., Redondas A., Eskes H., Allaart M., Amiridis V., Dahlback A., De Bock V., Diémoz H., Engelmann R., Eriksen P., Fioletov V., Gröbner J., Heikkilä A., Petropavlovskikh I., Jarosławski J., Josefsson W., Karppinen T., Köhler U., Meleti C., Repapis C., Rimmer J., Savinykh V., Shirotov V., Siani A. M., Smedley A. R. D., Stanek M., Stübi R.: 2017, Detecting volcanic sulfur dioxide plumes in the Northern Hemisphere using the Brewer spectrophotometers, other networks, and satellite observations, Atmos. Chem. Phys., 17, 551–574, doi: 10.5194/acp-17-551-2017.

Other Publications

Arsenovic P., Rozanov E., Anet J., Stenke A, and Peter T.: 2017, Implications of potential future grand solar minimum for ozone layer and climate, Atmos. Chem. Phys. Disc., doi: 10.5194/acp-2017-818.

Ball W. et al.: 2017, Continuous decline in lower stratospheric ozone offsets ozone layer recovery, Atmos. Chem. Phys. Disc., doi: 10.5194/acp-2017-862.

Caldwell M. E. et al.: 2017, The VUV instrument for Solar-Orbiter: ground testing of performance, Proc. SPIE, 10397, UNSP 1039708, doi:10.1117/12.2272980.

Cessateur G., Schmutz W., Ball W., Finsterle W., Walter B.: 2017, The Total Solar Irradiance as measured by PREMOS/PICARD, EGU General Assembly Conf., Abstracts 19, EGU2017-17720.

Davies R., Egli L., Schmutz W.: 2017, Preface. In: R. Davies, L. Egli, W. Schmutz (eds.) Radiation Processes in the Atmosphere and Ocean (IRS2016), Proceedings of the International Radiation Symposium (IRC/IAMAS), AIP Conf. Proc. 1810, 010001-1–010001-5 doi: 10.1063/1.4975496.

Dietmüller S. et al.: 2017, Quantifying the effect of mixing on the mean Age of Air in CCMVal-2 and CCMI-1 models, Atmos. Chem. Phys. Disc., doi: 10.5194/acp-2017-1143.

Drosoglou T. et al.: 2017, Total ozone data retrieval from the Phaethon DOAS system, in Perspectives on Atmos. Sci, 989-994, doi: 10.1007/978-3-319-35095-0_141.

Gkertsi F. et al.: 2017, Comparison of ground-based tropospheric NO_2 columns with OMI/Aura products in the Greater Area of Thessaloniki by means of an air qualit modeling tool, in Perspectives on Atmos. Sci, 1075-1080, doi: 10.1007/978-3-319-35095-0_153.

Gray L. J., Ball W., Misios S., 2017: Solar Influences on climate over the Atlantic / European Sector, AIP Conf. Proc., Rad. Processes in the Atmos. and Ocean, 1810, doi:10.1063/1.4975498.

Gröbner J. et al.: 2017, Spectral solar variations during the eclipse of March 20th, 2015 at two European sites, AIP Conf. Proc., Rad. Processes in the Atmos. and Ocean, 1810, doi: 10.1063/1.4975539.

Heikkila A. et al.: 2017, UV Exposure in artificial and natural weathering: A comparative study, AIP Conf. Proc., Rad. Processes in the Atmos. and Ocean, 1810, doi: 10.1063/1.4975566.

Karha P. et al.: 2017, Monte Carlo analysis of uncertainty of total atmospheric ozone derived from measured spectra, AIP Conf. Proc., Rad. Processes in the Atmos. and Ocean, 1810, doi: 10.1063/1.4975567.

Kosmopoulos P. G. et al.: 2017, Estimation of the solar energy potential in Greece using satellite and ground-based observations, in Perspectives on Atmos. Sci, 1149–1156, doi: 10.1007/978-3-319-35095-0_165.

Marshall L. et al.: 2017, Multi-model comparison of the volcanic sulfate deposition from the 1815 eruption of Mt. Tambora, Atmos. Chem. Phys. Disc., doi:10.5194/acp-2017-729.

Maycock A. et al.: 2017, The representation of solar cycle signals in stratospheric ozone. Part II: Analysis of global models, Atmos. Chem. Phys. Disc., doi: 10.5194/acp-2017-477.

Orbe C. et al.: 2017, Large-Scale Tropospheric Transport in the Chemistry Climate Model Initiative (CCMI) Simulations, Atmos. Chem. Phys. Disc., doi: 10.5194/acp-2017-1038.

Raptis I. P. et al.: 2017, Actinometric platform for solar spectral and air quality measurements, in Perspectives on Atmos. Sci, 1181–1186, doi: 10.1007/978-3-319-35095-0_170.

Walter B., Finsterle W., Koller S., Levesque P.-L., Pfiffner D., Schmutz W.: 2017, The Compact Lightweight Absolute Radiometer (CLARA) for Total Solar Irradiance Measurements on the NORSAT-1 Satellite, EGU General Assembly Conf. Abstracts 19, EGU2017-13027.

Walter B., Finsterle W., Koller S., Levesque P.-L., Pfiffner D., Schmutz W.: 2017, First TSI observations of the new Compact Lightweight Absolute Radiometer (CLARA), AGU Fall Meeting 2017, abstract #SH43B-2811.

Walter B., Winkler R., Graber F., Finsterle W., Fox N., Li V., Schmutz W.: 2017, Direct solar irradiance measurements with a cryogenic solar absolute radiometer, AIP Conf. Proc., Rad. Processes in the Atmos. and Ocean, 1810, doi: 10.1063/1.4975538.

Edited Book Chapters

Radiation Processes in the Atmosphere and Ocean (IRS2016). Proceedings of the International Radiation Symposium (IRC/IAMAS) held in Auckland, New Zealand 16–22 April 2016. Edited by Roger Davies, Luca Egli, and Werner Schmutz, 2017, AIP Conference Proc., 1810, Melville, New York.

Media

CLARA press release on 25 August 2017, reporting on successful first light measurements of the Total Solar Irradiance by the PMOD/WRC CLARA radiometer onboard the Norwegian NORSAT-1 satellite.

www.pmodwrc.ch/en/research-development/space/clara-norsat-1

WMO/MeteoSwiss/PMOD-WRC release of video on 31 October entitled "Measuring solar radiation".

https://www.pmodwrc.ch/en/2017/10/31/the-measurement-of-solar-irradiance/

International media coverage on 6 February 2018 on scientific paper by William Ball (Ball et al., 2018) concerning "Evidence for Declining Lower Stratospheric Ozone".

www.pmodwrc.ch/en/2018/02/06/evidence-for-declining-lower-stratospheric-ozone/

Personnel Department

Barbara Bücheler

Ready for the challenges of upcoming special events and highlights in 2017, we are once again proud to report from the front row about "our" world concerning solar science, instrument development and as a calibration centre.

The FUPSOL (Future and Past Solar Influence on the Terrestrial Climate) project ended in March 2017, which was funded as a Sinergia project by the Swiss National Science Foundation. This collaborative multi-institute research project produced 66 scientific publications as registered on the ISI Web of Science, which was cited 966 times up to April 2017. The last project meeting in Davos, where all partners participated, was reported in the television evening news and in the «Echo der Zeit» radio programme. Reactions from science and public circles were numerous.

MeteoSwiss welcomed our supervisory board on 9 May 2017 to the annual regular spring meeting held this year at Zurich Airport.

The beat of the New Orleans Jazz Festival transformed the Alps into a cultural scene on 12 July 2017. Lovers of Dixie, Swing, Blues and Jazz gathered in large numbers in our car-park to hear the likes of Dean Ross from the US and Ben Blue Martyn in a new formation. Together with joy and enthusiasm, we provided visitors with drinks and grilled food. Everyone enjoyed the beautiful sunny day with music, food and drink and the fantastic panoramic view of Davos.

Our scientists conducted a UV calibration campaign from 19 June to 18 August 2017, in the framework of the WMO/GAW programme, and were pleased with the positive feedback from our customers.

As part of our public outreach, we were once again able to arrange tours of our institute for prominent visitors from science and education as well as for the general public. Visiting groups from the Offices for Migration and Civil Law as well as the KIGA Canton Grisons challenged our experts with profound questions about space research and development, and other curious subjects such as the characteristics of tides. Building an electronic cube and taking it home at the end of the day was the inspiration for our 11 – 15 year-old visitors during holiday activities organised by the Pro Juventute.

Truly phenomenal and the absolute highlight of this year's projects was CLARA. The scientific community eagerly watched the NorSat-1 launch on 14 July 2017 which would bring CLARA into orbit. Silvio Koller and Daniel Pfiffner were present in the NorSat Mission Center in Oslo, while Wolfgang Finsterle was at the rocket launch itself, in Baikonur, Kazakhstan. Staff at PMOD/WRC enjoyed the spectacle from a safe distance by watching the launch on a live-stream. Our researcher-hearts were aflame and the enthusiasm continues.

Again, we are proud to report on the progress at the PMOD/WRC, and the changes in the staff this year.

Dr. Thomas Carlund, a scientist of the WORCC section, successfully completed his PMOD/WRC project on 31 March and returned to his native Sweden, following a new offer. Back home in Greece since 1 November 2017, Ioannis Panagiotis Raptis, a PhD student, continues to provide helpful support in the area of H2020 projects, where the PMOD/WRC will continue to be on board in the future. With Dr. Hongrui Wang we were able to make great progress in the Chinese cooperation project. He returned to China on 28 December 2017, where the collaboration with his home institute also continues.

With the employment of Matthias Gander (development engineer) and Mustapha Meftah (structual and thermal engineer), our technology section was further strengthened as of 1 February 2017. At the end of June 2017, Pierre-Luc Lévesque returned to Canada to join a new institution. We also continue to keep in touch with him. For Fabrice Eichenberger, his career path was manifold. He joined the PMOD/WRC as a civilian servant in January 2017 and remained with us from 1 July 2017 to 28 February 2018 as an Embedded Systems Engineer (HES). Johnathan Kennedy , a software engineer, left at the end of December 2017 after having successfully contributed to a number of projects. A big thank you to our guests, Franciele Carlesso, PhD student from Brazil, and Gian-Andrea Heinrich, Bachelor student at the ETH Zurich.

We congratulate Kathrin Anhorn and Alexandra Sretovic on the excellently passed final apprenticeship exam as a Business Woman EFZ E-Profile. We are grateful that Kathrin stayed with us until 31 December 2017. Diana Dos Santos took over in August, following in Kathrin and Alexandra's footsteps. We also congratulate Jeanine Lehner on her successfully completed commercial year internship. In August 2017, she started the next step of her further education at the Handelsschule in Chur.

With the energetic support of our committed civilian workers Marcel Schläppi, Martin Steiner, Fabrice Eichenberger, Thierry Solms, Elias Hagmann, Oliver Schaub, Stefan Steiner, Flurin Pestalozzi, Yannik Zimmermann and Lorenz Matter, we were able to set the next milestone in the development of our institute this year.

Our will to break new ground is limitless - we rely on the support of each individual person and their boundless energy. Together we hope to take our planet a step forward. Thank you for your trust and your inspiration.

Scientific Personnel

Prof. Werner Schmutz	Director, physicist
Dr. William Ball	Postdoc climate group, physicist
Dr. Thomas Carlund	Scientist WORCC section, meteorologist (until 31.03.2017)
Dr. Luca Egli	Scientist WCC-UV section, physicist
Dr. Tatiana Egorova	Scientist, climate group, climate scientist
Dr. Wolfgang Finsterle	Head WRC-section solar radiometry, physicist
Dr. Julian Gröbner	Head WRC-sections IR radiometry, WORCC, and WCC-UV, physicist
Dr. Nuno Guereirro	Postdoc solar physics group, physicist
Dr. Margit Haberreiter	Head solar physics group, physicist
Dr. Gregor Hülsen	Scientist WCC-UV section, physicist
Dr. Stylianos Kazantzis	Scientist WORCC section, physicist
Dr. Natalia Kouremeti	Scientist WORCC section, physicist
Dr. Stephan Nyeki	Scientist IR radiometry section, physicist
Dr. Eugene Rozanov	Scientist climate group, physicist
Dr. Timofei Sukhodolov	Postdoc, climate group, climate scientist
Dr. Benjamin Walter	Postdoc solar physics group, physicist
Dr. Hongrui Wang	Postdoc, WRC-section solar radiometry, physicist (until 28.12.2017)
Alberto Remesal Oliva	PhD student, 2nd year, University of Zurich
Christine Aebi	PhD student, SNF project, 4th year, University of Bern
Ioannis Panagiotis Raptis	PhD student, 3rd year, National and Kapodestrian Univ. Athens, Greece (until 31.10.2017)
Franciele Carlesso	PhD student, guest from Brasilia (01.04.2017 – 31.07.2017)
Gian-Andrea Heinrich	Bachelor student, ETH Zurich (06.03.2017 – 31.12.2017)

Technical Personnel

Silvio Koller	Co-Head technical dept., project manager space, quality system manager, elec. engineer
Daniel Pfiffner	Co-Head technical dept., project manager space, electronic engineer
Lloyd Beeler	Electronics engineer MSc
Fabrice Eichenberger	Embedded Systems engineer HES (since 01.07.2017)
Matthias Gander	Electronic engineer BSc (since 01.02.2017)
Manfred Gyo	Project manager space, electronic engineer
Jonathan Kennedy	Mechanics engineer MSc (until 31.12.2017)
Philipp Kuhn	Systems engineer
Patrik Langer	Mechanics engineer BSc
Pierre-Luc Lévesque	Instrument engineer (until 30.06.2017)
Mustapha Meftah	Structural and thermal engineer (01.02.2017 – 31.03.2017)
Pascal Schlatter	Mechanic, head workshop, security officer
Yanick Schoch	Electronics apprentice, 2nd year
Marco Senft	System administrator
Ricco Soder	Project manager technics, deputy quality system manager, electronics engineer
Marcel Spescha	Technician

Technical Personnel within the Science Department

Nathan Mingard	Physics laboratory technician
Christian Thomann	Technician

Administration

Barbara Bücheler	Head Administration/Human Resources
Kathrin Anhorn	Administration apprentice, 3rd year (until 31.07.2017), book-keeping (01.08.2017 – 31.12.2017)
Irene Keller	Administration, import/export
Angela Lehner	Administration, book-keeping
Jeanine Lehner	Trainee administration (until 31.07.2017)
Diana Fern. Dos Santos	Administration apprentice, 1st year
Alexandra Sretovic	Administration apprentice, 3rd year (until 31.07.2017)
Christian Stiffler	Accountant

Caretaker

Maria Sofia Ferreira Pinto	General caretaker, cleaning
Eufémia Soares Ferreira	General caretaker, cleaning (back-up)
Ana Rita Alves Ferreira	General caretaker, cleaning (back-up 2)

Civilian Service Conscripts

Fabrice Eichenberger	09.01.2017 – 09.06.2017
Marcel Schläppi	03.10.2016 – 31.01.2017
Martin Steiner	28.11.2016 – 31.01.2017
Elias Hagmann	30.01.2017 – 31.03.2017
Thierry Solms	30.01.2017 – 31.03.2017
Olivier Schaub	27.03.2017 – 11.07.2017
Stefan Steiner	26.06.2017 – 08.09.2017
Yannik Zimmermann	11.09.2017 – 25.12.2017
Flurin Pestalozzi	31.07.2017 – 01.12.2017
Lorenz Matter	02.10.2017 – 26.02.2018

Public Seminars

05.01.2017 Pavle Arsenovic, ETH Zürich
The influence of Spectral Solar Irradiance and Energetic Electron Precipitation on Climate.

09.02.2017 Lukas Widmer, Hospital Davos
Why carbs might not be your best food choice.

03.03.2017 Mustapha Meftah, Université Paris-Saclay
Recent Solar Spectral Irradiance Obs. and high interest to develop new space based instrs.

09.03.2017 Christian Stricker, Davos
Genomic prediction: From using 50'000 DNA markers to whole genomes in 10 years.

06.04.2017 Stephan Bolay, Geotest AG, Davos
100 years research of Davos geology evolution.

18.04.2017 Maria Thomann, University Basel
Physical Activity: Our society and some recommendations.

04.05.2017 Franciele Carlesso, Nat. Inst. Space Res., Brazil
Sensor Element Development for Total Solar Irradiance (TSI) Measurements.

01.06.2017 Markus Suter, Davos Instruments AG
Celebrating 40 years of PMO6.

29.06.2017 Prof. Ye Xin, CIOMP Changchun Institute of Optics, Fine Mechanics and Physics, China
FY-3E Total Solar Irradiance Measurement.

17.08.2017 Gael Cessateur, Belgian Inst. Space Aeronomy
First in-situ detection of halogens in a cometary coma.

21.09.2017 Arseniy Karagodin, St. Petersburg University
First results and further plans to couple GEC and climate models.

24.09.2017 Alvar Daza, King Juan Carlos University
Fractal basins: final state unpredictability in dynamical systems.

16.11.2017 Dmitry Kulyamin, Institute of Numerical Mathematics of Russian Academy of Science
Numerical modeling of Earth climate recent advances of INM RAS climate models.

Meetings/Event Organisation

09.03.2017	CLARA/NorSat-1 meeting
27-28.03.2017	FUPSOL meeting
25-26.04.2017	Swiss Space Center meeting
09.06.2017	SFI Stiftungsratsitzung
13-14.06.2017	SNSF Division II meeting of the National Research Council
19.06-18.08.2018	International UV calibration campaign
26.06-07.07.2017	JTSIM-DARA/FY-3E meeting
12.07.2017	Davos Sounds Good 2017 (Führungen)
08.08.2017	Ferienpass, PMOD/WRC day
29.08.2017	QM meeting
05-07.09.2017	SOLSPEC workshop
30.10.2017	Group C meeting for Quality Audit of Graduate School of Graubünden
15.12.2017	SFI Stiftungsratsitzung

Davos/Klosters Sounds Good

By Kathrin Anhorn

On 12 July 2017, the PMOD/WRC was part of the *New Orleans Jazz Festival of the Alps* which took place in our car-park from 12:00 to 14:00. The festival was part of the Davos Klosters *Sounds Good 2017* during which 17 bands performed 96 concerts throughout the week. Lovers of Dixie, Swing, Blues, New Orleans and Big Band Jazz appeared in their numbers on this sunny day and enjoyed the Rhythm'n 'Blues, Martyn Band. This band is a new and exciting Blues and Jazz band. The pianist Dean Ross from the USA teamed up with Ben Blue Martyn. The audience enjoyed the concert amid wonderful views of Davos.

The PMOD/WRC team organised a refreshments stand with various drinks and hot-dogs from the barbecue, rounding off the event nicely. The crowd of visitors was so great that several members of the institute had to spontaneously help at the stand. Between the acts there was the opportunity to join a free tour of the PMOD/WRC, which was appreciated by the visitors. The *Sounds Good 2017* event was a great success and we are looking forward to the next jazz festival!

Donations

A contribution from Mr. Daniel Karbacher (from Küsnacht, ZH) made it possible to cover the expenses of one research project in solar physics, in addition to the project planning within the allocated budget. The 3D-SOLSPEC project addresses the problem of calculating the solar radiation from the Sun with its 3D structure, in contrast to simulations which treat the Sun as being spherically symmetric. The more realistic treatment makes a difference in particular in the far UV part of the solar spectrum.

Lecture Courses, Participation in Commissions

Werner Schmutz	Examination expert in Astronomy, BSc ETH-ZH Honorary Member of the International Radiation Commission (IRC, IAMAS) Member of the Comité Consultatif de Photométrie et Radiométrie (CCPR, OICM) Swiss delegate to the Science Programme Committee, ESA Member of the Space Weather Working Team Steering Board of ESA Swiss delegate to the council of the Committee on Space Research (COSPAR) President of the National Committee on Space Research, SCNAT Member of the Commission for Astronomy, SCNAT Member of the GAW-CH Working Group (MeteoSwiss)
Wolfgang Finsterle	Member of CIMO ET-A3-II on Instrument Intercomparisons Member of CIMO TT Radiation References Member of EURAMET TC PR Chairman of ISO/TC180 SC1 (Solar Energy, Climate-Measurement and Data) Member of the PROBA-3 Science Working Team Lecture on *Solar Radiation as key source to be measured* at the *Forum on Regional Cooperation: Developing Quality Infrastructure for Photovoltaic Energy Generation*
Julian Gröbner	Lecture course in Solar Ultraviolet Radiation WS 2017, ETH-ZH GAW-CH Working group (MeteoSwiss) Member Scientific Advisory Group for UV, WMO GAW Chair of the NEWRAD Scientific committee Chairman of Infrared Working group of Baseline Surface Radiation Network (BSRN) Member IAMAS International Radiation Commission Member of the CIMO Task Group on Radiation, Vice Chairman Member of the EURAMET task Group on Environment Member International Ozone Commission (IO_3C)
Margit Haberreiter	President of the EGU Division on Solar-Terrestrial Sciences Member of the EGU Programme Group Vice-President of the Swiss SCOSTEP Committee, SCNAT Treasurer Swiss Rep. of the Interprog. Team on Space Weather, Inf. System and Services (IPT-SWISS) Member of the IAU Organizing Committee of Commission E3 *Solar Impact throughout the Heliosphere* Topical Editor Annales Geophysics Associate Member of the SPICE Operations Team
Stelios Kazadzis	Scientific Advisory Group Aerosol (WMO/GAW) Associate Editor in Atmospheric Chemistry and Physics Swiss delegate to the Management Group of COST 16202, WG3 Leader Co-Lecturer, *Fundamentals of remote sensing*, MSc in Space Science Technologies and Application, Univ. of Peloponnese, Greece Member of the GAW-CH Working Group (MeteoSwiss)
Eugene Rozanov	Co-Leader of SPARC SOLARIS-HEPPA WG3 Member of the Swiss SCOSTEP Committee Swiss representative in European COST CA15211, SCNAT WG3 leader Editor in *Atmosphere and Ocean Physics*, Russian academy of Science Associate Editor in *Frontiers in Earth Science (Atmospheric Science)* Editor in “Proceedings of Main Geophysical observatory”

Bilanz per 2017 (inklusive Drittmittel) mit Vorjahresvergleich

Aktiven	31.12.2017 CHF	31.12.2016 CHF
Flüssige Mittel	766'404.78	1'017'573.44
Forderungen	248'962.00	43'628.80
Warenvorräte	105'000.00	0.00
Aktive Rechnungsabgrenzungen	393'226.46	203'736.55
Total Aktiven	1'513'593.24	1'264'938.79

Passiven		
Verbindlichkeiten	322'323.75	151'914.51
Kontokorrent Stiftung	122'487.45	91'540.05
Passive Rechnungsabgrenzung	289'713.34	121'532.31
Rückstellungen	772'789.75	892'789.75
Eigenkapital	6'278.95	7'162.17
Total Passiven	1'513'593.24	1'264'938.79

Erfolgsrechnung 2017 (inklusive Drittmittel) mit Vorjahresvergleich

Ertrag	CHF	CHF
Beitrag Bund Betrieb WRC	1'460'000.00	1'460'000.00
Beitrag Bund (BBL)	102'139.75	158'003.30
Beitrag Kanton Graubünden	499'282.00	499'282.00
Beitrag Gemeinde Davos	651'168.00	651'168.00
Beitrag Gemeinde Davos, Mieterlass	160'000.00	160'000.00
Overhead SNF	59'977.00	117'461.69
Overhead EU	66'925.35	9'587.25
Profit Projekt ATLAS	0.00	30'844.00
Auflösung Rückstellungen für Instrumentenbau	120'000.00	0.00
Instrumentenverkäufe	184'897.85	114'947.95
Reparaturen und Kalibrationen	227'583.77	145'458.63
Ertrag Dienstleistungen	14'772.95	27'051.90
Übriger Ertrag	11'589.85	19'949.25
Finanzertrag	5.55	29.65
Ausserordentlicher Ertrag	44'224.60	13'623.30
Drittmittel	2'216'383.05	2'783'362.31
Total Ertrag	5'818'949.72	6'190'769.23

Aufwand		
Personalaufwand	4'446'910.85	4'338'549.10
Investitionen Observatorium	97'910.93	140'181.42
Investitionen Drittmittel	105'702.50	41'493.75
Unterhalt Gebäude (Beitrag Bund)	102'139.75	158'003.30
Unterhalt	27'745.05	48'485.26
Verbrauchsmaterial Observatorium	30'174.00	22'822.20
Verbrauchsmaterial Drittmittel	262'833.54	252'137.61
Verbrauch Commercial	171'284.34	126'897.56
Reisen, Kurse	183'074.89	160'966.71
Raumaufwand/Energieaufwand	195'912.90	206'804.75
Versicherungen, Verwaltungsaufwand	116'483.64	147'736.14
Finanzaufwand	2'262.39	2'839.72
Übriger Betriebsaufwand	49'908.15	41'449.32
Ausserordentlicher Aufwand	27'490.01	111'914.28
Nicht gedeckter Aufwand EU-Projekte	0.00	454'907.92
Total Aufwand	5'819'832.94	6'255'189.04
Jahresergebnis vor Auflösung Rückstellungen	-883.22	-64'419.81
Auflösung Rückstellungen zur Defizitdeckung	0.00	52'530.44
Jahresergebnis	-883.22	-11'889.37
	5'818'949.72	6'190'769.23

Abbreviations

AERONET	Aerosol Robotic Network, GSFC, USA
AOCCM	Atmosphere-Ocean-Chemistry-Climate Model
AOD	Aerosol Optical Depth
BIPM	Bureau International des Poids et Mesures, Paris, France
BSRN	Baseline Surface Radiation Network of the WCRP
CCM	Chemistry-Climate Model
CCPR	Comité Consultatif de Photométrie et Radiométrie, BIPM
CIMO	Commission for Instruments and Methods of Observation of WMO, Geneva, Switzerland
CIPM	Comité International des Poids et Mesures
CLARA	Compact Light-weight Absolute Radiometer (PMOD/WRC experiment onboard the NorSat-1 micro-satellite mission)
CMC	Calibration and Measurement Capabilities
COCOSIS	Combination of COSI Spectra
COSI	Code for Solar Irradiance (solar atmosphere radiation transport code developed at PMOD/WRC)
COSPAR	Commission of Space Application and Research of ICSU, Paris, France
COST	European Cooperation in Science and Technology
CSAR	Cyrogenic Solar Absolute Radiometer (PMOD/WRC research instrument)
DARA	Digital Absolute Radiometer (PMOD/WRC experiment onboard the ESA PROBA-3 formation flying mission)
EM	Engineering Model
EMRP	European Metrology Research Programme
ESA	European Space Agency
EUI	Extreme Ultraviolet Imager (international experiment onboard the Solar Orbiter mission)
EUV	Extreme Ultraviolet region of the light spectrum
FM/FS	Flight Model/Flight Spare
FUPSOL	Future and Past Solar Influence on the Climate, SNF Sinergia Project
FY-3	Feng Yun 3 series of Chinese space missions (FY-3A to E)
GAW	Global Atmosphere Watch, a WMO Research Programme
GCM	General Circulation Model
IACETHZ	Institute for Climate Research of the ETHZ, Switzerland
IAMAS	International Association of Meteorology and Atmospheric Sciences of IUGG
IAU	International Astronomical Union of ICSU, Paris, France
IPC	International Pyrheliometer Comparisons, held at PMOD/WRC every 5 years
IRIS	Infrared Integrating Sphere Radiometer (PMOD/WRC research instrument)
IRCCAM	Infrared Cloud Camera (PMOD/WRC research instrument)
ISO/IEC	International Oranisation for Standardisation/International Electrotechnical Commission
JTSIM	Joint Total Solar Irradiance Monitor (experiment onboard the Chinese FY-3E mission)
LASP	Laboratory for Atmospheric and Space Physics, Boulder, USA
LVPS	Low Voltage Power Supply (PMOD/WRC contribution to the Solar Orbiter mission)
METAS	Federal Office of Metrology
MITRA	Monitor to Determine the Integrated Transmittance (PMOD/WRC research instrument)
MPS	Max Planck Institute for Solar System Research
MRA	Mutual Recognition Arrangement
MRR	Manufacturing Readiness Review
NASA	National Aeronautics and Space Administration, Washington DC, USA
NIST	National Institute of Standards and Technology, Gaithersburg, MD, USA
NorSat-1	Norwegian Satellite-1
NPL	National Physical Laboratory, Teddington, UK
NREL	National Renewable Energy Laboratory, Golden, CO, USA
PFR	Precision Filter Radiometer (previously manufactured by PMOD/WRC)
PMO6-CC	PMO6-CC type of radiometer (manufactured by PMOD/WRC)
PROBA	ESA Satellite Missions (PROBA-1 to 3)
PRODEX	PROgramme de Développement d'Expériences scientifiques, ESA
PSR	Precision Spectroradiometer (manufactured by PMOD/WRC)
PTB	Physikalisch-Technische Bundesanstalt, Braunschweig and Berlin, Germany
QASUME	Quality Assurance of Spectral Ultraviolet Measurements in Europe
QM	Qualification Model
QMS	Quality Management System
SCNAT	Swiss Academy of Sciences
SLF	Schnee und Lawinenforschungsinstitut, Davos, Switzerland
SFI	Schweiz. Forschungsinstitut für Hochgebirgsklima und Medizin, Davos, Switzerland
SIAF	Schweiz. Institut für Allergie- und Asthma-Forschung, Davos, Switzerland
SNSF	Swiss National Science Foundation
SOCOL	Combined GCM and CTM Computer Model developed at PMOD/WRC
SOHO	Solar and Heliospheric Observatory (ESA/NASA space mission)
SPICE	Spectral Imaging of the Coronal Environment (PMOD/WRC contribution to the Solar Orbiter mission)
SSI	Solar Spectral Irradiance
TSI	Total Solar Irradiance
VIRGO	Variability of Solar Irradiance and Gravity Oscillations (PMOD/WRC experiment onboard the SOHO mission)
WDCA	World Data Centre for Aerosols
WISG	World Infrared Standard Group of pyrgeometers (maintained by WRC-IRS at PMOD/WRC)
WMO	World Meteorological Organisation, a United Nations Specialised Agency, Geneva, Switzerland
WRR	World Radiometric Reference
WSG	World Standard Group of pyrheliometers (realises the WRR; maintained by WRC at PMOD/WRC)

Annual Report 2017

Editors: Werner Schmutz and Stephan Nyeki
Layout by Stephan Nyeki

Publication by PMOD/WRC, Davos, Switzerland
Edition: 600, printed 2018

Front/rear covers: The 2nd international UV Filter Radiometer Comparison (UVC-II) was held at the PMOD/WRC from 25 May to 5 October 2017. This campaign followed three similar campaigns: 1995 in Helsinki (Finland), 1999 in Thessaloniki (Greece), and 2006 in Davos (Switzerland). A total of 75 broadband radiometers from 37 institutions participated in the most recent campaign.

Dorfstrasse 33, 7260 Davos Dorf, Switzerland
Phone +41 58 467 51 11, Fax +41 58 467 51 00
www.pmodwrc.ch